A C K N O W L E D G E M E N T

Preparation of this issue has been accomplished with excellent cooperation from the participants, particularly Frank F. Hines of Baldwin-Lima-Hamilton Corporation, Keith McFarland of Ames Research Center, Truman R. Curry of The Boeing Airplane Company, and Richard R. Tracy and Elmer Ward of the Task Corporation who have reviewed text material to ensure its accuracy.

Assistance and constructive criticism have been liberally supplied by the Executive Board of W.R.S.G.C. and Baldwin-Lima-Hamilton personnel. Mrs. Janet Withee supplied the secretarial effort, serving effectively in transcribing the tape recordings and preparation of the manuscript from which these "Proceedings" will be printed.

It has been a pleasure to work with these persons in preparing this material for "committee" delegates and their member organizations.

WESTERN REGIONAL STRAIN GAGE COMMITTEE
Philip O. Vulliet, Executive Director
Frank F. Hines, Executive Secretary

(NASA-TM-74879) PROCEEDINGS OF WESTERN REGIONAL STRAIN GAGE COMMITTEE (NASA) 119 p

N77-83285

Unclas
00/35 41897

CONTENTS

REPORT ON STRAIN GAGE DEVELOPMENTS

James Dorsey
B-L-H Corporation

Today we have three topics to discuss as strain gage developments. These items should be of interest since they cover,

Beneficial effects of post-cure techniques,
a new Stress-Strain Gage, and
NAS-942 qualification testing.

Beneficial Effects of Post-Cure A program has been initiated to determine what can be achieved with post-cure techniques. Figure 1 shows typical strain sensitivity curves as a function of temperature for three different quarter-inch bakelite strain gages. Run 2 shows considerably better performance than Run 1 because of the cumulative post-cure effect from temperatures of Run 1.

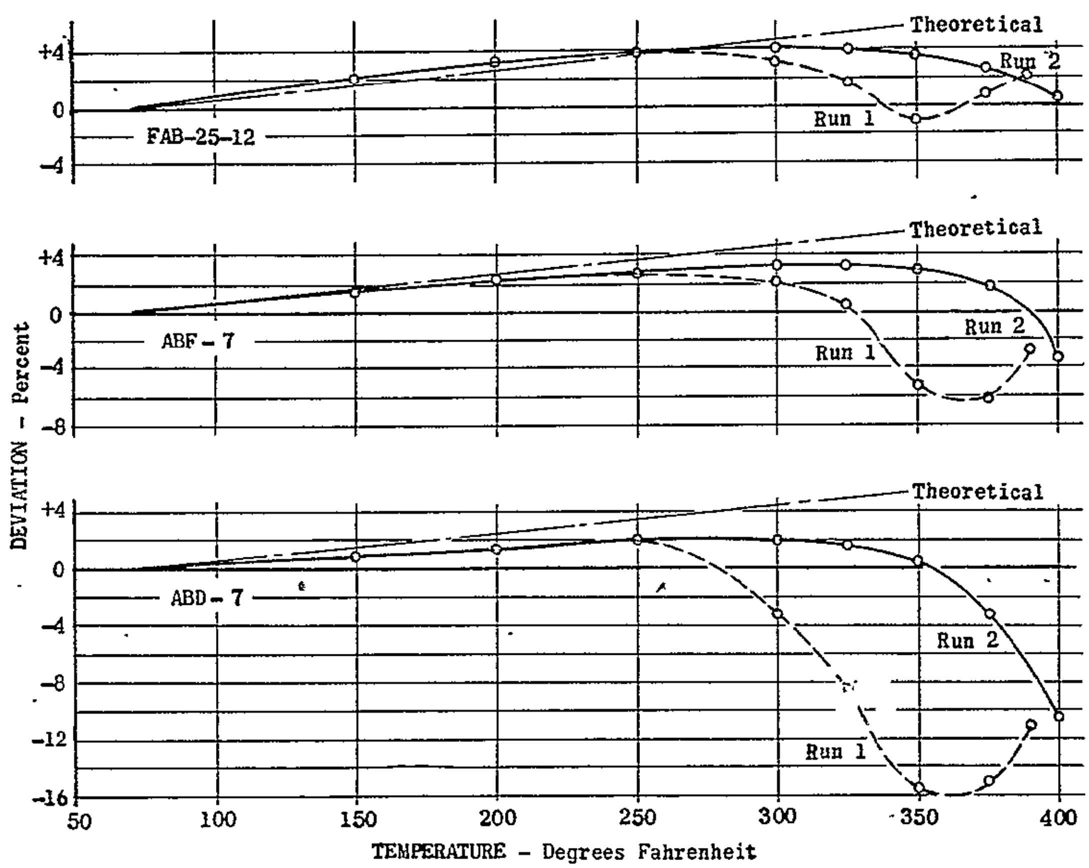

Figure 1 Strain gage strain sensitivity as a function of temperature for three typical bakelite gages.

Reliable strain response is shown to approximately 350°F for all gages on Run 2. Post-cure helps both the strain gage and adhesive in addition to raising the temperature limit of the installation.

Figure 2 shows a number of representative cures and strain sensitivity obtained from each. Data has been corrected for change in specimen material modulus due to temperature. That is, if the gage alloy did not increase its sensitivity with temperature, and if the specimen modulus of elasticity did not decrease with temperature, then the strain sensitivity or gage factor would lie along the zero axis for its entire length. The curves are typical and have been somewhat "idealized".

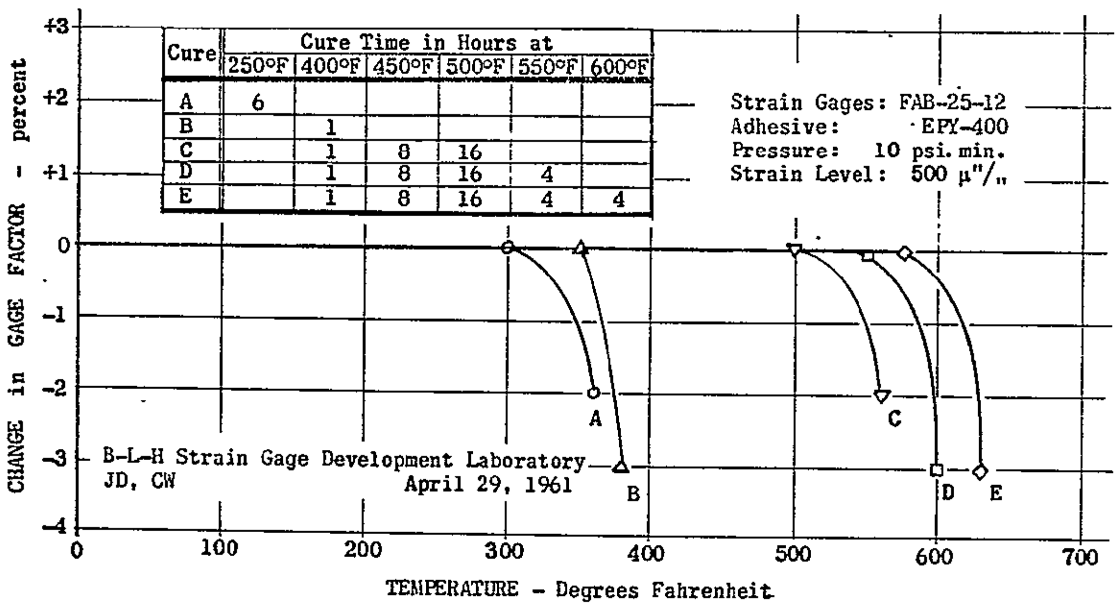

Figure 2 Effect of cure cycle on bakelite strain gage performance.

Curve A is for the nominal "package" cure of six hours at 250°F, and curve B is for one hour at 400°F. The difference between the two curves is interesting, since it indicates that bakelite is benefited more by a six-hour cure at 250°F than by one hour at 400°F. The other curves represent extensive post cures of twenty-five hours and longer. Increased strain sensitivity is demonstrated to above 550°F. The same gage installations represented by curve E, when temperature cycled for the second time, or recycled, should be "flat" to about 600°F.

Figure 3 shows a larger number of recommended cures for various maximum test temperatures. In most cases, the final cure temperature should equal or exceed the maximum test temperature. After the proper time at one temperature level during the curing cycle, we increase immediately to the next temperature range and hold. Figure 3 shows that two hours rather than one is usually recommended for the 400°F curing temperature. This is done because laboratory technicians often start timing the cycle before the specimen has reached the desired temperature.

There are two problems encountered with post cure of this type: They are;

1. Two materials are involved
    a. Strain gage matrix
    b. Adhesive
2. Bakelite polymerizes by condensation which releases minute quantities of water vapor

For this reason, an immediate post cure at 500°F, for example, does not work well at all, and I think it could cause deterioration of the bakelite. If heated rapidly to a high temperature, bakelite will blister around 600°F.

Maximum Test Temperature	Total Time at Cure Temps	Specimen Cure Time, hours at temperature							
		250°F	300°F	350°F	400°F	450°F	500°F	550°F	600°F
250°F	6	6							
300°F	6	6							
300°F	3		3						
350°F	6		4	2					
350°F	1				1				
400°F	4				2	2			
450°F	6				2	2	2		
450°F	10				5	5			
500°F	14				4	·4	6		
550°F	30				2	8	16	4	
575°F	34				2	8	16	4	4
600°F	35	Use 575°F cycle. Cool to room tempurature. Reheat to 600°F and hold for 1 hour							

Figure 3. Recommended Cure Cycles for SR-4 Bakelite Foil Strain Gages using EPY-400 Cement.

Creep at 550°F is definitely greater than it is at 350°F, but for some relatively short tests, the higher temperature does not seem to cause unreasonable creep. Our laboratory tested gages represented by Curve C of Figure 2 which showed failure at about 500°F for creep at 530°F. Total creep in one hour was about 1.5 percent and for five hours was about 6 percent. The longest we have been able to get a single installation to last in the oven has been ten hours, which seems inadequate when there is no sign of gage deterioration. We know that gages can operate at 600°F for some finite period of time, probably in the order of one hundred hours. This testing has been started, and we are going to expand it for more complete results. In time we expect to supply information on a greater variety of cures than those described. We are also working other combinations such as bakelite with low temperature epoxy, epoxy gages with other types of epoxy cements and Eastman 910 cement used with bakelite and epoxy gages.

There are two precautions concerning this information that should be noted.

1. Wire gages with bakelite matrix are good to about 350°F even under rather severe treatment. In some instances, if the gage is fairly long or if it is a flat grid of good proportions, they can be utilized to about 400°F. Wrap-around bakelite gages, however, have limiting temperatures considerably less than those mentioned previously.
2. Bakelite gages of the common variety are made with a polymeric reinforcing paper and soldered wire joints which can be considered reliable to 450°F. If one anticipates any elevated temperature strain gage work in the range of 500°F or above, special gages should be ordered for the purpose. Ultimately, we plan to produce only gages which will withstand 600°F.

If someone orders 600°F foil gages from my company, the order department consults with me concerning what is desired. These gages look identical to other foil gages, but they have leads attached by welding or with 600°F solder. One can usually cure a gage above the melting temperature of solder since the solder will remain in position during curing despite its molten state.

Question: Will the same cure cycles apply if one were to use other than a bakelite gage, i.e., a strippable foil gage?

Answer: It will not work with a strippable gage and epoxy cement because the modulus of elasticity of epoxy cement decreases rapidly at 350°F to 400°F regardless of the post cure. We do not understand why this works with bakelite, but apparently the glueline is thin enough that the shear strength is maintained sufficiently to get good sensitivity. We constructed some gages of epoxy similar to the EPY-400, and they just do not perform properly at 350°F. The curve drops right off regardless of post cure. It seems that the curve for phenolic materials also drops off at about this temperature, but if one keeps curing them, the modulus of elasticity goes back up. When the temperature is raised and lowered, the line stays at a high level. The epoxy does not do this, but is more like a thermoplastic material.

Question: Are you implying that EPY-400 is a phenolic, not an epoxy?

Answer: No, it is an epoxy. It will not work in construction of a gage nor for putting down a strippable one, but it does work as an adhesive for bakelite gages.

Question: How about gages with an epoxy matrix?

Answer: We have never been able to get these above 350°F on any kind of static testing.

Question: Why not use the bakelite cement, then?

Answer: The only reason is because it requires pressure for polymerization, which is sometimes more difficult to get than one would think. Bakelite cement with pressure is actually the better system. We expect that it will give as good or better results than the systems shown here, and one can cure it in considerably shorter time. It does require pressure, however.

Question: Why don't you make epoxy-backed gages that are good at higher temperatures, i.e., carry EPY-400 to 600°F?

Answer: The problem is the decreasing modulus of elasticity with temperature. We cannot find an epoxy which will retain its modulus above 350°F. In fact, at room temperature the modulus of most epoxies is 500,000 psi, while at 400°F it is only 3,000 psi. The properties that accompany this low modulus do not provide enough shear strength to give a good strain-sensing assembly.

A New Stress-Strain Gage. The material of Appendix A fully describes this device. Figure 4 is a standard transducer that has been available. The angle θ bears a direct relation to Poisson's ratio for the material on which it will be installed. Figure 5 shows the new stress-strain gage. The theory of operation is fully described with sample calculations and graphs of the error functions.

This gage is unique, since with proper switching and readout equipment, one can obtain axial stress and biaxial strains from the same installation. Gage element resistances have been selected such that the major element is 350 ohms and the minor element is approximately of 100 ohms, i.e., 98 ohms in one case and 115 ohms in the other. The gages have been made for material with Poisson's ratio of 0.33 and 0.28, and will be supplied in bakelite matrix only at this time. With proper construction and proper post cure, they can be used at temperatures up to 600°F.

Graphs for error in calculated stress, using these gages in various combinations of specimen properties and stress-strain gage characteristics have been developed. These figures appear quite similar, but actually they are different.

Included in the text is the topic of Poisson's ratio with a discussion of values available and accuracies of these values. A correct method for obtaining Poisson's ratio of any material by experimental techniques is given. A graph for the error in calculation of Poisson's ratio when using strain gages with various transverse sensitivities is included. The errors for a large number of wire and foil gages are shown in the plots so that one can make reasonable corrections if working with Poisson's ratio.

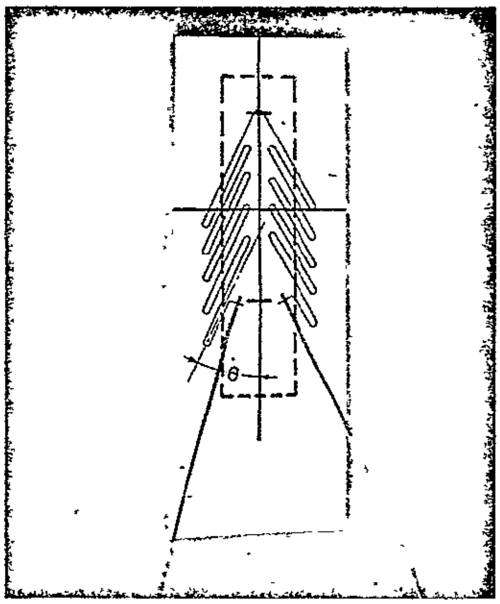

Figure 4 Typical Wire Stress-Strain Gage

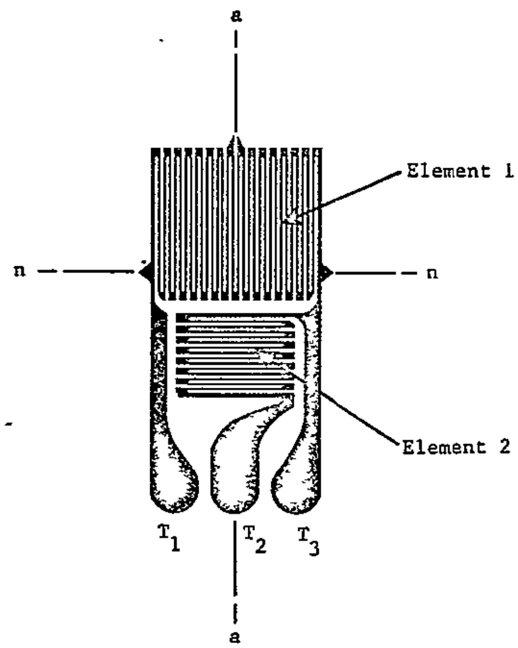

Figure 5 Typical Etched Foil Stress-Strain Gage

Question: Would these error factors and other data be satisfactory for use with a stress-strain gage of different size and area?

Answer: At this time we have one size only, so we do not know what effect size and shape will have. The supposition that these figures apply is not necessarily correct. It is a matter of the transverse sensitivity of that particular gage.

Question: What bonding do you use for this stress-strain gage?

Answer: Bakelite, EPY-400, or any epoxy.

Question: Is this true for 600°F application?

Answer: For 600°F, one would use EPY-400.

<u>NAS 942 Qualification Testing.</u> This last item, which has considerable interest, concerns specimens that Frank Hines has designed and worked on for the NAS 942 testing. Figure 6, B-L-H Drawing 206701-1, is a channel specimen designed for tension and compression tests at temperatures up to and above 1000°F. Figure 7, B-L-H Drawing 206683-1, is a sheet specimen intended for determination of creep, zero drift and mechanical hysteresis at temperatures up to approximately 600°F. This specimen can be changed quickly and has low thermal lag which permits rapid temperature variations.

The reasoning behind the design of the channel specimen involved a desire to conduct evaluation tests of strain gages mounted on the centroidal axis of the test specimen. This reduces bending effects on the gage to a minimum. The average strain at the centroidal axis is not a function of the amount of bending; therefore, strain calibrations are more accurate and more applicable to data taken on gages on the same specimen.

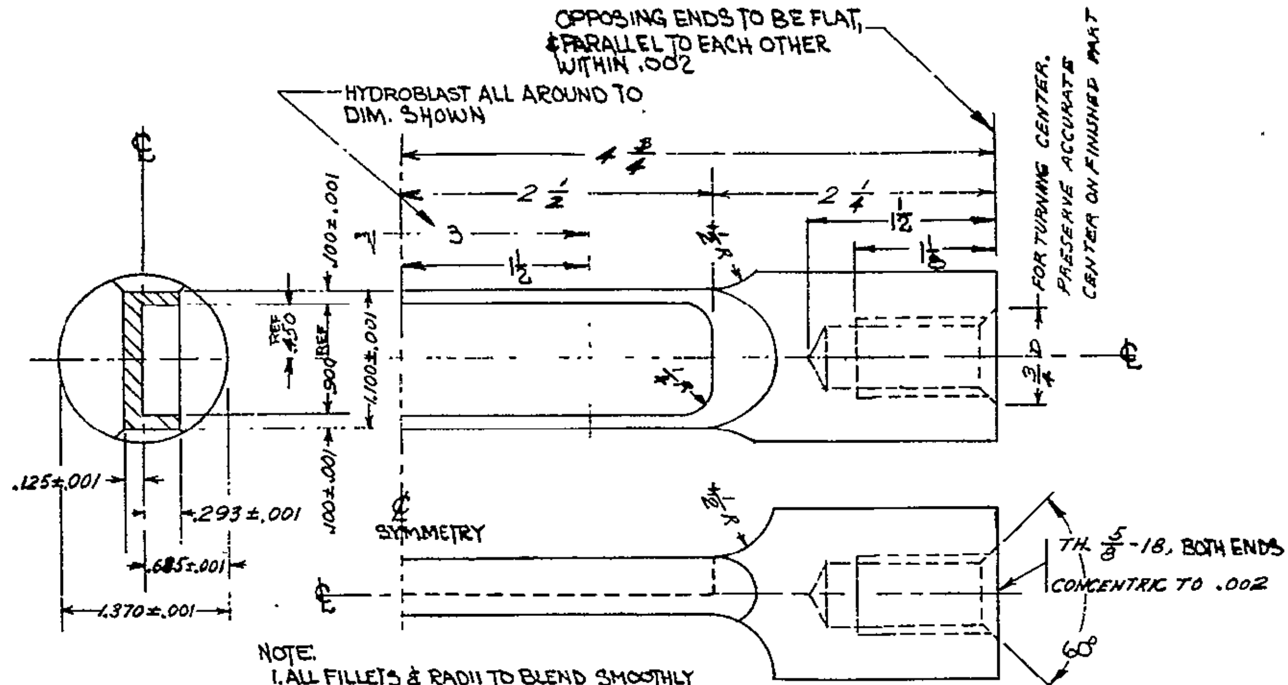

UNLESS OTHERWISE NOTED FRACT. TOL. ±1/64 DEC. TOL. ±.005 ANGULAR TOL. ±1/2° ALL CORNERS .005-.015R. MACH FINISH 32/MIN	DRAWN FH 11-6-60	BALDWIN-LIMA-HAMILTON CORP. ELECTRONICS AND INSTRUMENTATION DIVISION WALTHAM 54 MASSACHUSETTS
PROTECTIVE FINISH —//—	CHECKED	
	APPROVED J.D. 5/4/61	TENSION - COMPRESSION TEST SPECIMEN, HIGH TEMP.
	RELEASED	
MATERIAL INCONEL "700"	E R W	
	SCALE FULL	206701 -1

Figure 6 Channel type universal strain gage evaluation specimen for high temperature testing.

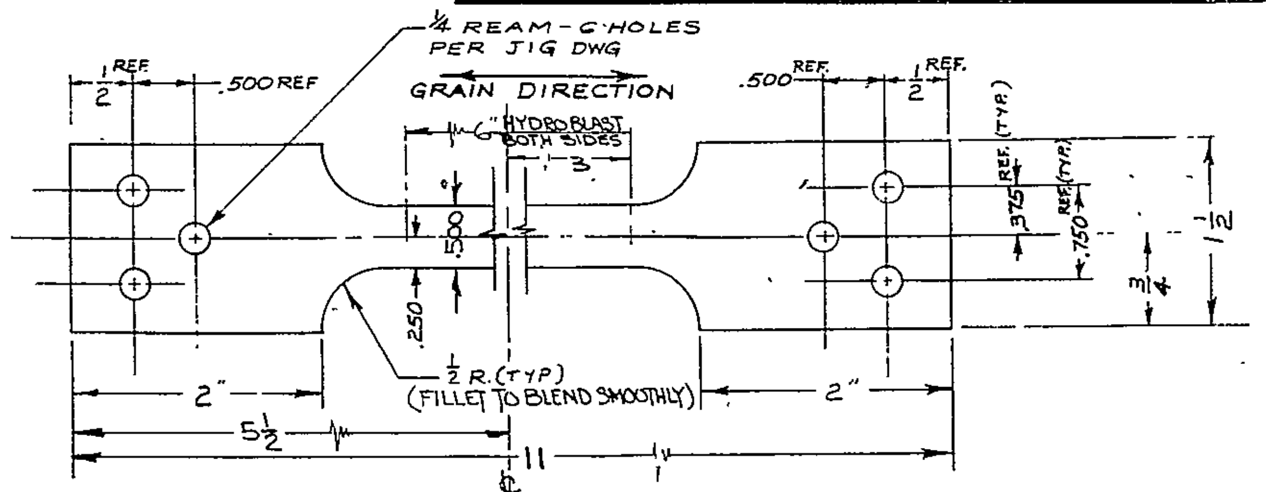

DWG NO	MATERIAL	THICKNESS
206683-1	ARMCO 17-7PH	.060/.064
206684-1	ALUM. 2024-T4	.060/.064
206685-1	ALUM. 7075-T6	.060/.064

UNLESS OTHERWISE NOTED FRACT. TOL. ±1/64 DEC. TOL. ±.005 ANGULAR TOL. ±1/2° ALL CORNERS .005-.015R MACHINE FINISH 32/MIN.	DRAWN R.G. Evans 5-30-61	BALDWIN-LIMA-HAMILTON CORP. ELECTRONICS AND INSTRUMENTATION DIVISION WALTHAM 54 MASSACHUSETTS
PROTECTIVE FINISH —//—	CHECKED	
	APPROVED J.D. 5/9/61	SHEET TYPE GAGE EVALUATION SPECIMEN
	RELEASED	
MATERIAL SEE CHART	E R W	
	SCALE 1 = 1	206683-1 THRU 206685 -1

Figure 7 Strain gage test specimen from sheet stock for evaluation of creep, zero drift and mechanical hysteresis.

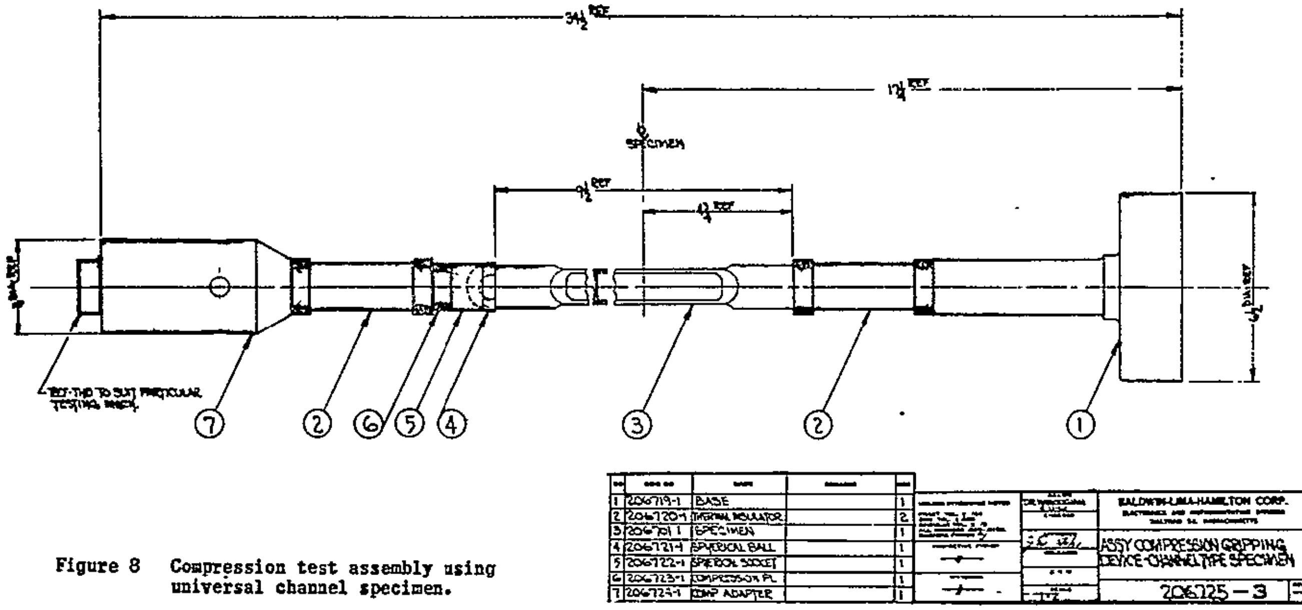

Figure 8 Compression test assembly using universal channel specimen.

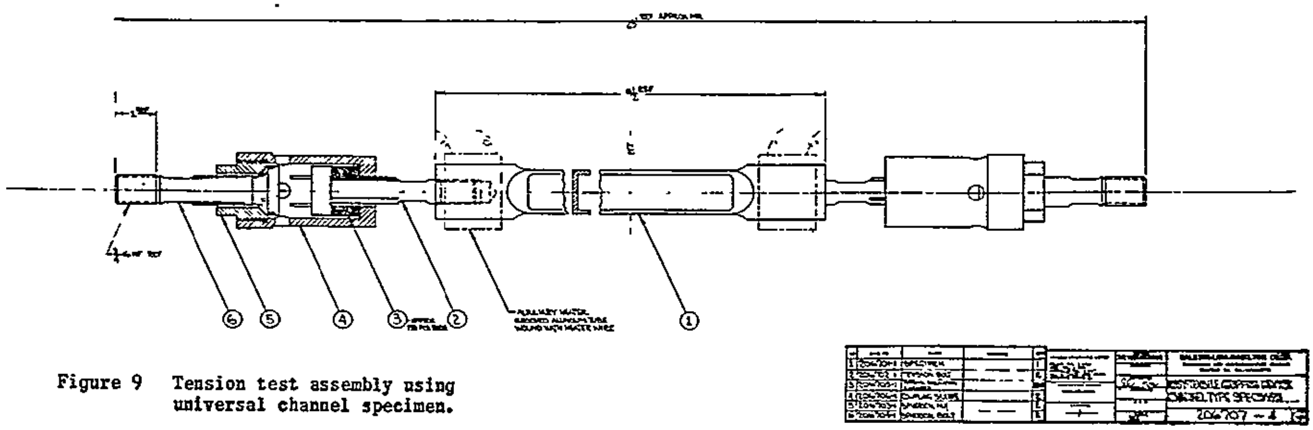

Figure 9 Tension test assembly using universal channel specimen.

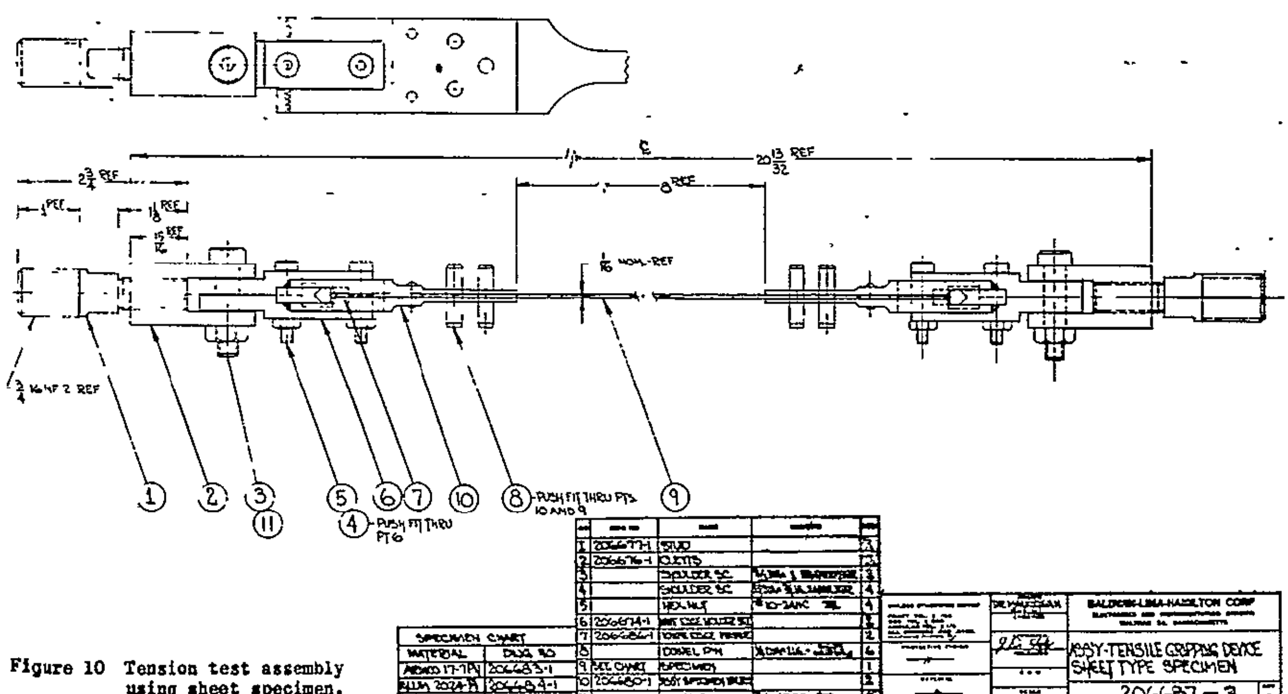

Figure 10 Tension test assembly using sheet specimen.

The specimen is wide enough to permit the use of a Tuckerman strain gage. The specimens and their jigs have been thoroughly evaluated.

The evaluation was begun with the channel specimen by clamping it at one end in two mutually perpendicular directions for two different tests as a cantilever beam. The strain on the flange of the beam was over one thousand microstrains while the indicated strain on the gaging area was less than eight microstrains in all cases. This is considerably better than one can do with loading devices intended to eliminate bending. Figure 8, B-L-H Drawing 206725-3 represents the channel specimen in the compression jig. The specimen is located in the center with the dowels acting as ceramic heat barriers. These have caps which are cemented to them, and are not numbered, but are shown with an arrow. Joints 4 and 5 on the assembly drawing are ball and socket joints. The system is rigid from the socket to the upper cross head shown on the left hand end of Drawing 206725-3, and from the ball to the bottom of the pedestal which is free to be placed in any position on the lower cross head. It is so arranged that the upper section of the jig is installed before positioning the lower pedestal, thereby aligning everything properly. Thus, the jig consists of two rigid halves. The ceramic pieces have been checked for maximum load capacity which was found to be about 12,000 pounds. Actually, the manufacturer's strength value on the ceramic pieces is very high. To make sure that the jig was adequate, the system was tested many times with the pedestal in various positions, and the results of these tests were considered very satisfactory.

The effectiveness of the thermal barriers on the compression specimen was checked since their function was to prevent a large heat sink at the end of the specimen rather than to protect other components. The specimens in both tension and compression on the channel jigs are provided with end heating elements which slide over the specimens. We use an oven with three-zone control and controls on each end heating element. With these controls at 1000°F, we can maintain temperature at the center of the specimen within about 4° of the ends. Figure 9, B-L-H Drawing 206707-4, shows the channel specimen in the tension jig and utilizes identical end arrangements with the specimen located in the center. The end heaters are shown dotted. At each end there is a ball and socket which is shown between the numbers 4 and 5 on the drawing, and in our particular setup, the bolt number 6 is also in a ball and socket on the testing machine. This bolt goes through the cross head of the testing machine and is secured by a convex washer. The thermal barrier in this case is provided by stainless steel discs indicated by the number 3 on the drawing. About one hundred and fifty of these are required at each end. The interface heat transfer is very low, and provides the desired end result. In the case of our tubular furnace, this extends over the piece indicated by the number 4 on the drawing. This arrangement does not prevent piece number 4 from increasing in temperature, but it does provide the desired isolation of the specimen. As stated before, the temperature is controlled within 4°F or 5°F over the entire specimen gage length at 1000°F.

Figure 10, B-L-H Drawing 206687-3 shows the assembled tension sheet metal specimen. This specimen is designed for testing in a creep chamber rather than in a tubular furnace. The specimen is shown on edge in the center. The holes in the specimen are drilled with a jig to insure rapid change and maintaining good alignment in the test jig. The knife edge shown near the number 6 and 7 is identical at both ends. These provide a degree of freedom in one direction, while freedom in the other direction is provided by pin number 3 shown on the drawing. The knife edge is a tool bit which has been ground to proper configuration. It is not fastened by welding since it is held in place by the other pieces that make up the assembly number 10. The knife socket that fits on the knife edge is also held by friction, and the other system fits between two sidearms. Two specimens were checked with this jig. One was essentially straight and the other one was offset about one-eighth inch over its entire length. A preload of three hundred pounds was required with the bowed specimen, but the one that was straight required about fifty pounds. Loads above the preloads gave good straightening differentials as well as very accurate strain differentials on both sides of the specimen. The fundamental principal involved in the test is that use is made of a strain measuring device with the specimen. At present, nothing is available which is considered very acceptable for this purpose. The device has been designed for the evaluation of gages, not of specimens. The aircraft industries have specified that true strain is to be measured, presumably by extensometers, and they have given stringent specifications concerning the design of the specimen. The specimen shown here does not match these specifications in length. It would be preferable to have a larger area that we could put gages on. The sheet metal specimen is for creep testing that would be taken off, principally after 600°F. Creep or drift at 1000°F is going to be a more difficult problem and we will probably try to solve it with our extension or universal testing machine and with a channel specimen. Anyone desiring prints of these drawings and details of the parts used in the assemblies may obtain them by writing to:

Baldwin-Lima-Hamilton Corporation
Electronics Division
Waltham 54, Massachusetts

These specimens and testing procedures were brought about largely by NAS 942. One of our serious problems right now with both of these specimens is the lack of an extensometer that is better than a strain gage. Please inform us where we can get one because, at the present time, within the normal ranges of some of these specimen materials, strain gages are far better than any extensometer we can get to compare them to. The Tuckerman is good, as long as you stay within its temperature limitations.

HIGH ACCURACY ASPECTS OF TRANSDUCER DESIGN

Frank F. Hines
B-L-H Corporation

It is well known that a strain gage, bonded to an elastic member and calibrated in terms of force or pressure, can be termed a transducer. To be completely general the strain gage itself is a transducer. However, the term "transducer" is usually reserved for a combination of elements including one or more gages bonded to some kind of a mechanical structure which is used to convert some physical phenomena such as pressure, force, load, torque or displacement into strain of the gage which results in an electrical signal.

This involves two elements in the transducer which can create errors:

a. The mechanical transduction element
b. The strain gage installation

One cannot always separate the effects of the two, but at least one can reasonably describe what is happening with both. The paramount cause of error in this type of transducer is a change in temperature during operation. The effect of temperature change can appear in the zero reading of the instrument, the output of the bridges, or on the stability of the bridge circuits. The zero shift is probably the easiest of these to correct. The difference in the temperature coefficient of the gages that form the bridge circuits often cause serious error. For a half bridge and the full bridge, there is opportunity to obtain compensating effects from the absolute temperature coefficient of the gages because of the inherent nature of the bridge circuit. This is true theoretically, but rarely do two gages on a load or pressure sensing element have exactly the same temperature coefficient. Inevitably, there is some random difference between the two or four gages on an element, and therefore, there is a residual temperature coefficient in the bridge.

The difference in gage behavior can be caused by a number of things such as a random deviation of the gage itself, or a difference in the expansion characteristics of the structure on which the gages are cemented. There can be a curvature effect where some of the gages are applied to surfaces with relatively sharp radii and others are on flat surfaces. There can also be variations in the basic temperature coefficient of the bridge circuit. These are relatively easy to correct for by temperature cycling the transducer to determine the deviation of the zero reading versus the temperature. Knowing this, one can open the bridge circuit and introduce into the appropriate arm another resistor having the known temperature coefficient which will compensate for the residual temperature effect on the bridge. Therefore, by adjusting the bridge, one can achieve a zero temperature coefficient under no load conditions. Theoretically, this can provide a zero temperature coefficient; actually, it is more difficult since one has to repeat the process several times.

Another very important effect of temperature is on the output of a transducer caused by two major effects. First, the mechanical structure of the element is like a spring; the amount of deformation is dependent on the modulus of elasticity of the material. This modulus is not constant with temperature, but will change from one and a half to two percent per 100°F. Second, in addition to this error is the gage factor change with temperature. Some of these errors are compensating, but usually no attempt is made to separate the various effects. The simple way to compensate for such errors is to introduce a temperature-sensing resistor into the input leads of the bridge circuit, thus reducing the actual voltage on the bridge by the same amount that the modulus is decreasing and the output is increasing. If all these parameters are adjusted correctly, the output versus temperature under any given load conditions will be linear. The conventional circuit diagram for load cells using modulus compensation resistors in the circuit is a temperature sensitive voltage attenuator that adjusts the voltage on the load sensing portion of the bridge to compensate for the change in output versus temperature.

Going further into the various effects on the bridge, one finds the problem of creep and hysteresis of gages, or of the metal on which the gages are mounted. Another effect is zero drift which is different from zero temperature coefficient shift. Terminology can confuse these two effects. There is thermo-electric effect which is usually no problem in bonded strain gages because there are two thermocouple junctions on each gage which are opposed and so close together the residual thermo-electric voltage is negligible. Linearity may be considered either an error or a fact, but many transducers can be linearized deliberately, either electrically or mechanically.

Probably the most difficult thermal effect to correct for is an unequal distribution of temperature throughout the physical structure of the transducer. To be completely honest, I do not know how to correct for this because it is unpredictable. It is difficult to place gages to compensate for random temperature gradients within the transducer. The best advice for these conditions, is to insulate the transducer and they do not experience transient temperatures or gradients. When worse comes to worse, however, one can compensate each and every individual strain gage in the bridge in a normal temperature compensation. This will do much for elimination of effect of uneven temperature distribution within a transducer but it will not correct it all.

Another problem that will arise for missile people is that they are going to have to decide which is to be measured, weight or force. It so happens that most of the standard units at the present time are based on the gravitational constant of Washington, D.C. and the particular calibrated masses in Washington. If one takes those same weights to another part of the country, one no longer has the same force. In other words, the accuracy of many load transducers is such that one can see the difference in the gravitational constants over the various areas of the country. What one does about this is a matter of definition. What gets the missile off the ground is the excess of thrust over weight at that particular location.

Question: What order of magnitude is this gravitational change?

Answer: It amounts to a fraction of a hundredth of a percent or a couple of hundredths of a percent. Between Waltham, Massachusetts and Washington, D.C., it amounts to 4 pounds in 10,000. For a 10,000 pound weight calibrated in Washington, four more pounds must be added to the weight to make it correct.

Question: Is this effected by latitude or longitude?

Answer: Latitude, I believe. As a matter of fact, it is difficult to find the real standard number for the gravitational constant, or anyplace where the gravitational constant fits the standard figure.

SPECIAL PURPOSE TRANSDUCERS

Keith McFarland
Ames Research Center

The Ames Research Center is a complex of some six major wind tunnel systems plus a relatively large number of smaller wind tunnels and special research facilities. These research facilities include such things as a high velocity ballistic range, supersonic preflight tunnels, atmosphere entry simulators, a low density and heat transfer facilities, iron beam apparatus, flight simulators, etc. The primary function of the Ames Research Center has been research in the field of high speed flight, and with the advent of the NASA, we are working more in the field of space research in support of space projects. We are continuing work in high speed supersonic flight and at the present time have a very important mission in VTOL and STOL aircraft, which is an important field.

In support of these particular programs and these facilities, the Facilities Instrumentation Research Branch is required to provide a wide variety of mechanical, electrical, and optical measuring systems and transducers. A relatively large portion of these transducers utilize resistance strain gages. There are a number of reasons for this. First, is the basic advantages of the resistance strain gage, and second, is the availability of a wide variety of excellent strain gage instrumentation. A third reason is that Ames has been fortunate enough to assemble a small but highly skilled group of strain gage technicians.

Assuming that a strain gage transducer is the most economical way to make a large number of our measurements, one might ask why commercial transducers are not always used. Of course, this is the best solution to many of the problems, and this is what is done except for the conditions requiring special purpose transducers. These may involve a peculiar configuration, special range, special accuracy, or practical consideration of economy and time.

Special configurations may require a transducer on a strut in a model, on the end of a sting, or the transducer may be required in a minimum shape or size to measure more than one parameter. A higher or a lower range transducer than is available commercially may be needed, or it may have to withstand any number of parameters such as extreme temperature, shock, vibrations, or any number of special conditions which a standard commercial transducer is not specifically designed to withstand. In the case of accuracy, there are now available some very high accuracy transducers on the market, but there are certain conditions where high accuracy is required in a particular range where one might need to build his own transducer. In the case of economy, there are situations that would justify the use of special purpose transducers, although commercial transducers usually cost less than a specially built transducer. Changes in test schedules can require transducers on short notice which means fabrication at the test facility.

There is an almost unlimited variety of shapes and types of strain elements that can be used in meeting various specifications. These include bending beams, columns, rings, diaphragms and torque bars. There is seldom only a single design that would satisfy the requirements of any given situation. Here are a few considerations that might help in the development of a transducer for a given set of conditions. First, the transducer should be made as simple and rugged as possible, since in most cases, minimum deflection is desirable. Try to avoid all pins and screw joints in the actual body of the transducer. The figures show that most of the Ames' transducers are machined from one piece, which has not been found uneconomical. A second item concerns the actual beam stiffness. The beam element, particularly in bending, should be made as stiff as possible so that the strain gages carry a negligible portion of the load. For high accuracy transducers, we try to design for modest strain levels, primarily in the range of 500 microstrain. Another consideration is to design with thermal problems in mind, particularly thermal gradients. The gage placement should minimize these effects during operation of the transducer. The same thing is true of loads. A transducer to measure normal force should ignore lateral and torsion forces. To do this, it is best to design the mechanical system of the transducer so that this force does not effect the strain element. Often gages can be arranged to cancel out unwanted stresses, but it is better to design the mechanical system so they are eliminated. Using these various design considerations, we have made many transducers at Ames.

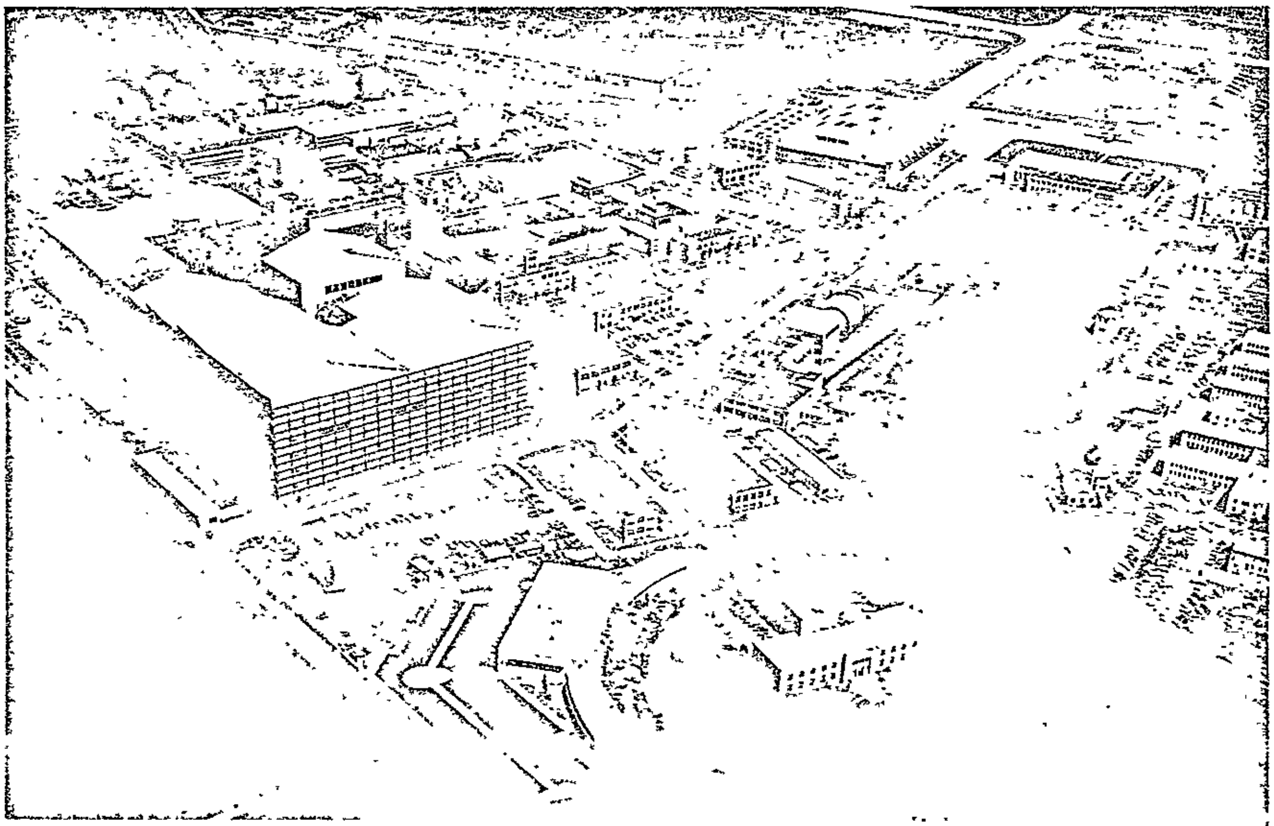
A-27777-7 NATIONAL AERONAUTICS AND SPACE ADMINISTRATION AMES RESEARCH CENTER, MOFFETT FIELD CALIFORNIA

Figure 1. Ames Research Center of National Aeronautics and Space Administration, Moffett Field, California.

Figure 1 is a view of Ames-Research Center. The big building at the left of the picture is the 40' x 80' Wind Tunnel where we are doing a relatively large amount of strain gage work in connection with VTOL testing. The complex immediately above the 40' x 80' Wind Tunnel is the Unitary Wind Tunnel composed of three major transonic-superxonic tunnels operating on the same power system. At the extreme upper left are vacuum spheres for the three and one-half foot facility which has capabilities of mach 10 to 15 in the high temperature range.

Figure 2 is a transducer milled from a rectangular block of 17-4PH steel to obtain the desired beam shape. The block is slotted to form a shear beam or a double cantilever with no moment across the center of the beam length. An advantage of this design, beside simplicity, is its lack of sensitivity to bending moments. This transducer also has flexures on it to make it even less affected by moments. The thermal gradients through the transducer are such that their effect on the gages is minimized. The deflection is very low, the deflectionbeing less than a thousandth of an inch for the gage beam length of one inch. This particular unit has been equipped with stops so that when overloaded in tension or compression it becomes a rigid structure. Consequently, this type of transducer can carry loads almost 100 times the rated capacity without damage.

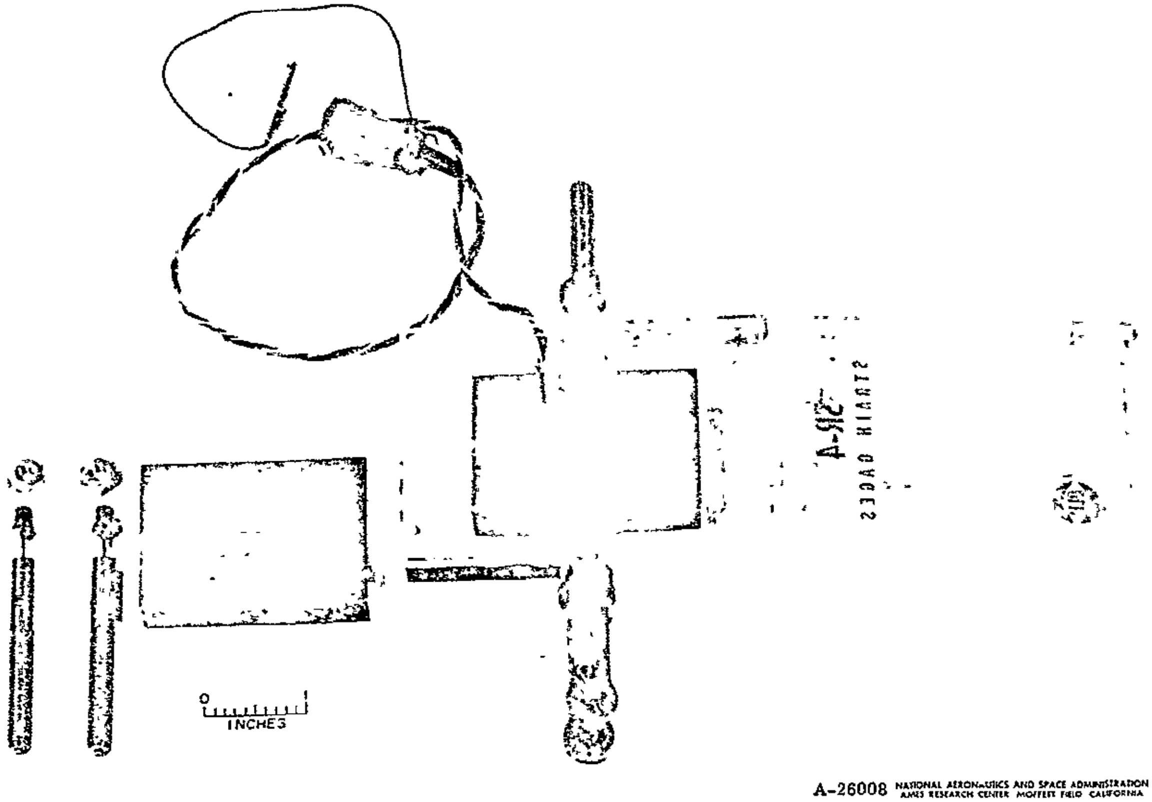

Figure 2. High Accuracy 27 lb. Force Transducer (tension)

The transducer of Figure 2 was designed for twenty-seven pounds full scale, with a tare load of nine pounds and operates with an accuracy of approximately one-tenth percent at room temperature. This type has been built in enough quantity to obtain statistical data concerning the performance. Twelve were made of 17-4 PH steel of which six were instrumented with ABF-11 gages, which are bakelite fine wire flat grid gages, and six had foil gages on them. All installations were satisfactory, but the ABF-11 gages were significantly better in terms of hysteresis and linearity. This unit is used in electronic computing of the platform forces in the 40' x 80' Wind Tunnel.

Figure 3 shows a similar type transducer for moment-balancing compressor blades for one of our wind tunnels. Figures 4, 5 and 6 show transducers that were developed for a special purpose and to fit a particular configuration. The 40' x 80' Wind Tunnel is now being used for vertical takeoff and landing studies, but the massive floating frame platform has too low a frequency to respond to dynamic changes in lift and other parameters. It was desirable to have a multiple component force unit to fit on the end of the existing strut system and mount on the models under test.

Figure 4 shows a transducer designed for 3000 pounds normal and 2250 pounds axial force. The normal force produces a double bending in the two outboard flexures, while the axial force transmits a tension and compression through the outboard flexures and produces bending on the inboard flexures. All forces are measured in bending, and the resolution between the applied loads is very good; i.e., when a normal force is applied, there are negligible effects on the chord force.

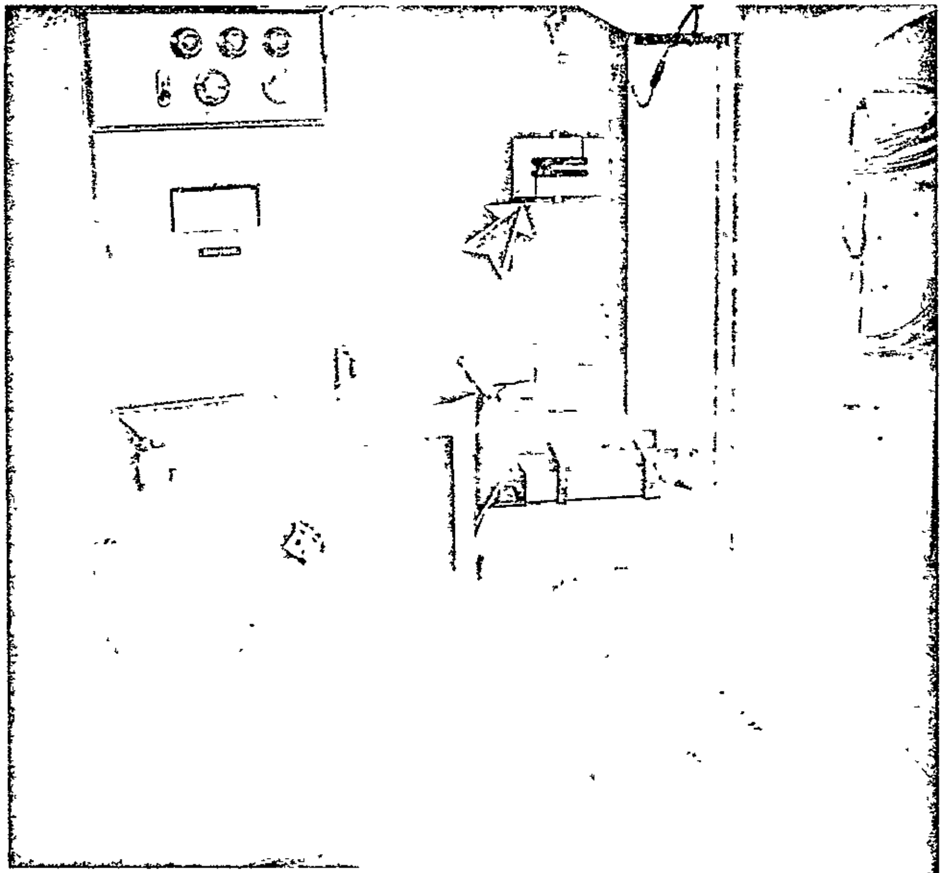

A-26021 NATIONAL AERONAUTICS AND SPACE ADMINISTRATION AMES RESEARCH CENTER, MOFFETT FIELD, CALIFORNIA

Figure 3. 100 lb. Precision Load Transducer

Figure 4. Two-Component Force Transducer
3,000 lbs. Normal
2,250 lbs. Axial

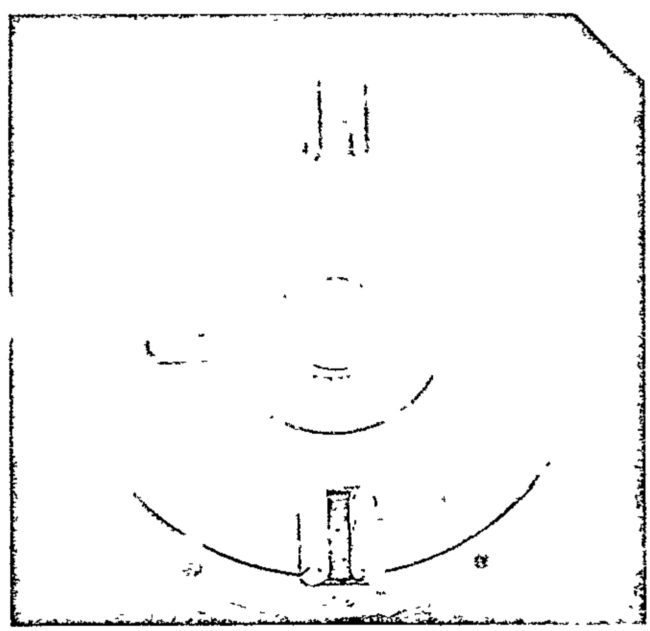

A-26007 NATIONAL AERONAUTICS AND SPACE ADMINISTRATION AMES RESEARCH CENTER, MOFFETT FIELD, CALIFORNIA

Figure 5. Two-Component Force Transducer;
8,000 lbs. Normal, 7,000 lbs. Axial

Figure 5 shows an 8,000 pound unit which could not use the bending beams. Because of space limitations, two columns were used. Although the inter-action error was relatively high to begin with, a very small change in angular position of the gage reduced it to one percent.

Figure 6 is a 15,000 pound load cell of a different design. Each time the load increased substantially, we ran into different problems which necessitated new designs. We tried to go back to the first two component unit of Figure 4 and use tension-compression beams in place of bending flexures. Deflection was excessive and the design of Figure 6 was evolved as the solution.

Figure 7 is an entirely different type of transducer. In our ballistic facilities, and we have quite a few of them, we use strain gage devices to measure the ballistic pressures which vary from 10,000 psi up to 400,000 psi. A piston with a strain gage wound around it is clamped into the ballistic barrel. The pressure is sealed with a neoprene "O" ring which withstands the very high temperatures and high pressures that act over a very short period of time. The piston diameter is about an eighth of an inch for the standard unit. Unit A of Figure 8 is a 100,000 psi unit; and the one on the right is a two step measuring device which is a bending beam for measuring low pressures plus a column.

Figure 9 shows some older type pressure transducers. These units are flush diaphragm pressure cells, and the ones in the center are about 0.2 of an inch inside diameter. We used ABF-11 gages for a while, and then wound our own spiral gages, flattened the wire and mounted them. At present we are using Baldwin spiral gages one-eighth inch in diameter.

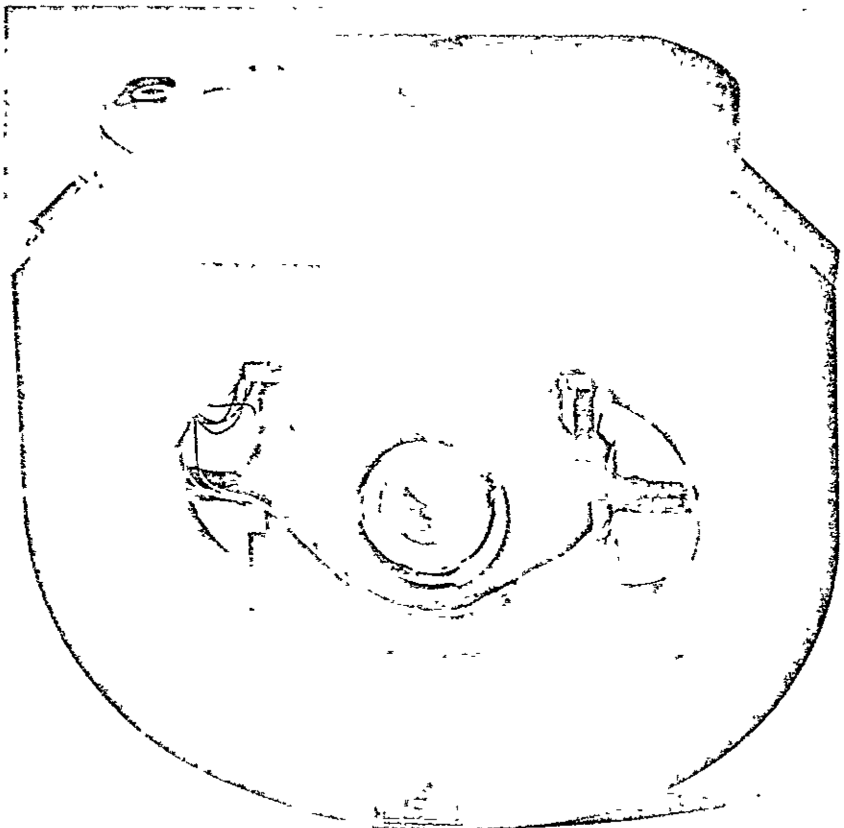

A-27779 NATIONAL AERONAUTICS AND SPACE ADMINISTRATION AMES RESEARCH CENTER, MOFFETT FIELD CALIFORNIA

Figure 6. Two-Component
Force Transducer
15,000 lbs. Normal
12,000 lbs. Axial

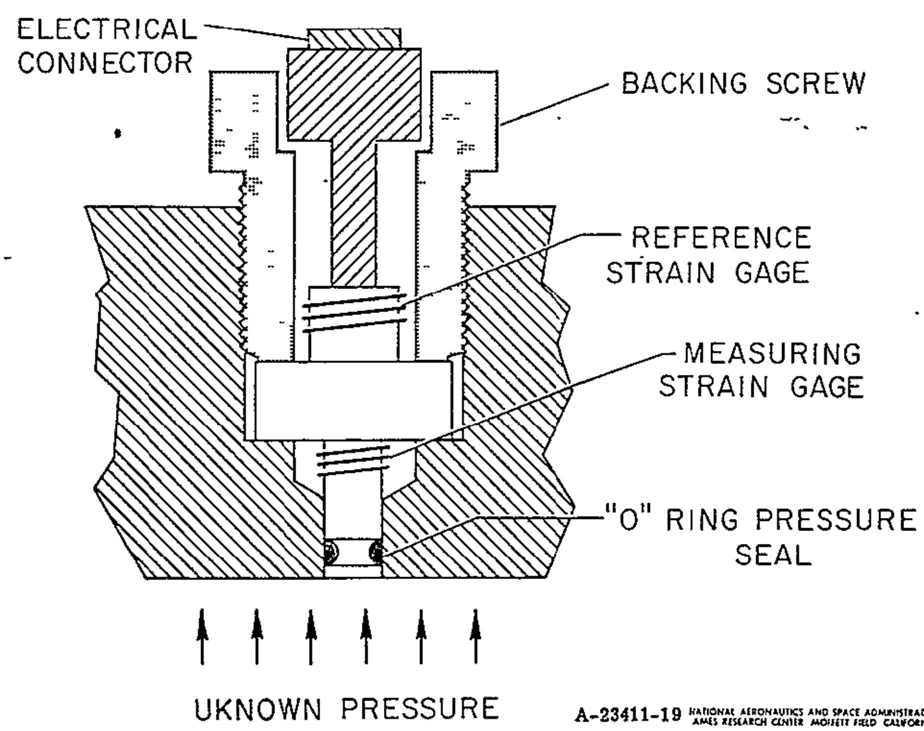

A-23411-19 NATIONAL AERONAUTICS AND SPACE ADMINISTRATION AMES RESEARCH CENTER MOFFETT FIELD CALIFORNIA

Figure 7. Ames piston type pressure cell (schematic)

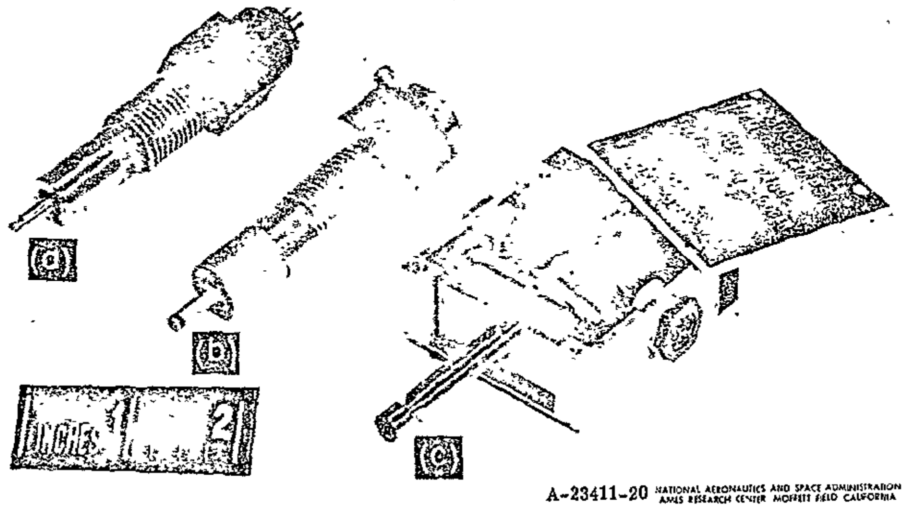

Figure 8. Ames piston type pressure cells.

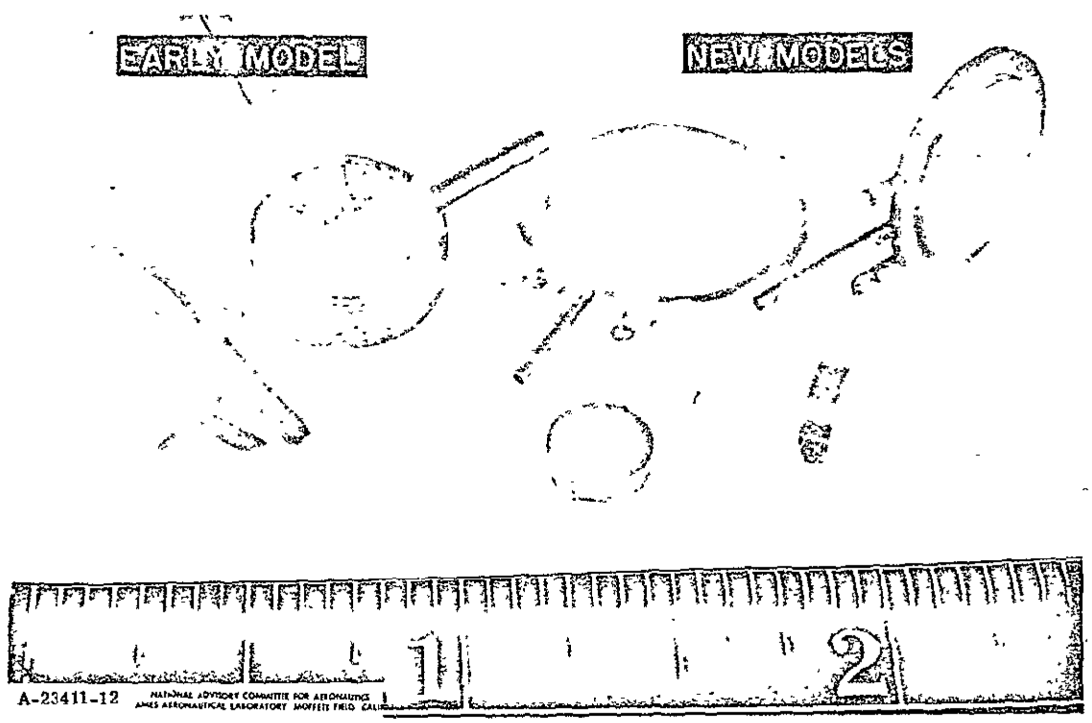

Figure 9. Diaphragm mounted strain gage pressure cells for dynamic measurement.

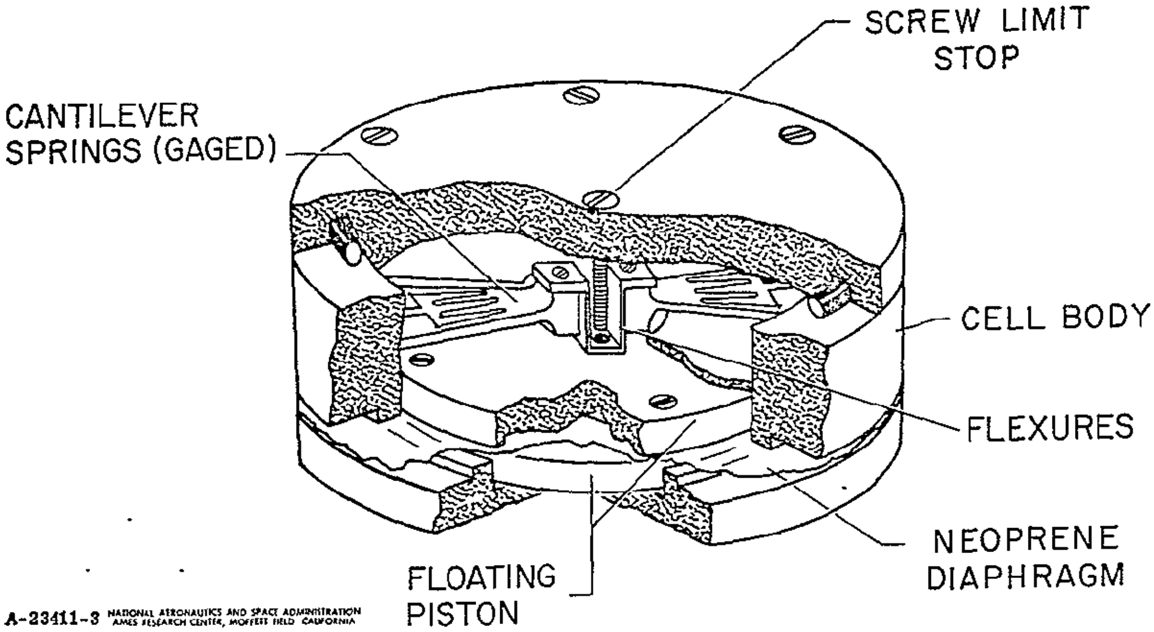

Figure 10. Ames Precision Strain Gage Differential Pressure Transducer.

Another type of pressure device, shown in Figure 10, which has turned out to be quite successful is the pressure transducer used to replace our liquid monometer. The strain gages are cemented to a cantilever beam passing over to a small flexure attached to a floating piston which is sealed from the differential pressures by a neoprene diaphragm. The total diaphragm area is a small angular ring which takes up very little of the pressure and produces negligible hysteresis and other bad effects. This is used for relatively low pressure, that is, about 4 psi. We have made some 1 psi and many 15 psi transducers. Figure 11 shows the actual cell body. The large size contracts with the small flush mounted diaphragm cell and, of course, there is a tremendous difference in their accuracy.

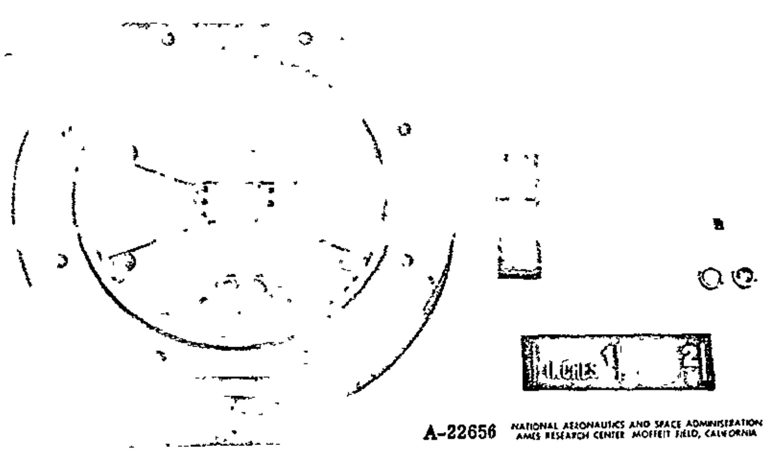

Figure 11. Ames Pressure Cell Bodies

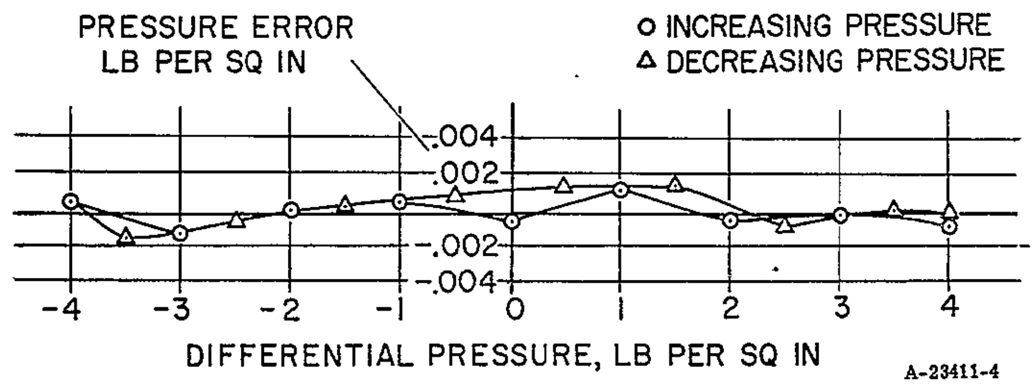

Figure 12. Calibration Curve for typical Ames Precision Differential Pressure Cell.

No presentation is complete unless one can show a curve as in Figure 12 and prove that his transducers are better than any available elsewhere. There is about .05 percent overall scatter of these data and have an overall accuracy of 0.1 percent when housed in temperature controlled cabinets.

Figure 13 shows a fail-safe stick force transducer for measuring pilot control forces.

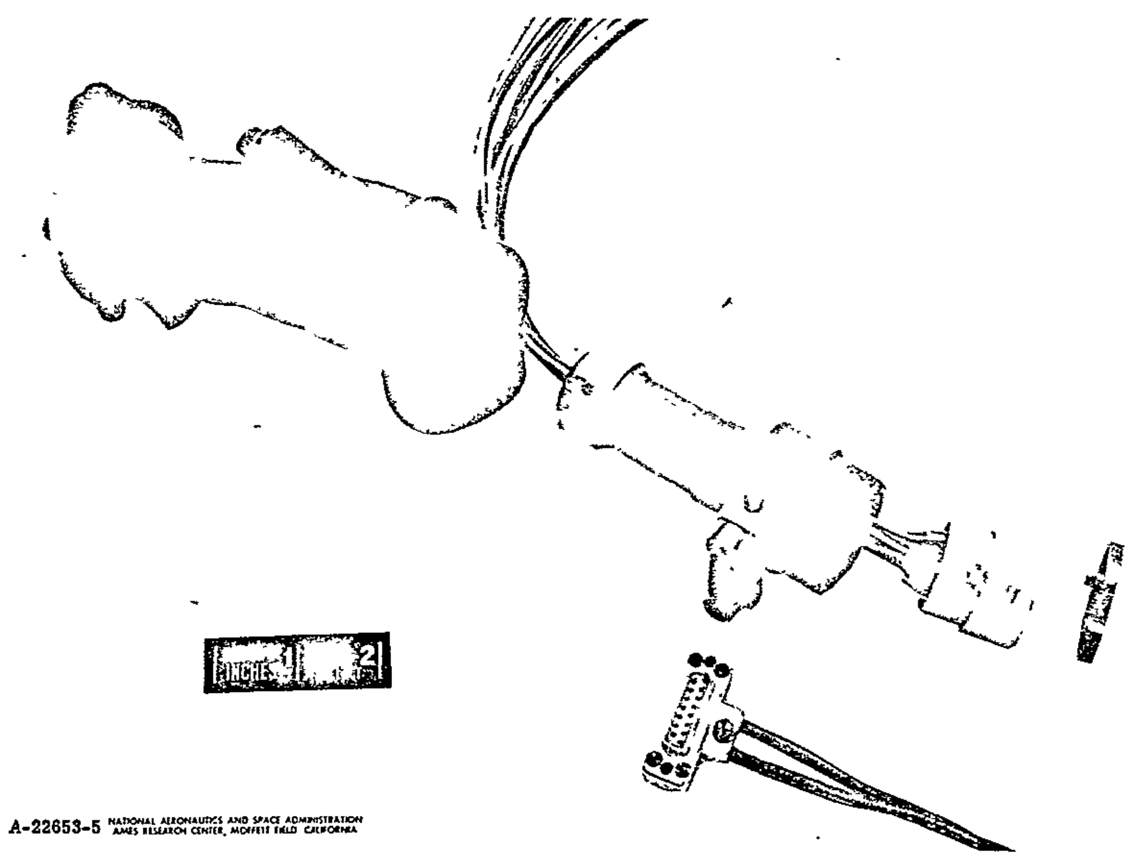

Figure 13. Two Component Aircraft Control Stick Transducer.

UNIQUE STRAIN GAGE INSTRUMENTATION
IN BOEING WIND TUNNELS

Truman R. Curry
Boeing Airplane Company

At this time the Boeing Company has in use approximately 90 internal sting balances. A three-page tabulation in Appendix B shows most of them and the facilities for which they were designed. Each page of the tabulation contains balances associated with a specific type of vehicle. There is considerable variation in appearance for we have no philosophy tending to standardize configuration; instead, we try to select the measuring technique that is most suitable to the situation.

The Boeing Wind Tunnel Laboratory Unit consists of five major wind tunnels in addition to two pilot tunnels, two shock tunnels, one hypersonic aeroballistic range. In addition, we conduct force tests in out-of-town facilities, and keep approximately a dozen facilities occupied with our force tests.

We are now working on our six hundredth model in the last 16 years. Consequently, we use our balances for more than just the models for which they were designed. Most of our balances are designed for a specific model and tailored to a specific Boeing facility. Design criteria differ for balances used in different facilities. For example, in our transonic tunnel, temperature is one of the most significant quantities which must be considered in design. Our supersonic tunnel, which is a blowdown tunnel, requires a design

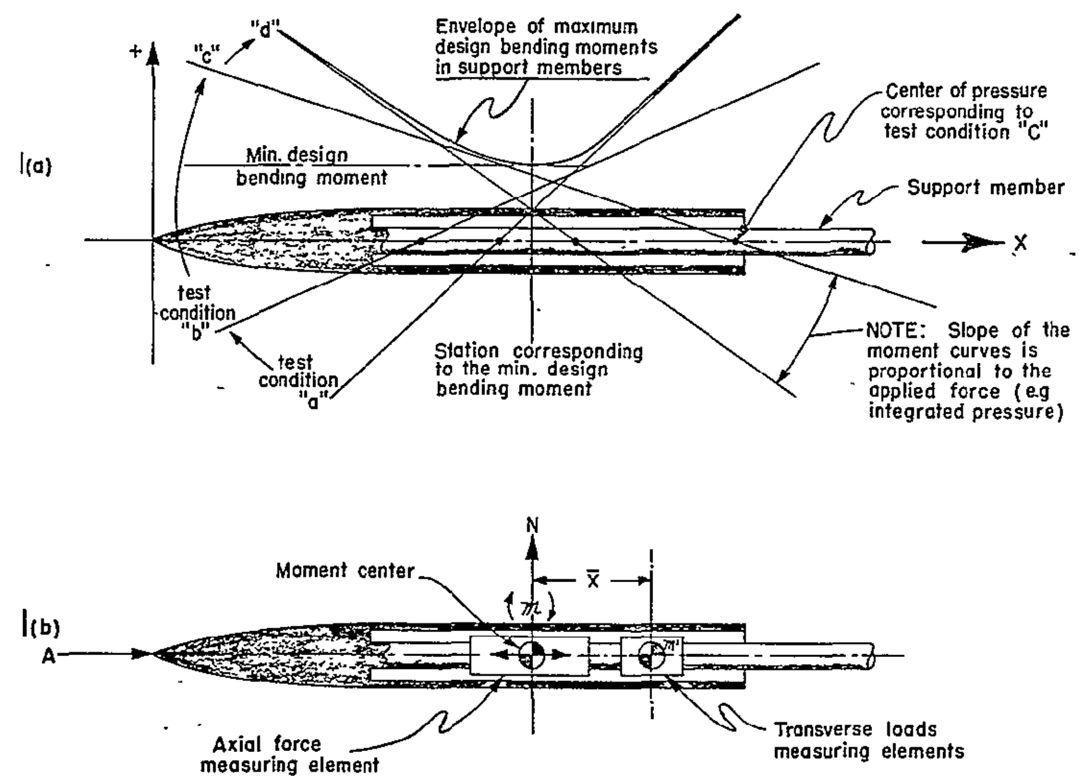

Figure 1. Typical internal force balance installation and external loads.

with factors of safety which consider starting and shock loads. In our hypersonic tunnel we must watercool the balances, and in hot-shot testing, frequency response is of prime importance. Our balance designs comply with test requirements, and reflect the facilities at our disposal for design, fabrication, gaging and calibration data reduction.

Boeing places considerable emphasis on wind tunnel testing, and gives priority usage of computers to aid in selection of configurations for balances, in doing stress analysis on the selected configurations, and in reducing calibration data. We have two electric discharge milling machines: a Japax, which is a Japanese machine, and a Swiss copy of this Japanese machine called an Eleroda. These machines give more freedom in design than conventional milling machines, allowing best usage of the space available.

Great emphasis is placed on reliability in design and development of our balances, since this is more important than accuracy, which seems to have been realized. A greater effort is made to minimize random and unpredictable errors rather than predictable errors, such as interactions, because we have facilities for handling them. Extra compensation equipment is minimized that would be associated directly with the models, balances and readout systems. To simplify test installations, mathematical compensation is relied upon heavily.

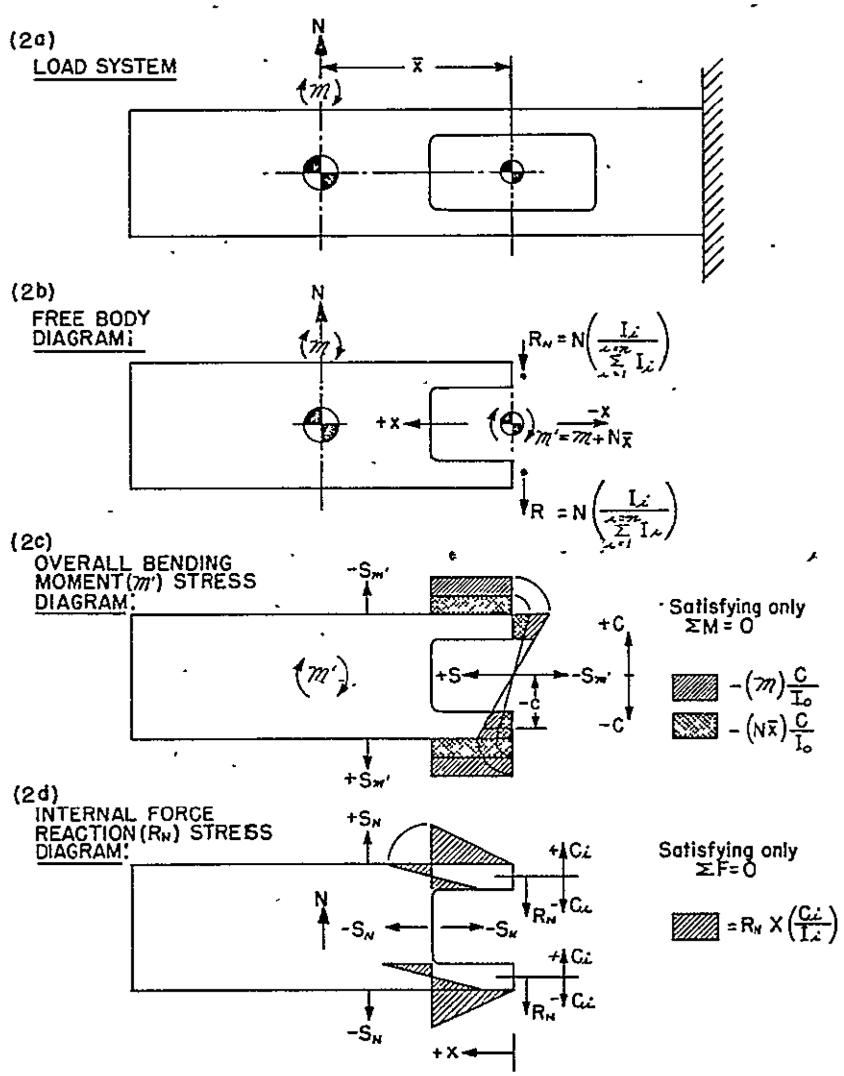

Figure 2. Load, reaction and stress diagrams.

The first topic that I will discuss relative to specific designs is the technique we call "stress-cancellation moment transfer". Because of space limitations in these balances, the axial force element is the weakest section in bending. Figure 1 represents a model supported by a sting showing the moment diagrams of the support member for various critical test conditions. If one draws an envelope of maximum design bending moments on the sting, this locates the position of minimum design bending moments; therefore, the axial force measuring element being weakest to moments is placed there. The transverse load measuring elements must thus be located remotely from the point where we want to reduce data. In the past, moment data has been electrically transferred with an analog device or mathematically in data reduction to the point where we want to reduce data. The subject of this mechanical stress cancellation technique takes advantage of two different sources of stress due to normal force, applied at the desired moment center, that tend to cancel each other in the structure. We place the moment gages at a point of zero stress due to normal force on the structure. Therefore, they are out of the influence of the normal force irrespective of its magnitude.

Figure 2 shows the development of the princeples that have been mentioned. Figure 2a is a diagram showing a simple two-legged device with forces and moment applied at the moment center which is remote from the center of the cage. Figure 2b is a free body diagram of the split cage. External loads are balanced by the vertical reactions and internal moments. Figure 2c is the stress diagram due to the bending moment about the center of the cage. The heavily shaded portion is that part of the moment which is due to normal force times transfer distance. The lesser shaded area is that portion of the moment which is caused by pitching moment. Figure 2d is a stress diagram due to the vertical shear (normal force) only.

Figure 3 superimposes the stress due to the vertical shear caused by normal force on top of the bending stress due to normal force times transfer distance. The upper surface of the top beam (AA) has a point (X_m) where there is zero stress due to normal force. On the under surface of the beam the point of zero stress is behind the center of the cage. Either of these two points would be satisfactory for locating pitching moment gages.

Figure 4 shows a small stress cancellation moment transfer type balance designed for three component testing of "Dynasoar" in our eight inch Hotshot tunnel where the importance of natural frequency was stressed. We achieved 250 cycles per second in the pitch plane and 1000 cycles per second in the axial force direction. The front end of this balance is made out of hardcoated aluminum, which is an electro-chemical process that deposits alumina on the surface about 3 thousandths of an inch thick.

The large balance of Figure 5 was designed for boost glide testing, and is a six-component balance. The left end of this balance is the moment cage which is completely formed by conventional milling techniques. The design of this five-component cage is similar in complexity to a seven-component cage since it is designed for stress cancellation moment transfer. Stress levels must be controlled

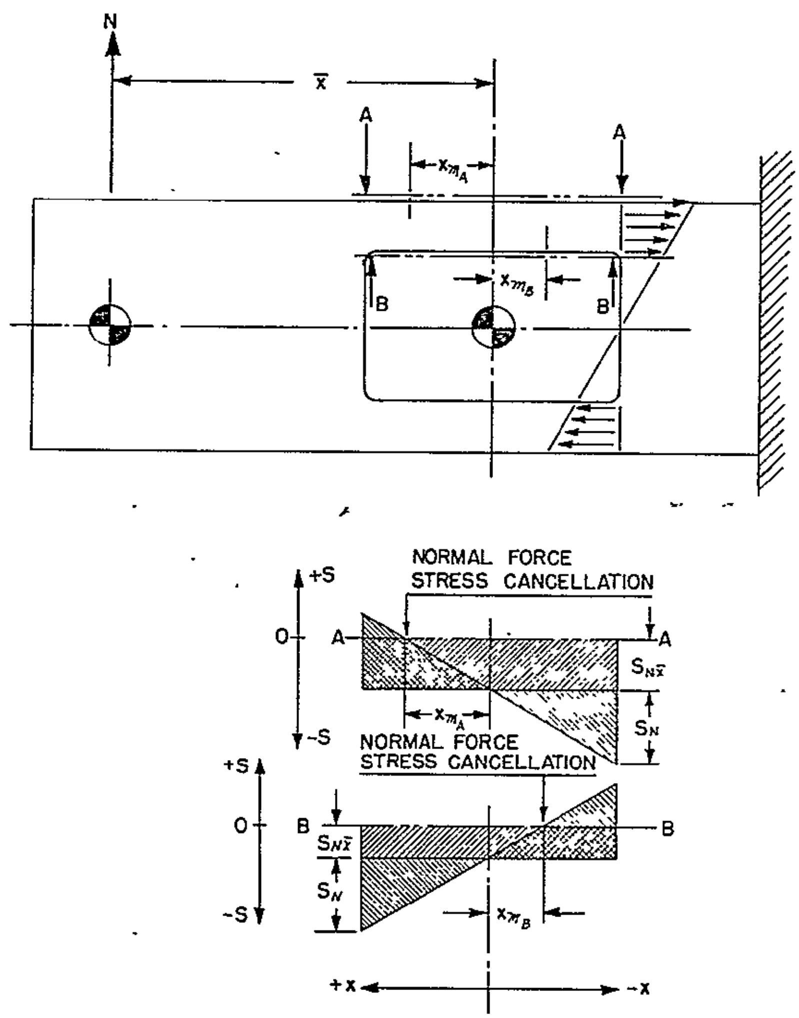

Figure 3. Normal force, stress cancellation.

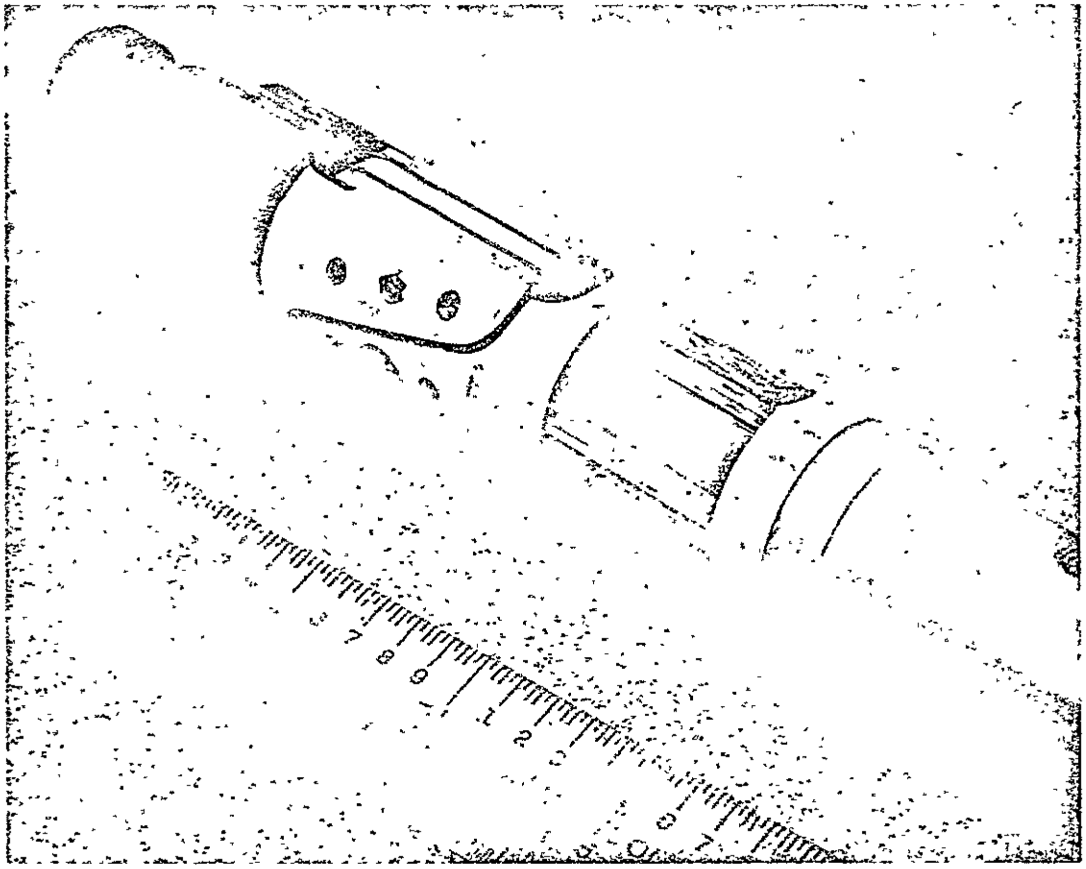

Figure 4. Balance Number 3124-A

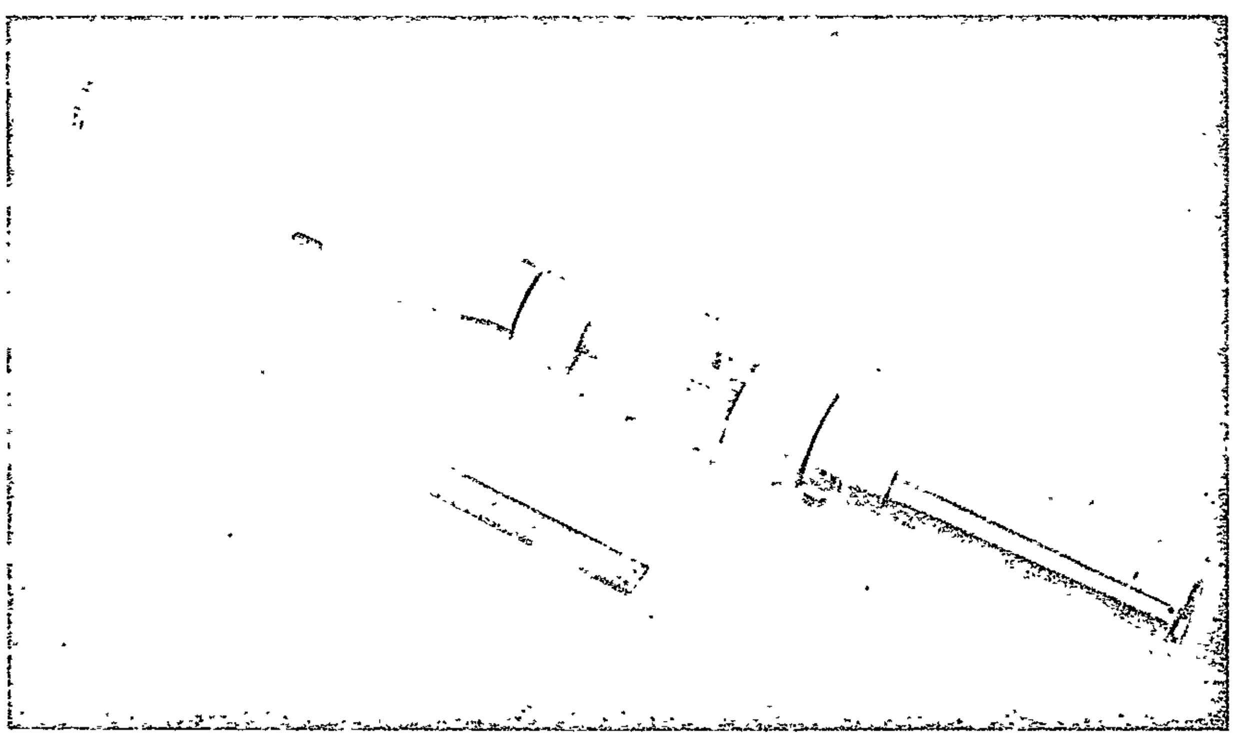

Figure 5. Balance Number 6132

for normal force vertical shear reactions, as well as for normal force times transfer distance; also for vertical shear due to side force, and the overall bending moment of the side force times the transfer distance. To satisfy the requirements for a good working balance with suitable factors of safety and adequate measured stress under these conditions is very difficult. Included in Supplement 2 of Appendix B are the development of mathematics and derivations for a five-component moment transfer cage. The asterisked equations have been programmed for digital computing to aid in configuration selection, which is done on an iterative basis.

A general mathematical statement is given in Supplement 3 of Appendix B for the stress analysis of a parallel member prismatic beam after the configuration has been selected. The first part contains the derivation of expressions for internal reactions in terms of geometric configuration and external loads. The next section in the analysis is the tabulation of these internal reactions. The three internal forces and three internal moments acting on each member are determined, followed by the computation of overall safety stresses which are the combined stresses; i.e., combined effective tensile and combined effective shear. Equations are written in terms of such things as the moment of inertia, and area. Written sub-routines are included for computing various inputs to the program for different cross-sectional shapes. These sub-routines aid in a stress analysis, since one merely has to indicate the beam geometry by indicating the configuration number with dimensions of the members. This program has been worked out for rectangles, octagons, vertical I-beams, horizontal I-beams, vertical "T's" and horizontal "T's".

The design of a balance for a Hotshot facility is quite simple since loads are low for a given size model and compact assembly is not mandatory. In addition, temperature is a minor problem because thermal inertia of the model prevents the balance from changing temperature during the "blow", which lasts about a 25th of a second. However, high frequency response is extremely important. We do not use inertia compensation but design our balances to such high natural frequencies that inertial response frequencies are separated from the frequency components of the aerodynamic forcing function by as much as possible. The inertial frequencies are then filtered out with electronic filters.

Figure 6. Balance Number 6143 assembly.

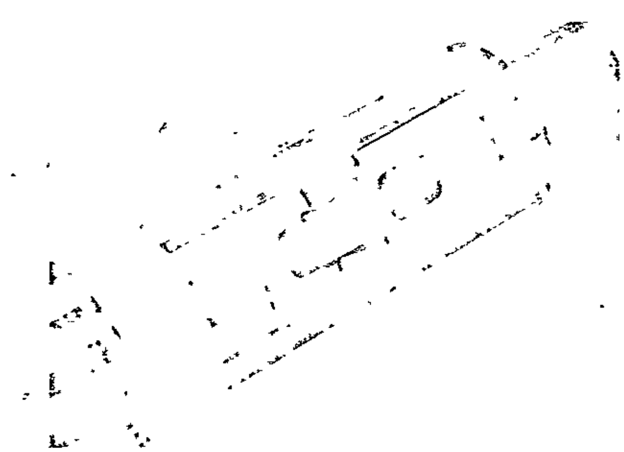

Figure 7. Balance Number 6143 closeup.

Figures 6 and 7 depict a balance configuration for the Hotshot facility in which the measuring elements are as "stiff" as possible to the quantity which they are measuring and limber to other components not being measured by them. Thus, a great percentage of the total load is carried by members which are designed with large sections which contributes to their high natural frequency. The outer flexures (normal force) are cut out at the center to make them very limber to pitching moment and drag. The center element is very stiff to pitching moment and drag and very limber to lift because of small flexures that have been cut in its ends.

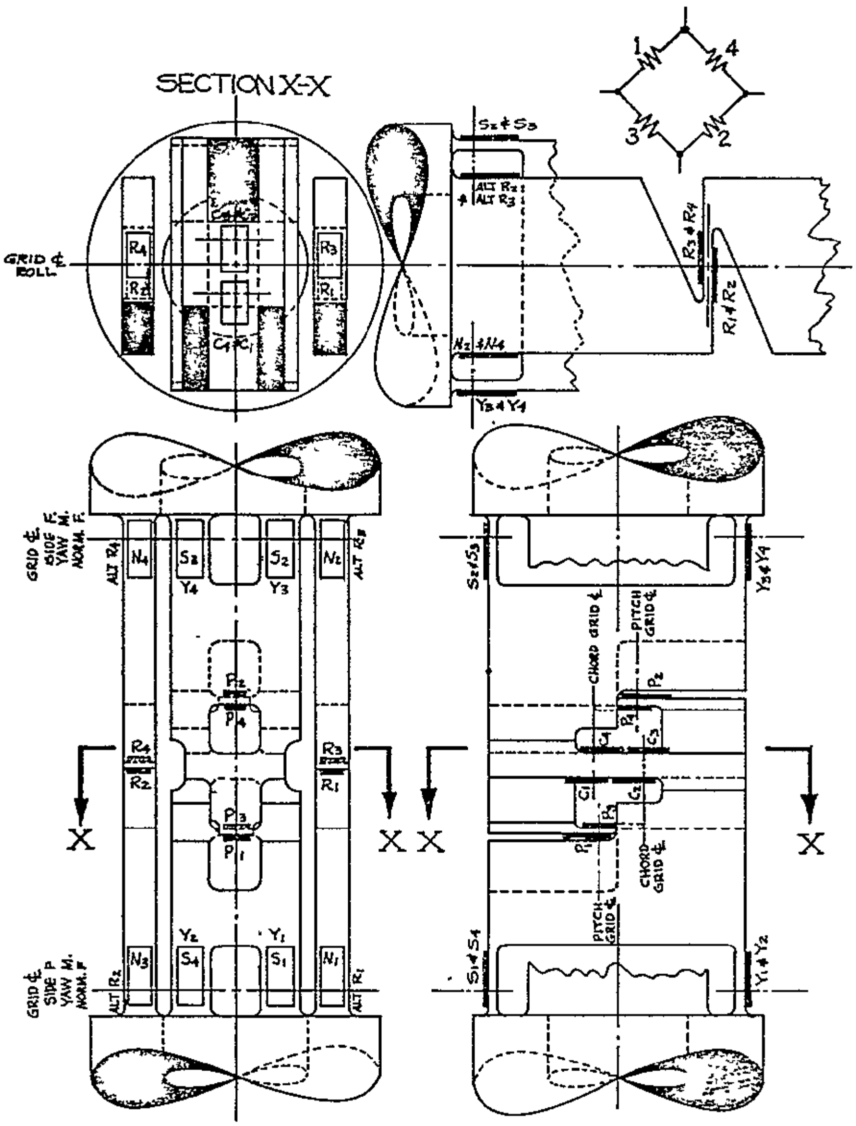

Figure 8. Balance number 6143, design wiring and gaging diagram.

Figure 8 is a diagram of the balance shown in Figures 6 and 7 showing the placement of the gages for six-components measurements.

Force measurement at Boeing has shown that high temperature gages have not acheived the degree of reliability and accuracy required for making force measurements in our wind tunnel. In the past we have built water-cooled balances by making water jackets which are essentially in series with the balance and the model using flexible jumper tubes to supply the water.

The balance shown in Figure 9 is a one-piece balance utilizing drilling and boring to form tubes and reservoirs for water within the one-piece balance structure. The water goes through the inlet tube on the right end of the balance, branches out through a "Y" and goes down through the two side members. The lower left section shows the hollow beams for the tubes. Water enters the reservoir, reverses back through the reservoir, up through the top and bottom beams, back through the drag section, down through a "Y", and into the aft reservoir which empties via the outlet tube. We have been building balances like this for about a year. This particular balance was designed for missile tests in a hypersonic tunnel.

One of the smallest balances we have ever built is shown in Figure 10. It is a five-component balance and could not have been six because we were unable to find or make room for more gages. This balance is 0.40 inches in diameter. It measures 0.40 of a pound of drag, and three pounds of lift. It was designed for Dynasoar testing, and it is water-cooled very similarly to the diagram of Figure 9.

Calibrations are performed manually because of the flexibility required to calibrate a wide variety of balances. The calibrator's ingenuity is relied upon to make his own setups for the particular balance since the calibration equipment is easily modified. However, load application accuracy is controlled within 0.10 percent. Every component is assumed to have twenty-seven possible interaction terms. Our calibration procedure determines the presence and magnitude of the coefficients that go with all twenty-seven of these terms. Data

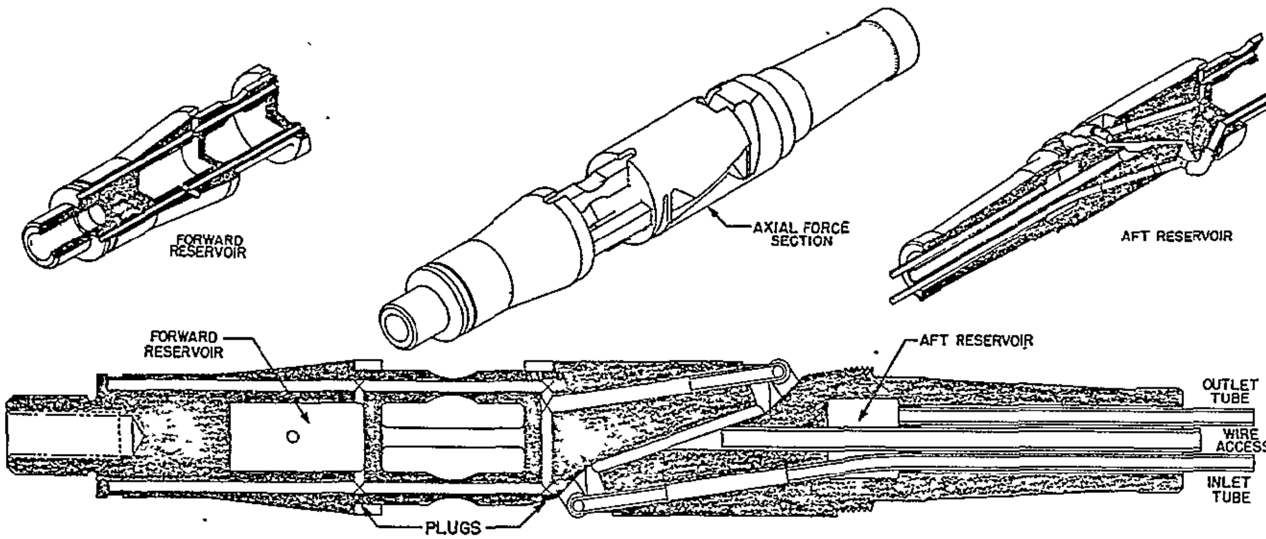

Figure 9. Plumbing for balance number 6148-W

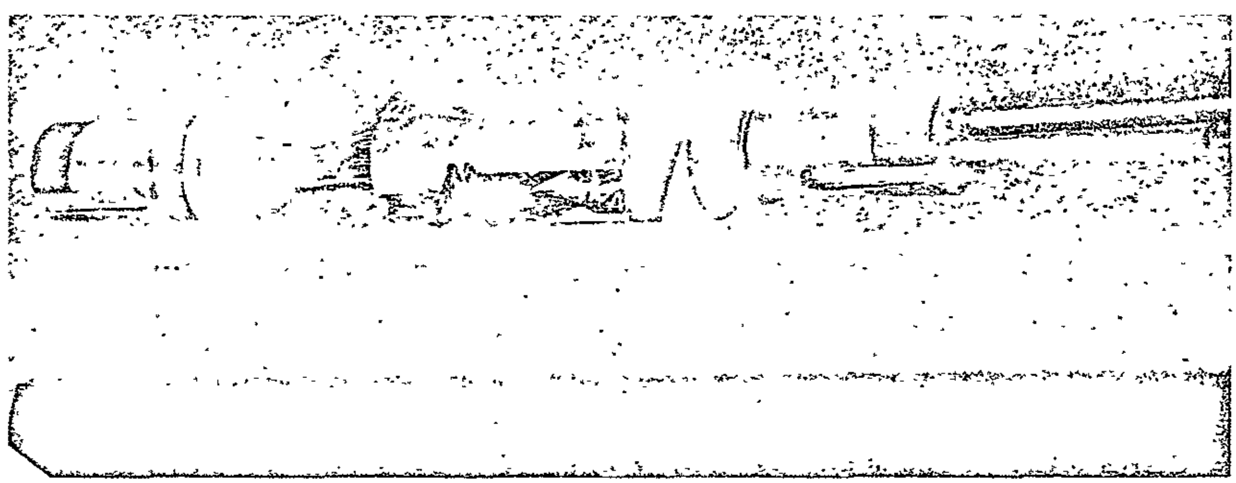

Figure 10. Balance number 5158-W

is reduced by digital computers and monitored by a complex system that assists in evaluating the quality of the balance and the data.

Question: What quantity of water is required to cool the balance and will variation in water pressure affect the gage response or the balance itself?

Answer: For a balance of this size, (Figure 9 or 10) repeatability is about 5 percent. This is a very small balance, only four inches long, and is made of aluminum, hard coated on the ends. Water pressure is regulated at 50 psi.

Sometimes the water pressure can be shut off while gathering data if it is turned on immediately after the data is taken. On this small balance, one pint of water per minute will affectively cool the unit. There are reservoirs in the model support and sting support.

Question: Is the difficulty largely the determination of the gage location or its placement?

Answer: No, the problems are:

1. to determine the exact center of the gage.
2. to place the gage where it is supposed to be.

Question: What temperatures are you isolating the balances from?

Answer: We are testing in wind-tunnels at temperatures between 1000°F and 2000°F.

WIND TUNNEL STING BALANCES

Richard R. Tracy
The Task Corporation

The term "balance" warrants an explanation since it is obtained from the earliest use of force measuring devices in wind tunnels which were balances. Dead weight was either hung from pans or moved on beams to counteract applied aerodynamic forces. The original devices were called external balances and are still used to some extent in numerous facilities with high accuracy where there is no space restriction. However, other limitations led to the development of "sting balance". This was made possible by use of resistance wire strain gages which allowed a localized strain measurement.

The first sting balances were essentially beams milled to provide a surface for strain gages and were fairly crude in a modern sense. A later development, brought about by reduction of the strain gage size, is the floating frame internal balance which is philosophically similar to the external balance except it is turned inside out. Instead of supporting the model with external stress members attached to force transducers; the model is supported by internal stress which carries force transducers attached to an interior structural member.

It is worthwhile to delineate between the "single piece balance" and the "floating frame balance". The principle of the single piece balance is that a set of applied forces on a cantilever member uniquely determines the state of strain throughout the body of the cantilever member. Of course, it is impossible to measure the state of strain throughout a body which eliminates the possibility of obtaining forces from partial strains. If such a thing were possible, then it could be written in the form of equation (1) in Appendix C. This is an equation for the output of a strain gage or a bridge of strain gages mounted at the unique location on the surface of the body and its output is a linear combination of products from all the applied forces or moments, taking 1, 2, 3, 4, 5 and 6 at a time. This is not the most elaborate equation that could be written for the output of these components, but a mathematician would guess that it is probably adequate. However, it is a difficult equation to use to determine forces from an electrical output. There are six of these equations and each equation has six major terms which are a summation involving about 300,000 coefficients. One could not calibrate such a balance, much less reduce the data involved.

A practical limit is represented by equation (2). This is an equation containing two terms, each of which is a summation of forces taken one or two at a time. This equation is worth mentioning in more detail because it is typical of the actual equation used in reducing wind tunnel balance data. This equation says the output of each element is a sum of six terms, each of which is a constant times a single applied force, plus another sum involving a constant times the product of pairs of forces taken two at a time. It is practically reducible or invertible so you can solve for the applied forces in terms of the electrical output. The first terms in this equation are called linear outputs. They are first order terms, one term being the float coefficient and the remaining term being the first order interaction. The second term involves quadric non-linearities of primary outputs. These are interactions that arise as a result of two forces being applied simultaneously and is based on the single piece balance which has been shown to be very successful. Mr. Tom Curry stated their facility uses this type of balance in various configurations. I think, however, they exhibit some difficulties which led to consideration of a different type of balance. One of the difficulties mentioned was performance which is sensitive to location of the strain gages.

Reduced strain gage size led to the attempt to build an external balance inside out which was done some 15 years ago for the first time. The system is "ideally" a statically determinate system involving isolated transducers to measure six force or moment components supporting a model. To accomplish this statically determinate "ideal" depends to a great extent on the applied loads, the ratio of loads, and the means used to isolate the transducer. If you have seen rocket thrust stands, which are external balances philosophically similar to the internal balance I shall discuss, you are probably aware that there are a number of possible arrangements of these force measuring transducers. In fact, there are a limitless variety of arrangements which permit a resolution of applied forces into distinguishable, individual components of force. In the internal balance, the package space which contains the force resolution system is very limited and very repeatable. It is usually a cyclindrical body, circular in cross section, or nearly so and fairly long. This shape restricts the possible ways of resolving forces mechanically and results in a particular force resolution system which is shown in Figure 1. The tapered member at the back of the attachment is for mounting to the sting support. The pair of vertical elements which we call forward and aft normal force, resolve normal force and pitching moment. The pair of similarly spaced side force elements resolve side force and yawing moment; an axial member carries axial or cord force loads, and a torque tube measures rolling moments and carries the same. This arrangement is very successful. In principle, this balance has no difficulties in that each transducer is isolated from all of the loads but the one to be measured. By using a perfect pivot at each end a transducer is obtained which is insensitive to stray loads and only sensitive to a primary load so that interaction effects are non-existent.

Obviously, minimizing deflections in its crucial end, and improving the performance and reducing the second order interaction, in addition to the other criteria, such as natural frequency should be optimized if possible. The actual internal balance of the floating frame type deviates somewhat from an ideal balance for several reasons. The elements themselves deflect and cause deformation of the balance. The transducers may be sensitive to extraneous or lateral loads and its performance may not be ideal nor proportional nor repeatable, etc. Finally, the transducers may be sensitive to the thermal environment.

The floating frame balance is susceptible to a fundamental error which the ideal single piece balance is not. The error is its sensitivity to thermal environments, and the unwanted outputs due to thermal changes. This is not to be confused with thermal strain or lack of compensation on the bridges, but is an actual force that occurs on the transducer because of thermal gradients in the balance. This type of balance develops forces in the presence of a thermal gradient in a multiply-connected region. Modifications of the transducer such as moving the axial and roll element to the center, halfway between the normal and side force element precluded thermal forces arising from the model and the balance. This mutation of the original force resolving arrangement is the one that we currently use. It is the most acceptable force resolving arrangement and is thermally inert.

Let us now consider, in detail, the floating frame balance and not consider in detail the single piece balance because it has been discussed, and I am more familiar with the floating frame balance. The design of this balance is a very highly integrated problem involving a great deal of structural and electronic transducer design. I will divide the design into that of a mechanical force resolution problem, structural problem, pivot design, transducer design, and odds and ends such as an attachment, calibrations and selection of a balance. We shall, henceforth be dealing with the system shown in Figure 2. The figure is a cutaway view of a typical balance and with careful inspection, one can see the normal force elements at each end, and the side force elements at inboarded ends, two axial members sharing the applied axial load and two torque tubes sharing the applied rolling moment. This is the thermally compensated floating frame balance. The structural problem for this balance is severe. Strength of the inner member, which has the sting attachment joint, is the load limiting factor. Pivots in this type of balance are very definitive on the performance of the balance. They have backlash, and hysteresis resulting from occasional large deflections affects the balance performance adversely. The only pivot that approaches our requirements is the elastic pivot, and the simplest type is composed of flat strapped flexures. These pivots have one drawback, and that is that they are not rotationally free, since they have an elastic restoring moment. It is necessary to examine the nature of that restoring moment and its effect on balance performance, which is accomplished in equations 3 through 8 and explanations. Equation 8 is very important because it shows the analytical results correct in that flexure length is not dominant, but thickness and spacing is dominant in making an internal balance, rocket component stand, or any force resolving system using transducers and flexures.

The length of a flexure beyond a certain point does nothing to improve the quality of the system, and such an elastic pivot is a very complex device. Figure 5 shows some of the most important characteristics. Further discussion of the behavior of an elastic pivot or flexure under applied axial loading will attempt to answer how applied load affects the center of rotation change and what angle of rotation is allowable. Also, further discussion will explain the restoring moment change, which may be a surprising fact to some. Analysis shows that the flexure is not a device that has a given fixed stiffness to deflection, but depends on how much axial load is being carried.

Figure 5 shows the change of center of rotations, non-dimensionalized by the length of the flexure strap, as a function of applied load over the yield load. The left hand plot of Figure 6 has an abcissa of P over Pcr and the right hand plot is P over Pcr, while the center plot also has P over Pcr. In the center of Figure 6 is a plot of allowable angular rotation undimensionalized by the maximum allowable rotation as a function of applied load over yield load. Deflection for several yield load over critical buckling load are shown and as the yield load approaches the critical buckling load, the allowable angular rotation drops off very rapidly. This is not very important for balances for which these angular rotations are of the order of milliradians. Finally, the most important plot for our purposes shows the rotational stiffness divided by the rotational stiffness at no load as a function of applied load over critical buckling load. The rotational thickness increases with compression load and is essentially infinity at the buckling load.

By increasing the length of a flexure, the buckling load is reduced so that the fixed rate of axial load is a bigger percentage of the buckling load. Thus, the change in restoring moment is greater and greater as the flexure is lengthened. The flexure is lengthened to improve force resolution; however, the flexure becomes more non-linear so the restoring moment depends heavily on the load it is carrying which is a first order interaction.

In our balances we use circular arc flexures which are very difficult to analyze, so we relate it to an equivalent flat strap. In other words, a circular arc flexure whose total length is equal to the diameter of the hole that forms it is equivalent to a flat strap of shorter length with thickness equal to the minimum thickness of the circular arc flexure. These effective lengths are shown in Figure 6. The effective length with which we are operating in most of our balances is between 1 1/2 and 2 1/2 times the flexure thickness; a very short, thick flexure, and the critical buckling load is far above the yield load so that we are operating in a very small band of the restoring moment change curve shown at the top of Figure 6. If we find that the force resolution is not as complete as we like it, that the redundency is high, rather than lengthening the flexures by making long straps of them or by making larger hole diameters, we reduce the thickness. Reducing the thickness reduces the bending and improves the resolution of forces because the thickness over the flexure separation appears squared in the expression indicating how well they resolve forces. We have made balances with fairly long flexure straps, and we have come up with very significant second order interactions which we will eventually trace to this effect.

We use the equation (9) through flexual redundency equalling $6 \frac{t}{H}^{2}$ as a means of establishing a load criteria within which the balance should operate well. The allowable normal force capacity for an ideal or good balance is about 500 pounds for a one inch balance, with scales up and down according to the square of the diameter. If we double the load capacity, then we have to double the required flexure thickness, and this increases the redundency of the balance by a factor of four. This factor very quickly becomes significant if we consider balances with a 10 to 1 normal to cord force ratio. Instead of losing 3 to 10 percent of the applied cord force through the other flexures, 50 or 60 percent of the applied force is lost.

The transducer has to fit into the balance and it has to be sensitive to the loads if one desires a sense in the balance. Beyond that, it should have low deflection, linear output, low hysteresis, repeatibility, insensitivity to extraneous moments, insensitivity to thermal environment, insensitivity to pressure change, humidity and should be readily manufacturable with accuracy. The transducers that are usually used in balances are the tension type reading direct uniaxial stress; eccentric column which is a bending type element and ring type which is also a bending element. Probably the most important criterion, which should be optimized is deflection. Deflection is calculated using principles of conservation of energy. We use this method because it shows a very important consideration in transducer design which is illustrated by equation (20).

The analysis has been carried out for the case of a pure bending member. For the same surface strain level, comparison of the equation (22) with equation (20) shows the deflection to be approximately 1/3 as much for a bending member as it is for an axial member. Unfortunately, all of the transducers that appear in a floating frame balance are axially oriented members so our bending members are essentially eccentric columns. In addition to a bending strain, we have an axial strain; consequently, the equation (22) does not strictly apply to our transducers. This correction has been made resulting in equation (27) as an expression for axial deflection. An eccentric column is minimized at an eccentricity ratio of 0.3. When the eccentricity is reduced below this value, a constant bending stress is maintained, but less, because the member is getting thinner and thinner, and it is deflecting in the mode of a tension type element. Since this stress is not being measured, this is the optimum eccentric column; i.e., eccentricity from a deflection standpoint.

A ring element has much more deflection than an eccentric column or a tension type. There are reasons for using rings in situations where one can tolerate these excessive deflections. It appears that there are no restrictions to deflections if one is able to make the thickness of the gage or strain member approach zero. This is not practical since the gage must dissipate heat to prevent serious thermal effects. However, some shear elements can be made with very thin webs because the member that is carrying shear has heavy flanges. This type of gage can be used for measuring shear, with resulting small deflections because the volume of the strain material is very small.

Linear members are more useful in data reduction since non-linearity is a second order interaction or equivalent. A tension type element is non-linear in the sense that output decreases with applied compressive loads and increases with applied tensile loads. A bending element of this type, either a ring or eccentric column, is non-linear in the opposite sense. Output increases in compression. The results are due respectively to the fact that a tension type member or compression member will increase in its cross sectional area under compressive loading due to Poisson's ratio. On the other hand, a bending type element has its eccentricity increased under compressive loading due to the bending. Equation (28) is an approximate expression for non-linearity in an eccentric column, and includes both the bending of an eccentric column and the Poisson's ratio increase of the section due to axial strain in the column. The expression shows that if the column length or the column thickness is equal to about twice Poisson's ratio the non-linearity disappears. This usually is not possible since strain gages have a finite length and Poisson's ratio is rather small. In the denominator we have the expression eccentricity over thickness so that by increasing eccentricity we reduce non-linearity. However, it was previously pointed out that the eccentricity should be 1/3 or less for minimum deflection. This is one of the many dilemas we are faced with, and we normally allow the non-linearity and try to obtain the minimum deflection in our bending element, although there are cases where this is not done.

The attachments shown in Figure 9 are considered to be a disadvantage by many people because they are a joint in the system which permits friction, motion and hysteresis. They have an advantage in that they permit adjustments to be made in the positioning of elements that eliminate interactions in the first place.

They permit removal of the elements without cutting the balance apart for repair or changing the load range. This configuration also permits stops to be placed in the balance between the outer sleeve and inner structural member to carry overload. In ordering a balance, regardless of the type, bear in mind that when it is smaller than will fit into the model, a very severe penalty is present because of the increased flexure thickness that is required for such a model. Allowable force and roll capacity are associated respectively, with balance diameter squared and cubed. One loses very rapidly by going to smaller balances than required. Ordering a balance with a very high output or using high bridge voltages can materially depreciate balance performance.

INEXPENSIVE STRAIN GAGE TRANSDUCERS

Pierre M. Hahn
Lockheed Missile and Space Division

Any transducer, except perhaps a friction scale, is rather expensive when it requires strain gages. Instrumentation is required which increases the cost. For most of the testing involved in the development of rocket engines and attachments to these engines, loads and forces must be measured. This often is accomplished expediently and economically using an eccentric bending beam or hollow link.

Figure 1 is a cutaway section of a hollow link . This load link is used for thrust or drag and bending at the same time using a bending bridge and a tension or compression bridge. Interaction and non-linear response is not serious if held to minimum since calibration data is stored in the computer used for data reduction. The first units sent to the Santa Cruz test base for calibration were constructed using Eastman 910 cement and waterproofing compound.

Figure 2 shows a transducer returned from the test sight. After removing the outside coating, inspection indicated that someone must have grabbed the end of the wire and used it like a yo-yo. It appeared to have

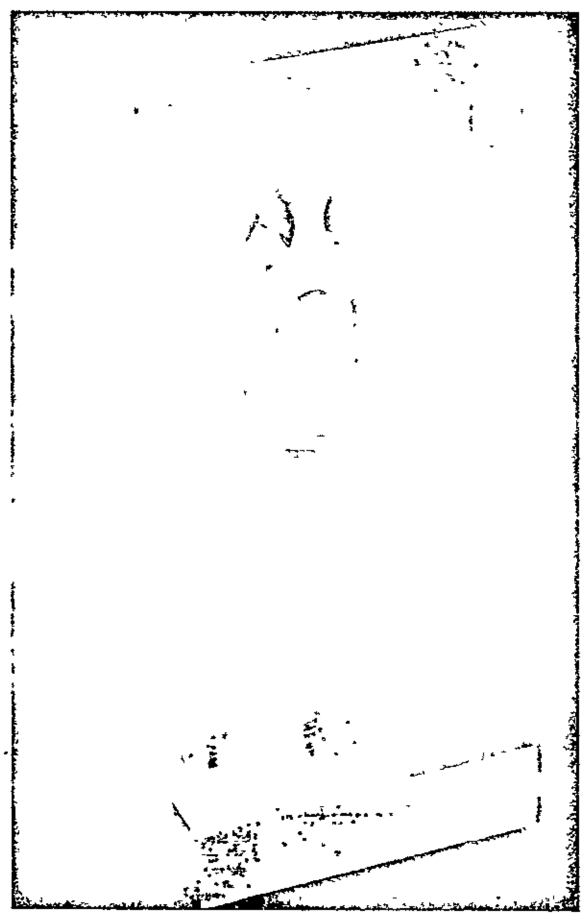

Figure 1. Sectional view of hollow force link.

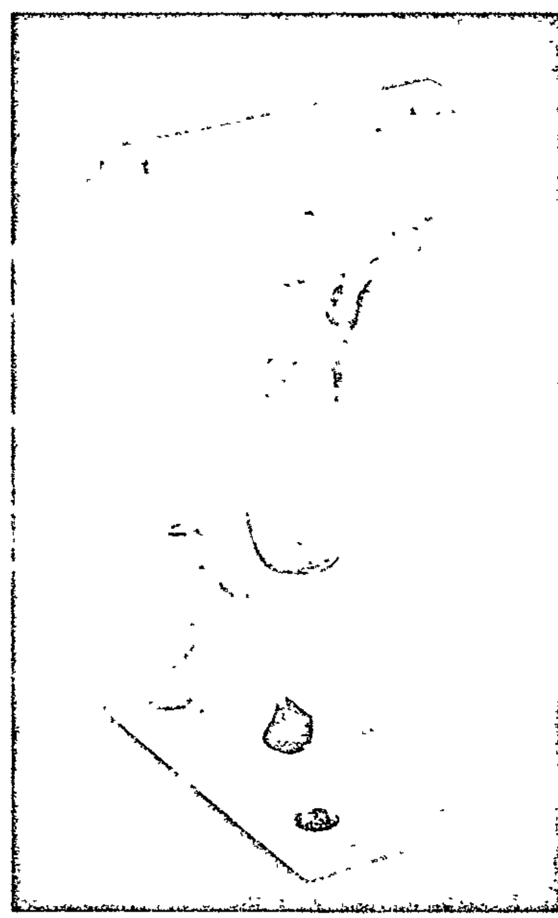

Figure 2. Used and abused transducer returned for repair.

been overheated, for the gages peeled off easily. Part of the problem was assumed to be aged Eastman 910. However, it is still not certain why the gages came off. Eastman 910 cement is good for certain applications, but only in the laboratory under very careful supervision and extreme care.

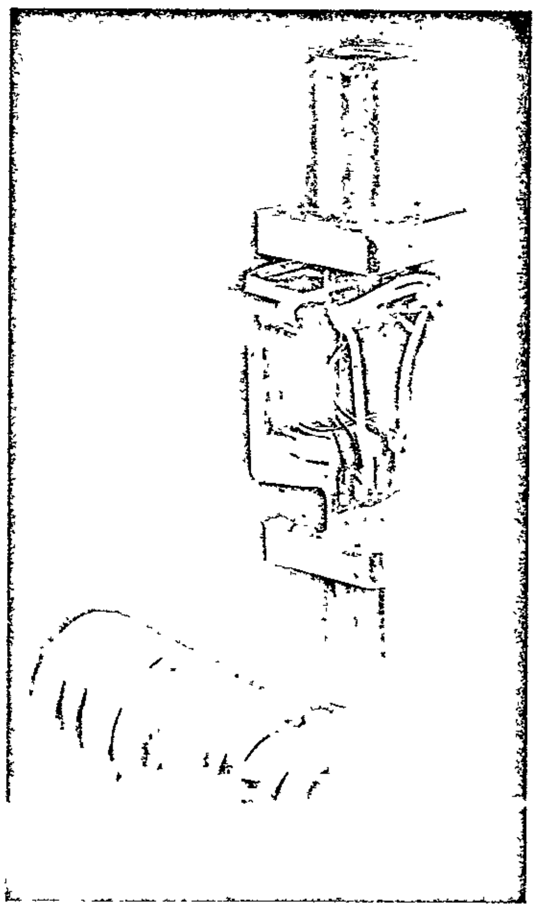

Figure 3. Improved model of axial force transducer.

Figure 3 shows a more reliable method; i.e., bakelite gages applied with EPY 400 cement. Transducer installations of this kind seem to last much longer with the mishandling in the rugged operation which these load links have to endure. The lead wires still get pulled off, which has yet to be remedied. Perhaps this is why some of the Baldwin manufactured load cells are better than many laboratory built load links.

The other problem has been spring action or deflection under load which has led to the use of semiconductor strain gages. The output of the semiconductor is kept at approximately the same level as the standard strain gage, thereby keeping the strain on the element much lower and reducing our spring effect. This is done to increase the natural frequencies of the rocket stand beyond the range of the rocket engine. This has produced the desired structural effects but it has developed a temperature problem. If the spring constant is changed by a factor of 50 the temperature sensitivity is increased by a factor of 50. This is a problem, in most of the cases, does not interfere because duration of the tests is a second or a second and a half. The transducer is protected with thermal insulation and the ends are made thermally large, to eliminate the effect of the temperature change due to external sources. The maximum temperature change noticed has been 25 to 30 degrees which gave only one-half percent of full scale. This is not the high accuracy needed for most cases, but is the least expensive, and is adequate for this particular purpose. Repeatability is of more concern than linearity, and it has been within one-tenth of one percent for all our transducers. This is quite good. Other factors are included in the calibration· applied load versus output. This is an old method of transducer construction which is reliable and inexpensive because almost any machinist can produce a serviceable unit without having to worry about dimensional tolerance.

WORKSHOP SESSION I

.Transducer Problem Areas

At this time we will welcome questions from anyone, on any subject having to do with transducers and we have questions that have been mailed in which will be considered.

Question: In preparing EPY-400 for laboratory use, have difficulties such as "stringing" been noticed?

Answer: We have some of this "stringy" EPY-400 cement, and I haven't been able to find any strings in it. In my opinion, the manufacturer's method is difficult to use when mixing this cement and I would suggest that you simply take the bag apart and transfer the contents into the container and mix it.

Question: Does the filler cause trouble?

Answer: This is definitely true. If we remove the filler we will have about a 300 or 350 degree cement because of the lower modulus of the epoxy. It is generally possible with a little bit of practice to obtain good EPY-400 installations with a glue thickness approximating 0.001 inch. This is one reason why bakelite cement will always maintain some of its popularity. On internal transducer work we use a phenolic material which has no filler in it at all.

There is one other thing we have had some trouble with occasionally and that is quality control of the cement. If you get some you think is not good, put a little on a specimen and send it back, and we will see that you get a return supply for it.

The offer of replacement is appreciated, but what about the gage installations we lose and the time that we could be "down" waiting for replacement? Our solution to this problem is to buy EPY-400 in larger quantities, then re-package and weigh the components. When we need cement, it is mixed in quantities to suit the job, using proportions determined by the weight of components in each bag. It is used in a warmed condition on a preheated specimen. This seems to have solved our problems.

Your question of who is going to replace the money and the time expended in the installation is certainly valid. It is the same one that confronts us when the manufacturer of one of our adhesives makes a mistake in a lot of 1000 units. When this gets out into the field, we have to replace not only the cement but the gages. When we go back to our supplier and ask him who is going to replace this ten fold amount of gages, he just shakes his head the way I'm going to shake mine at you.

Cost per package of the cement is not worth the effort to get it replaced even though you are willing to do it. There are elements of time and paperwork, as far as the user is concerned, that make replacement impractical. It is more economical to throw it away and get another package.

Question: Would you people say that if there is a possibility that you could buy this material in bulk, you might like the arrangement?

Answer: Yes.

Question: I know that there are a number of people here who use nothing but bakelite powder and mix their own. I believe Baldwin also sells the bakelite powder, is that right?

Answer: I do not think that we do except in foreign countries, but we certainly could. This group can do many things that the average man cannot do. This is one reason we do not push bakelite because it is necessary to have pressure for the chemical reaction to take place.

Question: We have had a little trouble with the EPY-150. It just does not set up unless you put a heat lamp on it.

Answer: There was a lot of about 1000 units that went into the field, and we have been unable to determine what was wrong with it, but there is no doubt that it wasn't right. You obtained some of this bad batch.

Question: Has anyone found the difference between the EPY-400 and Mithra? I am interested in cements for high temperature which are easy to apply and conveniently packaged like EPY-400. Is Mithra any better?

Answer: As far as I know, they are approximately equivalent cements. They are the same two-component system, but do not mix well when you try to cross breed them; that is, using liquid Mithra with powdered EPY-400 or conversely even though they use the same catalyst. It seems that Dupont Company made the catalyst for these systems and has decided that it is not worthwhile manufacturing. Our supplier says they are not using this material or they have sufficient quantities on hand to cover development of another supply or a substitute material. One or the other of us is going to have trouble.

We have done some work with both of them and we have a feeling that Mithra is better for higher temperatures. It does not seem to carbonize quite as rapidly. We mix the entire batch of cement, use what we need and put the rest in the freezer.

Question: Are the NASA pressure transducers as good as indicated?

Answer: We have had considerable experience making several hundred transducers ourselves, and by having more than a hundred made for us. Although they could be made quite temperature stable, they are kept in temperature controlled cabinets so they experience very small temperature changes. We believe that they meet specifications to better than 0.10 percent full scale, in a range of 4 psi, which is below the range for which you usually get this degree of accuracy in pressure cells.

Question: Do you feel they are better than Statham's precision units?

Answer: We have not compared them recently. Generally speaking, Statham has tried to make units accurate to a tenth of a percent, but .15 percent seems to be their best effort. They bid on our design, which is rather unusual.

I might mention there is nothing particularly perfected about this design, and we have others that would decrease the deflection by a factor of 10. I do not think there is any real basic limit to the accuracy.

Question: What is the price of your unit?

Answer: I know we have paid approximately $300 per cell, but I do not know if this includes the whole system.

Question: What is the leak rate of your pressure transducer?

Answer: I am not sure there is a leak-rate problem. When they are used in banks of 100, it is necessary to hold the pressure while the readout is being made for 100 channels. As far as I know, the leak rate is negligible.

Question: How do you calibrate these pressure pickups?

Answer: We have some standards we are using; an Exactal Manometer is more or less a primary standard.

The output of this is bucked against the output of the cell and plots an error curve. The curve you saw on the slide was essentially a plot of error output against what we consider to be standard.

Question: A number of people who sell load cells have asked me if there is a market for an inexpensive 2 percent load cell, opposed to the quarter percent ones which is about all you can buy. Do most of you people have some use for load cells that would be less accurate and less expensive to build?

Answer: I think the building of a load cell in that price range is not going to help much because of the many different applications.

I was thinking along the line that you wouldn't have to have modulus compensation; you wouldn't need specially heat treated material. Perhaps these load cells could be made in a general configuration and the user could just drill a hole to convert to 10,000 pounds instead of 30,000 pounds. Is any of this practical from a manufacturer's standpoint? It seem to me that if manufacturers made something that the user could modify for different ranges, they could do their own calibrating. I was thinking of something you could stock, like resistors.

I think it could be done. The corporation tried the technique of grading cells as they were made. They had an ultra-precision grade which was supposed to be that small portion which for one reason or another happened to be better than the rest. They put this list out and no one bought the middle class and they suddenly got a tremendous order for the high precision ones. It could be impractical from the scheduling standpoint. It is not a problem of can you make or supply one for a low price, but the fact that everyone wants something different makes it difficult to stock items economically.

It seems to me that the main reason for buying the cell is to obtain accuracy. The others can be made up in a hurry. The reason you get no one to order the lower grade ones is probably because they make their own.

WORKSHOP SESSION II

General Strain Gage Problems

Strain Gage Specifications. Most of you are familiar with NAS 942 since quite a few of you helped write it. After trying to use this specification for a little while, it became apparent that revisions were necessary. For those of you who are not familiar with NAS 942, it is a specification that told how to test strain gages and determine their characteristics. It was started under the auspices of the Aerospace Industries Association and was intended to be a purchase specification for strain gages, but the purpose was changed at its very beginning. During the past year or so, it has been in effect as a testing standard.

In its present form it attempts to set forth the standards for minimum qualification test data that the manufacturers of strain gages are required to supply. It specifies how the test data is to be obtained, the format in which it should be presented and the test procedures and instrumentation accuracies that should be used in obtaining the data. Once we started to apply the specification, some of the problems with it became readily apparent. In November, 1960 there was a meeting at the Bureau of Standards on strain gage evaluation which was attended by strain gage manufacturers, representatives of various government agencies and representatives from the Aerospace Industries Association. At this meeting there was considerable discussion on several things having to do with gage evaluation.

One of the things discussed was NAS 942 and some possible revisions that should be made. Several things were suggested that probably will be attempted. One of these was to eliminate the requirement for testing all gage types according to the specification. This could be accomplished in two or three different ways. For example, by grouping gages up into different types, or by grouping gages into various temperature spans. It was proposed that some of the measurements, for example, change in gage factor as a function of temperature could be made on a more qualitative basis. It requires absolute measurement of gage factor at each temperature and this data is not too useful; at least it is not required. The specification will probably be changed from its present form requiring steady state measurements to allow certain types of transient measurements and the use of automatic plotting equipment. Originally there were no requirements for the use of this equipment because people felt that someone could develop the world's best strain gage in a "garage shop", and he would be penalized if required to buy a bunch of fancy equipment to evaluate his product. On the other hand, established strain gage manufacturers could be inconvenienced or put out of business by the amount of data reduction if they cannot use automatic plotters.

The drift specification probably will be changed. It has been the experience of several people that requirements now set forth are impractical and not too useful. Most of the drift occurs during the first portion of gage heating and this is more critical than spelled out in the procedure. We may specify drift rather than drift rate. There have been several proposals in regard to how thermal output and hysteresis should be measured. One proposal was that the output should be recorded as a slope plus a deviation curve in order to get the required resolution with the results. It was also suggested that a simple check of self generated electrical output might be included by removing bridge exitation and measuring residual signal. This is a function of the installation, but it would be an indication of what can be expected in your own testing.

The leakage resistance tests could be automated to allow X-Y plots of leakage resistance versus temperature, possibly under low speed transient conditions. A requirement for measuring transverse sensitivity has been proposed for addition to the specification. Other portions of the specification are to be left unchanged such as requirements for fatigue testing and information on the gage installation procedure and previous history of the gage, physical description, etc. It has been strongly suggested that a required number of specimens to be tested be specified. Between 4 and 6 of each type should survive the test program, rather than leaving the number up to the manufacturer.

Since this meeting the ARTC Committee of the Aerospace Industries Association has authorized revision of NAS 942 and the project set in motion. At the ARTC meeting, it was again requested that NAS 942 be made a purchase specification. The first step is a questionnaire to Aircraft Industries Association members, various governmental agencies and load cell manufacturers to determine what the characteristics of a standard family of strain gages ought to be. This questionnaire by necessity is incomplete. Considering the possible parameters and combinations of parameters, you end up with a voluminous questionnaire. I tried to cover what appeared to be the main points and limit responses to require them to talk about a particular gage that they think would best fit their needs. We will put these responses together and try to generate a characteristic family from them. Just how successful this proposal will be, I do not know. We hope to have this completed by February 1962.

Question: The requirements for flight testing are much different than requirements for laboratory structural testing. Are there to be two separate specifications for this?

Answer: There will be one response per company division; include your more strenuous requirements. If you decide that grading is a good idea, it could be possible that for certain applications flight test may need a premium grade strain gage and the laboratory people might need something else.

The specification as it is now written, is sectioned. Section 1 is scope; Section 2 is applicable documents. The specifications as referred to the specific company purchase documents. The only thing that is covered now is how to measure physical quantities. It does not say anything about what they should be.

Question: Is the revision trying to say what they should be?

Answer: Yes, to set minimum requirement.

Question: Isn't this achieved automatically when grading is included?

Answer: Not necessarily. Manufacturers may feel that they have to produce different grades. From the standpoint of buying a reasonably priced strain gage in large quantities for high volume work, the accuracy requirements are not too high. If the minimum requirement is high enough to meet 50 percent of the required work, then the other 50 percent has to pay the premium.

Question: Does any document get down to specifying by type, because then you are specifying a manufacturer's type?

Answer: The following are proposed definitions for these various grades. The top grade would be a gage for which strict quality control is required and it would be subjected to all of the qualification tests that are presently required in NAS 942. The second grade would come with essentially the information that you get now, the nominal gage factor and the resistance, and if possible, the temperature coefficient for lot number. A third grade of gage would be for people who want something that gives a strain indication, and who do not require a gage factor.

Question: When this is done, don't you think the manufacturer ought to say that this is a grade A and this is grade B?

Answer: I do not know exactly what the manufacturers have in mind. Baldwin has been very good about helping with the specification. They have been running qualification tests under the existing specification and have a pretty good feel now for what is involved. One thing that has caused some consternation is that the definition of the word "type", the gage type. I think that for the most of our purposes, take the flat grid bakelite gages and perhaps call this a type. Manufacturers want to evaluate this type of gage, say this is typical of this line that everything will be this good or better.

Question: How do you settle a case where the strain gage installation is outside of standard procedures?

Answer: We try to determine the maximum limit of endurance as far as curing them out. We then use that cure to evaluate our gages. It makes a great deal of difference what adhesives we use and what cures we use. NAS 942 calls out that manufacturers specify the adhesives, cure cycle, handling and installation procedures in great detail. If you use the manufacturers' methods, results should be similar. This is one thing that you do not get now. We get the results, but little or no indication as to how they were obtained.

There is another problem that enters in here. We have the same trouble with strain gages that you mentioned with transducers. Purchasing people in various aircraft companies have rules that they operate by. With so many people getting into the strain gage business, if purchasing people buy the lowest price item, you may lose control over what you put on your airplane or test structure. This specification was intended to alleviate this problem.

As an example of this, we received some new gages that were supposed to solve all our problems, but no gage factor on the package. So we called the manufacturer and asked for the gage factor. He said I do not know; I do not have any way to measure it. I'll give you the name of the guy down the street where I bought the material and maybe he can tell you.

Question: The constant stress beam for fatigue has been shown photoelastically to be otherwise. In the interest of accuracy and correctness, shouldn't NAS 942 use a theoretically correct specimen for the fatigue tests?

Answer: Definitions and fundamentals should be compatible and in complete agreement with basic fundamentals of theoretical and applied mechanics. However, when it comes to evaluating competitive products, the evaluation is not required to be completely and one hundred percent compatibly oriented with theoretical and applied mechanics to obtain the last "gnats eyebrow" of refinement in our techniques. The prinicpal requirement in this case is for all evaluation tests to be conducted in precisely the same manner for comparative purposes. If we control the conditions, whether they are theoretically correct or not, we will still have the comparative data that we are looking for. NAS 942 is oriented to give a practical approach to comparative testing and establish techniques whereby we are controlling the testing conditions and environment for comparative data. There is more latitude possible when setting up a performance specification than in setting up basic definitions.

<u>Strain Gage Problems</u>. We will move into the area of general discussion and will be happy to have questions on any of the subjects. We have received questions on waterproofing materials for cryogenic and high temperatures. If someone will volunteer information in either area, we would all like to hear it.

Question: We have obtained pretty decent strain gage data from tests using liquid nitrogen, but have been unsuccessful in preventing atmospheric moisture from degrading the installation during warm-up to ambient temperature. The two or three materials tried have been failures even though liquid nitrogen does not appear to affect the installations. Can this be averted?

Answer: While working at cryogenic temperatures with liquid nitrogen, we conducted a number of immersion tests allowing frost to form on warm-up. We encountered the same phenomenon and solved the problem in the manner shown in the Douglas Seven Step Installation Technique that appeared in our Proceedings of the 1959 Seattle meeting. The lead wire electrical connection is made well in on the gage. Using some EPY-400 or other strain gage adhesive, work some of it over and around the end of the wire and connection to anchor the lead. This sealing attachment provides a mechanical bond and seals the wire end to prevent a "wicking" action. Closing off this end of the system in itself gives a very effective moisture seal for rather severe conditions, even for repeated immersion in liquid nitrogen.

Further precautions for mechanical handling were also described where we used some PRC products or equivalent. There are a number of products that have worked fairly well and should be applied lightly. Churchill Chemical Company 3C1300 worked quite well. There are a number of these rubber-like materials that are compatible with the epoxy and are rather easy to use. The key to the whole thing is closing off the wires in a satisfactory manner.

Question: Can you use Epon?

Answer: This method is applicable to any of the adhesives. It works well with EPY-400, Epon VIII, Epon VI, or any similar adhesive for high temperature work. It also works satisfactorily with the bondable type teflon wires.

Question: We have tried to do the very same thing, but the EPY-400 bond cracked after several cycles.

Answer: An excessive quantity of adhesive will tend to crack due to the mass present and its own thermal expansion properties resulting in a progressive failure. Other materials may be acceptable. One of the newer synthetic rubbers such as Viton B which is being used in high temperature areas could be used. They seem to be promising for higher temperature moisture proofing. If they are as compatible with other temperature extremes as they are with the 600 to 700°F environments they are used for, then they may be very serviceable for cryogenic temperatures until you get into problems from direct contact with liquid hydrogen and oxygen.

Question: Are these some things that come in tubes?

Answer: No. Liquid Viton is similar to liquid neoprene. It is soluble in methylisobutyl ketone (MIBK) until final cure at 600°F. Vitons are high temperature synthetic rubbers. They appear to be good sealants which are unaffected by other organic liquids which are encountered in the aircraft industry, including a lot of the hydraulic fluids. Wire manufacturers are coming out with high temperature cables using Viton jacketing with a higher service temperature than teflon.

Question: How does one improve adhesive action of Eastman 910?

Answer: Too many people have had trouble with it. We have had our troubles, although we use it extensively. There is one thing that we have to do, and that is buff the back of the gage. If you do not, you might as well not use it at all, especially on bakelite gages. One of the techniques for buffing the back of the gages to remove the gloss, is to use the pencil style, refillable fiber glass typewriter erasers. They are very handy. You do not use Eastman 910 with wire gages in paper matrix.

Question: Do you use it on epoxy backed gages?

Answer: We can and do, but do not use many epoxy gages.

Question: Have the data presented at the last meeting for Curvature Error Strain been verified?

Answer: We had an instrumented test part for use on an airplane with the gages laid on 5/8 inch diameter rod with the end of the rod enlarged to accept a bearing. The gages were on the cylindrical section and temperature error was about 10 times greater than the formula would predict. In order to determine the cause of this effect, we used simple specimens and checked the formula with good agreement. Temperature distribution seemed to be the trouble. We cured the immediate problem by installing the gages on machined flats.

I want to point out the effect of thermal masses on some parts can develop misleading data. If gages are to be applied on a section near some thermal mass, significant errors are still possible even under stable temperature conditions. Variable temperature conditions are even worse.

Question: Has anyone using the weldable type gages experienced a transverse buckling phenomona?

Answer: To increase the performance of premounted, weldable gages in compressive strain fields, apply a bondable teflon terminal on top of the gage and over the grid. This will stiffen the assembly for transverse buckling, provide mechanical and thermal protection and serve as an insulated point to attach a thermocouple for thermocouple compensation of the strain gage circuit. This method will permit the use of thinner shim stock for less stiffening effect and better installations. If you make your own assemblies, cut the piece large enough to cover the grid of the gage and cement it in position at the time strain gages are applied to the shim stock tab. In effect, this applies a geometric stiffening effect to inhibit transverse buckling effect obtained at higher compressive strain levels without the undesirable effect of localized buckling in the gage. Geometric mass and stiffening are added without adding strength to the total assembly because added material modulus is insignificant compared to the rest of the assembly.

Question: Why haven't strain gage manufacturers provided high temperature strain gages with one large and one standard tab for use in the single gage three wire system?

Answer: I do not think it has been mentioned before and it seems to be a very good idea.

High temperature gages made with one tab much wider than the other to accept the two wires attached at the same point would be convenient and helpful. We have found that installations give different outputs from temperature variation because of different lead attachment locations.

I think that tabs on the strippable back gages could be enlarged in many respects, either lengthened or widened. There seems to be space between the tabs which could be used for enlarging the tabs.

Question: Why not make both tabs larger, then you do not have to worry about an irregular installation?

Answer: This could increase the gage size to the point you would be unable to place the gage in the desired location.

WESTERN REGIONAL STRAIN GAGE COMMITTEE

Jack Tar Hotel, San Francisco, California
May 11 and 12, 1961

Thursday, May 11 PLANT TOURS

Lockheed Missile and Space Division
 Briefing Session
 Recess
 Tour of Lockheed Laboratories
Luncheon

Ames Research Center
 Briefing Session
 Tour of Ames Laboratories

5th Anniversary Dinner

Friday, May 12 TECHNICAL SESSIONS

Chairman's Convening Statements
 Ward B. Brewer, Lockheed Aircraft Corporation

Sponsor's Welcome to WRSGC Delegates and Guests
 John F. Kirkland, B-L-H Corporation

Recess

DESIGNING SPECIAL PURPOSE STRAIN GAGE TRANSDUCERS
 Introduction
  Ward B. Brewer, Lockheed Aircraft Corporation

 General Procedures for High Accuracy
  Frank F. Hines, B-L-H Corporation

 Special Purpose Transducers at Ames Research Center
  Keith McFarland, Ames Research Center

 Unique Strain Gage Instrumentation in Boeing Wind Tunnels
  Truman R. Curry, Boeing Airplane Company

 Luncheon

 Wind Tunnel Sting Balances
  Richard R. Tracy, The Task Corporation

 Inexpensive Strain Gage Transducers
  Pierre M. Hahn, Lockheed Missile and Space Division

WORKSHOP SESSION I - Transducer Problem Areas

Committee Business

Recess

Sub-Committee Reports

WORKSHOP SESSION II - General Strain Gage Problems

ATTENDANCE

May 12, 1961

COMMITTEE: Members and Delegates

Member	Division	Delegate
Aerojet General Corporation	Solid Rocket Plant P.O. Box 1947 Sacramento, California	Bruce Barclay Instrumentation Engineer
Boeing Airplane Company	Transport Division P.O. Box 707 Seattle, Washington	Theodore M. Mathison Unit Chief, Flight Test
Douglas Aircraft Company	El Segundo Division 827 Lapham Street El Segundo, California	John J. Shea Instrumentation Engineer
	Testing Division 3000 Ocean Park Boulevard Santa Monica, California	John Quinley Research Engineer
General Dynamics Corporation	Astronautics P.O. Box 166 San Diego 12, California	Donald J. Ferris Sr. Test Lab Engineer
	General Atomic Division P.O. Box 608 San Diego, California	T. A. Trozera Res. Staff Member
	San Diego Str. Lab P.O. Box 1950 San Diego, California	Dean O. Whitney Res. Test Engineer
Grand Central Rocket Company	Test Division P.O. Box 111 Redlands, California	Thomas P. Carpenter Test Engineer
Jet Propulsion Laboratory	4800 Oak Grove Avenue Pasadena, California	Bartc[illegible] [illegible]. Graves Ins[illegible]tation Group S[illegible]sor
Lawrence Radiation Laboratory	Weapons Engineering Division P.O. Box 808 Livermore, California	Ra[illegible]. Morton Group [illegible]der
Lockheed Aircraft Corporation	California Company P.O. Box 551 Burbank, California	War[illegible] [illegible]ewer Grou[illegible]ineer
	California Company P.O. Box 551 Burbank, California	Ch[illegible]. Buzzetti Gr[illegible]eer
	California Company P.O. Box 551 Burbank, California	Robert [illegible]. Merrill Rese[illegible]ngineer
	California Company P.O. Box 551 Burbank, California	Philip O. Vulliet Sr. Research Specialist
	Missiles and Space Company Sunnyvale, California	Sterling W. Davis Research Engineer
	Missiles and Space Company 7701 Woodley Avenue Van Nuys, California	Richard L. Hannah Sr. Res. Engineer

COMMITTEE: Members and Delegates (Continued)

Member	Division	Delegate
Martin Company	Avionics P.O. Box 179 Denver, Colorado	Carl R. Harris Group Engineer
North American Aviation	Flight Test Instrumentation L. A. International Airport Los Angeles 45, California	Robert W. Troke Design Specialist
	Space and Info. Systems Downey, California	Robert R. Walker Test Engineer
Sandia Corporation	Test Lab Department Sandia Base Albuquerque, New Mexico	Paul H. Adams Division Supervisor
University of California	Berkeley Radiation Laboratory Berkeley 4, California	Jack Gunn Mechanical Engineer

SPEAKERS:

Lockheed Aircraft Corporation	Missile and Space Company Palo Alto, California	Pierre M. Hahn Sr. Research Engineer
Boeing Airplane Company	Wind Tunnel Laboratory Seattle, Washington	Truman R. Curry
N.A.S.A.	Ames Research Center Moffett Field, California	Keith H. McFarland Research Engineer
Task Corporation	1009 E. Vermont Avenue Anaheim, California	Richard R. Tracy Project Engineer

GUESTS:

ACF Industries, Inc.	Development and Test Engineering P.O. Box 1666 Albuquerque, New Mexico	Grant W. Gray Sr. Electronics Engineer
Allegany Instrument Company	Sales 11801 Mississippi Avenue Los Angeles 25, California	Harold W. McAllister Application Engineer
Boeing Airplane Company	Aerospace Division P.O. Box 3707 Seattle 24, Washington	Darrell R. Harting Supervisor, Instrumentation and Data Reduction
Consolidated Electro Dynamics	Transducer Advanced Development 1400 So. Shamrock Avenue Monrovia, California	Val Davidson Manager Advanced Development
N.A.S.A.	Ames Research Center Moffett Field, California	Carl D. Kolbe Research Engineer
Sandia Corporation	Static Test Sandia Base Albuquerque, New Mexico	Howard W. Nunez Staff Member
Task Corporation	1009 E. Vermont Avenue Anaheim, California	Elmer F. Ward President
University of California	Mechanical Engineering 101 A Mechanics Building Berkeley, California	Don M. Cunningham Associate Professor
	Civil Engineering 230 Engineering Mat'l Lab. Berkeley 4, California	Louis J. Trescony Assistant Research Engineer

GUESTS: (Continued)

Member	Division	Delegate
White Sands Missile Range	Structures Branch White Sands Missile Range, New Mexico	Frank W. Stout Staff Engineer

SPONSOR:

Member	Division	Delegate
Baldwin-Lima-Hamilton	Electronics and Instrumentation Division 42 Fourth Avenue Waltham 54, Massachusetts	Frank F. Hines Consultant
	Electronics and Instrumentation Division 42 Fourth Avenue Waltham 54, Massachusetts	James Dorsey Chief Engineer Strain Gages
	West Coast Region 2929 - 19th Street San Francisco 10, California	John F. Kirkland Regional Manager

THE STRESS-STRAIN GAGE

BALDWIN-LIMA-HAMILTON CORPORATION
Electronics and Instrumentation Division
Waltham, Massachusetts

Appendix A

THE STRESS-STRAIN GAGE

Frank F. Hines
Staff Engineer
Baldwin-Lima-Hamilton Corporation
Electronics and Instrumentation Division

GENERAL:

The term Stress-Strain Gage is used to describe a unique bonded resistance strain gage whose change in resistance under applied strain can, at the option of the user, be made proportional to either the strain or to the stress in the direction of the principal gage axis. Figure 1 shows a typical configuration of an etched foil type of Stress-Strain Gage. Basically, this gage consists of two single uniaxial strain sensing elements of different resistance values oriented at 90° to each other. The two elements have one common connection so that only three lead connections are available. Either of the two elements can be selected and observed independently or the two elements can be read together, depending upon which two of the three gage terminals are connected to the readout instrument. Thus, by connection to Terminals T_1 and T_3, Element 1 only is in the measuring circuit and the observed readings are proportional to strain in a manner similar to any conventional single element strain gage. Connection to Terminals T_1 and T_2 places both Elements 1 and 2, in series, in the measuring circuit and the observed readings are a function of the strains in both elements. This latter hookup, through proper design of the gage geometry and the resistance ratio between the two elements, can be made to produce observed readings that are proportional to the stress along the major gage axis.

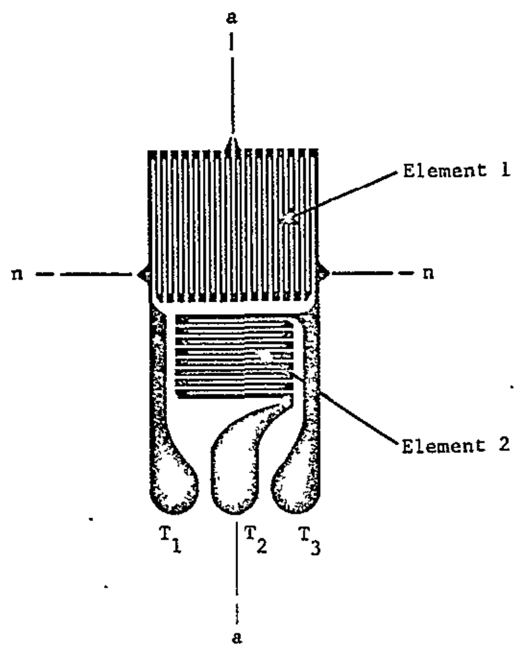

Figure 1 Typical Stress-Strain Gage Configuration in Etched Foil Construction

Measurement need not be limited to either strain or stress alone. By the use of three lead wires and suitable switching arrangements, both strain and stress along the principal gage axis can be obtained. In addition, by connection to Terminals T_2 and T_3, it is possible to obtain strain readings from Element 2 only, although limitations on the resistance of this element (approximately 1/3 that of Element 1) may make it unsuitable for use with some instrumentation.

STRESS GAGE THEORY

The theory of the bonded resistance stress gage, as applied to both T and V configurations and including rigid proofs, has been thoroughly explained in published literature.[1, 2] The following is a brief description intended only to reveal the essential characteristics required in a stress gage.

Let the following symbols apply to the combination of gage Elements 1 and 2 as shown in Figure 1 (leads connected to Terminals T_1 and T_2).

F_a = Strain sensitivity of the combination of gage elements for uniaxial strain along axis a-a for zero transverse strain. Ohms/ohm/in/in.

NOTE: Superscript numbers refer to references at end of discussion.

F_n = Strain sensitivity of the combination of gage elements for uniaxial strain along axis n-n, normal to a-a, for zero longitudinal strain along a-a. Ohms/ohm/in/in.

k_s = $\frac{F_n}{F_a}$ = Transverse sensitivity coefficient.

F_s = Stress gage factor as supplied with the gage. Ohms/ohm/in/in.

R_1 = Initial resistance of gage Element 1. Ohms.

R_2 = Initial resistance of gage Element 2. Ohms.

R = $R_1 + R_2$. Ohms.

ΔR_1 = Change in resistance of gage Element 1. Ohms.

ΔR_2 = Change in resistance of gage Element 2. Ohms.

ΔR = $\Delta R_1 + \Delta R_2$. Ohms.

The following symbols apply to the material on which the gage is bonded.

σ_a = Stress along axis a-a. Lbs/sq. in.

σ_n = Stress along axis n-n. Lbs/sq. in.

ε_a = Strain along axis a-a. In/in.

ε_n = Strain along axis n-n. In/in.

μ_o = Poisson's ratio of the material on which the gage is calibrated and designed to be used.

μ = Poisson's ratio of any test specimen material.

E = Modulus of elasticity of the material to which the gage is bonded.

From the general theory of elasticity, the stresses and strains along any two orthogonal axes are related as follows:

$$\varepsilon_a = \frac{1}{E}\left(\sigma_a - \mu\sigma_n\right) \tag{1}$$

$$\varepsilon_n = \frac{1}{E}\left(\sigma_n - \mu\sigma_a\right) \tag{2}$$

$$\sigma_a = \frac{E}{1-\mu^2}\left(\varepsilon_a - \mu\varepsilon_n\right) \tag{3}$$

$$\sigma_n = \frac{E}{1-\mu^2}\left(\varepsilon_n - \mu\varepsilon_a\right) \tag{4}$$

The unit change in resistance of a gage exposed to a general strain field is

$$\frac{\Delta R}{R} = \varepsilon_a F_a + \varepsilon_n F_n. \tag{5}$$

Substituting Equations 1 and 2 in the above gives

$$\frac{\Delta R}{R} = \frac{Fa}{E}\left(\sigma_a - \mu\sigma_n\right) + \frac{Fn}{E}\left(\sigma_n - \mu\sigma_a\right)$$
$$= \frac{\sigma_a}{E}\left(F_a - \mu F_n\right) + \frac{\sigma_n}{E}\left(F_n - \mu F_a\right) \tag{6}$$

By definition,

$$F_n = k_s F_a \tag{7}$$

Then

$$\frac{\Delta R}{R} = \frac{\sigma_a F_a}{E}\left(1 - \mu k_s\right) + \frac{\sigma_n F_a}{E}\left(k_s - \mu\right)$$

$$= \frac{F_a}{E}\left[\sigma_a\left(1 - \mu k_s\right) + \sigma_n\left(k_s - \mu\right)\right] \tag{8}$$

Under calibration conditions, in order to "fit" the material on which the gage is bonded, two conditions must be satisfied. The first condition is that when $\sigma_a = 0$, then $\frac{\Delta R}{R} = 0$, which means that the change in gage resistance must be independent of the transverse stress, σ_n. The second condition is that when $\sigma_n = 0$, then $\frac{\Delta R}{R} = \frac{\sigma_a}{E} F_s$, which means that the change in gage resistance must be proportional to the stress, σ_a, applied along the a-a axis. If these two conditions are met, the gage will respond only to the stress applied in the direction of the principal gage axis, a-a.

Applying the first condition to Equation 8 gives

$$\frac{\Delta R}{R} = \frac{\sigma_n F_a}{E}\left(k_s - \mu_o\right) = 0, \tag{9}$$

from which

$$k_s = \mu_o. \tag{10}$$

Applying the second condition to Equation 8 gives

$$\frac{\Delta R}{R} = \frac{\sigma_a F_a}{E}\left(1 - \mu_o k_s\right) = \frac{\sigma_a}{E} F_s, \tag{11}$$

from which

$$F_s = F_a\left(1 - \mu_o k_s\right) \tag{12}$$

Equation 10 shows that a stress gage, in order to have a change in resistance proportional only to applied stress, must simply have a transverse sensitivity coefficient equal to the Poisson's ratio of the material on which it is bonded. Equation 12 shows how the stress gage factor, F_s, is related to the other gage constants. Note that F_a, the strain sensitivity for uniaxial strain, is not the same as the conventional gage factor of a simple single element gage.

In the stress-strain gage configuration shown in Figure 1, Element 1 is the principal strain measuring portion of the sensing grid. Element 2 provides the necessary transverse sensitivity when the two elements are connected in series. The amount of transverse sensitivity introduced by Element 2, and hence the transverse sensitivity coefficient of the gage as a whole, may be controlled through the ratio of the resistance of Element 2 to Element 1. If the individual elements were perfect uniaxial strain measuring devices, then the ratio would be

$$\frac{R_2}{R_1} = k_s = \mu_o$$

This ratio is only approximate, however, because each individual element has a small but measureable transverse sensitivity coefficient of its own. Correction of the approximate resistance ratio can be made through actual calibration or by computation from the known characteristics of the individual elements.

Using the resistance ratio as a guide, the following table shows some possible combinations of gage resistance values for $\mu_o = 0.30$.

Case	R_1	R_2	$R_1 + R_2$
1	120	36	156
2	92.5	27.5	120
3	350	105	455
4	269	81	350

It appears that cases 1 and 3, in which the resistance of the single strain measuring element, R_1, conforms to conventional strain gage resistance values, are the more desirable. In general, instrumentation systems will accommodate an increase in gage resistance over the common values better than a decrease. In addition, an increase in gage resistance will reduce extraneous effects, such as those caused by lead wire resistance.

The "stress gage factor", F_s, should not be confused with the "strain gage factor" supplied with the more conventional single element or multiple element rosette type strain gages. Although both have the same dimensional units, ohms/ohm/in./in., they actually relate to different quantities. The "strain gage factor" is the proportionality constant relating the unit change of resistance of a strain gage to the total axial mechanical strain to which it is subjected. In contrast, the "stress gage factor" is the proportionality constant relating the unit change in resistance of a stress gage to σ_a/E, where σ_a is the stress along the gage axis and E is the modulus of elasticity of the material to which it is bonded. σ_a/E is, of course, a strain, but is not the total mechanical strain except under very special conditions. A stress gage may be regarded as an automatic computer that solves the general stress-strain equations, rejects the axial component of strain due to stress in a transverse direction, and responds only to that component of strain produced by the stress in the axial direction. The fundamental relationship, then, for interpreting the result of a stress gage measurement is

$$\frac{\sigma_a}{E} = \frac{\Delta R}{R} \times \frac{1}{F_s} .$$

ERRORS FROM MISMATCH OF TRANSVERSE SENSITIVITY COEFFICIENT TO POISSON'S RATIO:

Ideally, the transverse sensitivity coefficient, k_s, of a stress gage should be exactly equal to Poisson's ratio, μ, of the material to which the gage is bonded. This precise condition will seldom be obtained in actual practice, however, because of the wide range of Poisson's ratios exhibited by common structural materials, the lack of accurate data concerning the exact value of Poisson's ratio for the particular condition of the test specimen material, and because of normal gage manufacturing tolerances.

To determine the reading error caused by a mismatch of k_s and μ, consider the equation for the response of a stress gage when exposed to a general stress field as already derived in Equation 8.

$$\frac{\Delta R}{R} = \frac{F_a}{E} \left[\sigma_a \left(1 - \mu k_s \right) + \sigma_n \left(k_s - \mu \right) \right] \tag{8}$$

The apparent stress, $(\sigma_a)c$, obtained from the change in resistance given in Equation 8 and from the stress gage factor given with the gages will be, from Equation 11,

$$\begin{aligned} (\sigma_a)c &= \frac{E}{F_s} \times \frac{\Delta R}{R} \\ &= \frac{E}{F_s} \times \frac{F_a}{E} \left[\sigma_a \left(1 - \mu k_s \right) + \sigma_n \left(k_s - \mu \right) \right] \\ &= \frac{F_a}{F_s} \left[\sigma_a \left(1 - \mu k_s \right) + \sigma_n \left(k_s - \mu \right) \right] \end{aligned} \tag{13}$$

The true stress is, of course, σ_a. The error, e, in the calculated stress is

$$e = \frac{(\sigma_a)c - \sigma_a}{\sigma_a}$$

$$= \frac{\frac{F_a}{F_s}\left[\sigma_a(1 - \mu k_s) + \sigma_n(k_s - \mu)\right] - \sigma_a}{\sigma_a} \tag{14}$$

$$= \frac{F_a}{F_s}\left[(1 - \mu k_s) + \frac{\sigma_n}{\sigma_a}(k - \mu)\right] - 1.$$

But, from Equation 12,

$$F_a = \frac{F_s}{1-\mu_o k_s}. \tag{15}$$

Then, by substituting the above for F_a in Equation 14,

$$e = \frac{1}{1-\mu_o k_s}\left[(1 - \mu k_s) + \frac{\sigma_n}{\sigma_a}(k_s - \mu)\right] -1$$

$$= \frac{\left[(1-\mu k_s) + \frac{\sigma_n}{\sigma_a}(k_s-\mu)\right] - (1-\mu_o k_s)}{1-\mu_o k_s}$$

$$= \frac{k_s(\mu_o-\mu) + \frac{\sigma_n}{\sigma_a}(k_s-\mu)}{1-\mu_o k_s}. \tag{16}$$

Since $\mu_o = k_s$, the condition under which F_s was established, the error expression can be further simplified to

$$e = \frac{\left(k_s + \frac{\sigma_n}{\sigma_a}\right)\left(k_s-\mu\right)}{1-k_s^2}. \tag{17}$$

Equation 17, then, is the general expression for the error in a stress gage reading caused by mismatch of k_s to μ. Note that when $k_s = \mu$, the intended condition of use, the error is zero.

The general error expression contains three variables, k_s, μ, and the ratio σ_n/σ_a, and therefore canno. be represented on a single comprehensive graph. The following series of graphs, however, show error function plots under enough conditions to permit determination of the probable error for practically any combination of conditions.

Figure 2 shows the percent error in calculated stress versus the difference between the transverse sensitivity coefficient and Poisson's ratio, $(k_s-\mu)$, for fixed ratios of σ_n/σ_a ranging from -1 to +1 and for μ of 0.28. and 0.33. These are the only graphs in which the error function is not a perfectly straight line. The deviation from linearity is small, however.

Figure 3 shows the percent error in calculated stress versus Poisson's ratio for fixed values of σ_n/σ_a ranging from -1 to +1 and for fixed values of k_s of 0.28, 0.30 and 0.33, respectively.

Figure 4 shows the percent error in calculated stress versus Poisson's ratio for fixed values of k_s of 0.26, 0.28, 0.30, and 0.33 under uniaxial stress conditions only, when $\sigma_n/\sigma_a = 0$. These same conditions are presented separately as a part of Figure 3.

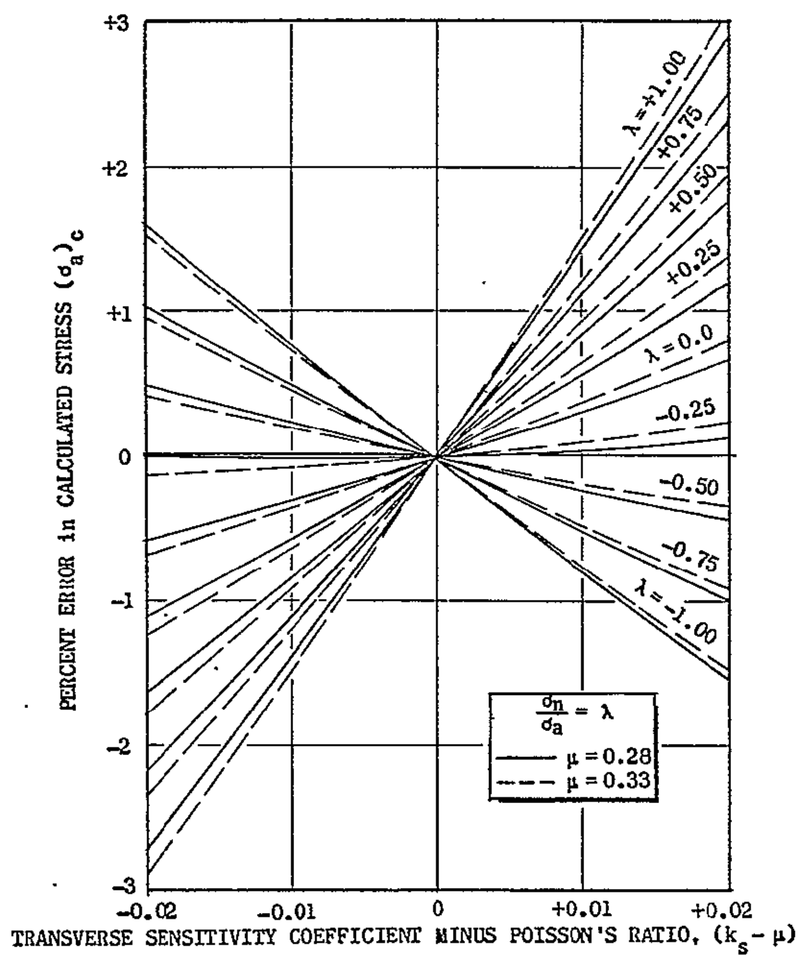

Figure 2 Percent error in calculated stress versus the difference between gage transverse sensitivity coefficient and Poisson's ratio for two values of Poisson's ratio.

Figure 5 shows the percent error in calculated stress versus the stress ratio σ_n/σ_a for a number of fixed combinations of k_s and μ. The combinations of k_s and μ have been chosen as representative of those that might be met in practice when using a stress gage on a material other than that for which it was intended. The stress ratio has been extended to -2 and +2 with the significant range limits marked at -1 and +1. Beyond this range the stress being measured is not the maximum and is therefore of lesser importance.

In all of the error function plots shown here, the basic variables cover rather wide ranges, and the magnitude of the error is consequently quite large at some of the limits. These extremes are not apt to be encountered in practice, however, if any effort at all is made to match the stress gage to the test specimen material.

TRUE STRESSES FROM TWO ORTHOGONALLY MOUNTED STRESS GAGES

In any case where μ does not match k_s, and where the best possible measuring accuracy is required, the true stresses can be obtained from two stress gages mounted at right angles to each other. The solution of two simultaneous equations based on Equation 13, and the relationship in Equation 15, gives

$$\sigma_a = \frac{(1-\mu_o k_s)\left[(1-\mu k_s)(\sigma_a)_c - (k_s-\mu)(\sigma_n)_c\right]}{(1-\mu k_s)^2 - (k_s-\mu)^2} \tag{18}$$

$$\sigma_n = \frac{(1-\mu_o k_s)\left[(1-\mu k_s)(\sigma_n)_c - (k_s-\mu)(\sigma_a)_c\right]}{(1-\mu k_s)^2 - (k_s-\mu)^2} \tag{19}$$

where $(\sigma_a)_c$ is the apparent stress calculated from the response of a gage on the a-a axis and $(\sigma_n)_c$ is the apparent stress calculated from the response of another gage on the n-n axis. In the denominator, the quantity $(k_s-\mu)^2$ is usually very small compared to $(1-\mu k_s)^2$ and can therefore be dropped with little loss in

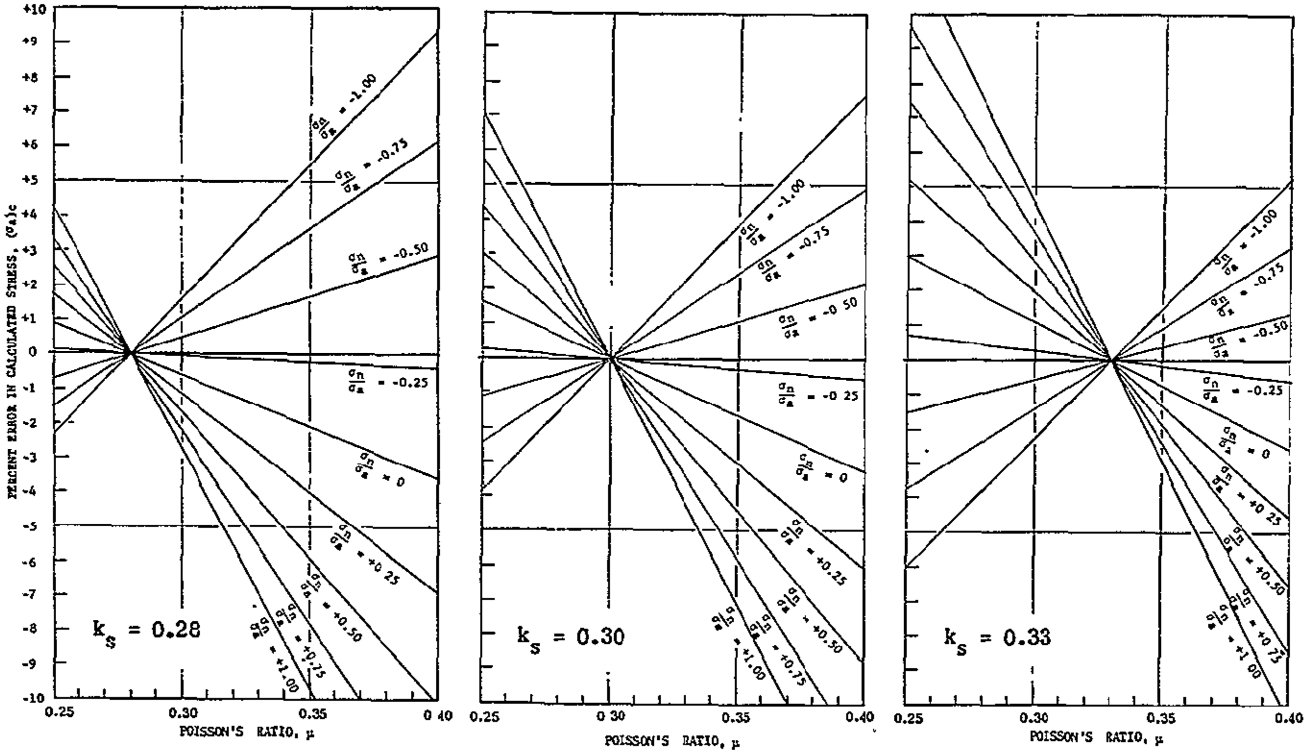

Figure 3 Percent error in calculated stress versus Poisson's ratio using three values of Transverse Sensitivity Coefficient k_s.

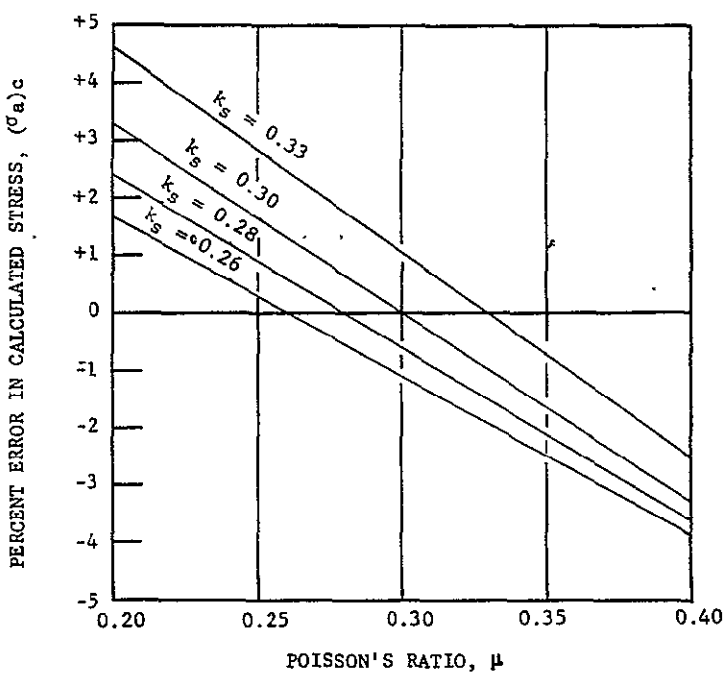

Figure 4 Percent error in calculated stress versus Poisson's ratio for uniaxial stress,

$$\frac{\sigma_n}{\sigma_a} = 0$$

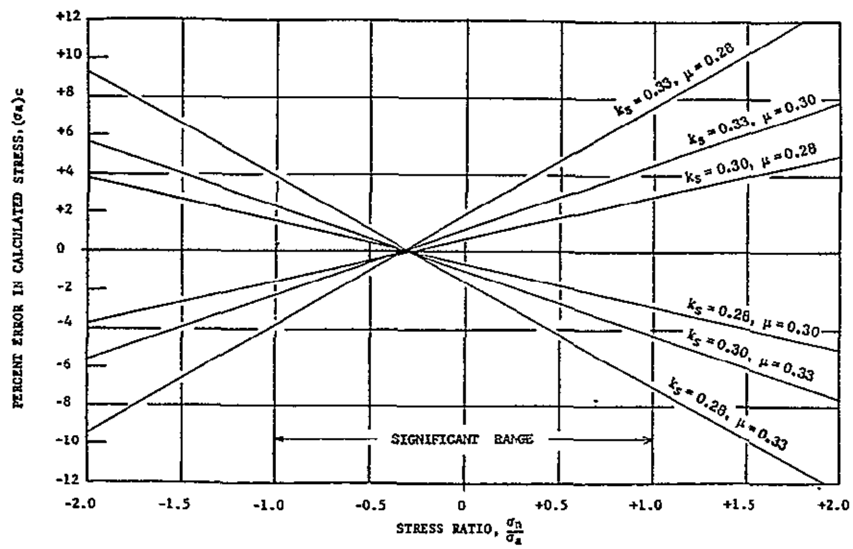

Figure 5 Percent error in calculated stress versus stress ratio for some combinations of k_s and μ.

accuracy. If $k_s - \mu = 0.04$, for instance, the error from dropping this term will be approximately 0.2 percent. Equations 17 and 18 then become

$$\sigma_a = \frac{1-\mu_o k_s}{1-\mu k_s}\left[(\sigma_a)_c - \left(\frac{k_s-\mu}{1-\mu k_s}\right)(\sigma_n)_c\right] \tag{20}$$

$$\sigma_n = \frac{1-\mu_o k_s}{1-\mu k_s}\left[(\sigma_n)_c - \left(\frac{k_s-\mu}{1-\mu k_s}\right)(\sigma_a)_c\right] \tag{21}$$

These simplified expressions will, except in extreme cases, give results that are more accurate than that with which the mechanical properties of the test specimen, such E and μ, are known.

POISSON'S RATIO

Poisson's ratio appears in all general stress-strain formulas and its value is, therefore, of some importance in experimental stress analysis.

Poisson's ratio is normally regarded as one of the fundamental mechanical properties of structural materials. A search of literature from manufacturers of metals and alloys, however, shows that it is omitted almost as often as it is included in the tables of mechanical properties. The indications are that Poisson's ratio and its determination are generally treated somewhat casually by most investigators of the properties of metals and alloys. Only infrequently is its value given beyond two significant figures, the probable accuracy is almost never mentioned, and the method of determination is rarely described. This general indeterminate nature of the value of Poisson's ratio should be recognized when applying stress gages and in solving stress-strain relationships, although it is probably of lesser importance in the latter case.

Table I lists values for Poisson's ratio obtained from various sources, including handbooks and manufacturer's literature. The accuracies of the listed values are unknown and none have been verified. This list is not intended as a reference source, but only to illustrate the range of values and the common practice used in

TABLE I

Material	Poisson's Ratio
Steel	0.28
Structural Steel, Hot Rolled	0.26
Aluminum Alloys	0.33
Magnesium, Pure	0.35
Magnesium Alloys	0.35
HK31A Magnesium-Thorium	0.34
17-7PH Stainless	0.28
Inconel	0.29
Inconel X	0.29
Monel	0.32
Duranickel	0.31
Permanickel	0.31
Zircoloy 2, Annealed, 27°C	0.368 to 0.380
Annealed, 150°C	0.425 to 0.460
Cold Worked, 27°C	0.382 to 0.406
Cold Worked, 150°C	0.392 to 0.432
Invar, 36 Percent Ni	0.290
Dumet, 42 Percent Ni	0.290
51 Percent Fe, 49 Percent Ni	0.290
Titanium, Comm. Pure	0.34
Stainless W, 75°F	0.20 to 0.23
300°F	0.19 to 0.24
500°F	0.20 to 0.24
700°F	0.21 to 0.27
Columbium	0.38
Rhenium	0.49
Tungsten	0.284
Vanadium	0.36
Copper	0.33 ±0.01
Brass	0.33
Cast Iron	0.21 to 0.30
Molybedenum, 100°F	0.324 ±4 percent
250°F	0.330 ±4 percent
500°F	0.319 ±4 percent
770°F	0.317 ±4 percent
1200°F	0.314 ±4 percent
1300°F	0.321 ±4 percent
1600°F	0.321 ±4 percent
Silver, Annealed	0.37
Hard	0.39
Platinum	0.39

reporting them. Strain gage users with a need to know accurate values of Poisson's ratio are urged to use original sources or to determine their own values experimentally.

In the absence of any evidence to the contrary, it may be assumed that a large percentage of the experimental measurements of Poisson's ratio have been made with bonded resistance strain gages. Such gages have been generally accepted in metallurgical and other laboratories for many years, the method of measurement is simple and easy to employ, and it will give results of adequate accuracy provided the applicable strain gage characteristics are known and used properly. It is the question of whether or not the gages were properly used and the results correctly interpreted that raises doubt concerning the validity and accuracy of much of the published data.

The conventional method of determining Poisson's ratio with bonded resistance strain gages is by measurement of axial and transverse strains on a standard tensile test specimen, either flat or round type, under applied load. Conventional single element strain gages or double element 90°X gages, not stress gages, should be used. The best arrangement of gages is that of two axial gages positioned directly opposite each other on a flat specimen or diametrically opposite on a round specimen, and two circumferential or transverse gages also positioned directly opposite each other. Readings of each pair of similarly positioned gages are averaged to cancel the bending strains always present in tensile specimens and which, incidentally, can be quite substantial in magnitude. The ratio of the transverse or circumferential gage readings to the axial gage readings, <u>properly corrected for the transverse sensitivity coefficient of the particular gages</u>, is Poisson's ratio. The need for making a correction based on the transverse sensitivity coefficient is emphasized because it is the operation most likely to be neglected or overlooked.

Simple formulas for applying a correction for transverse sensitivity to two similar gages positioned at right angles to each other have been published many years ago.[3] These formulas are

$$\varepsilon_1 = \frac{(1-\mu_o k)(\varepsilon_{c1} - k\varepsilon_{c2})}{1-k^2}, \tag{22}$$

$$\varepsilon_2 = \frac{(1-\mu_o k)(\varepsilon_{c2} - k\varepsilon_{c1})}{1-k^2}, \tag{23}$$

where ε_{c1} and ε_{c2} are the apparent strains given by the gages along ε_1 and ε_2 axes respectively based on the manufacturer's gage factor, F_c, as given with each package of gages, and where μ_o is Poisson's ratio of the bar on which the gages were originally calibrated to determine F_c. The symbol k designates the transverse sensitivity coefficient of the single element gages. Then by definition and from the above two equations,

$$\mu = \frac{\varepsilon_2}{\varepsilon_1} = \frac{(\varepsilon_{c2}-k\varepsilon_{c1})}{(\varepsilon_{c1}-k\varepsilon_{c2})} . \tag{24}$$

Equation 24 is the proper formula for determination of Poisson's ratio from strain gage readings taken from axially and transversely positioned gages on tensile specimens. Note that in the general correction Equations 22 and 23, the algebraic sign of ε_{c1} and ε_{c2} is positive for tensile strains and negative for compressive strains. The same sign convention must also be followed in the special case, Equation 24, so that the sign of μ actually is negative, although the negative sign is normally used only in formulas applying μ.

The magnitude of the error in the determination of Poisson's ratio caused by neglecting the correction for transverse sensitivity is of some interest. Some strain gages have very small transverse sensitivity coefficients and the correction may be omitted if the ultimate in accuracy is not required. To find the error, e, let μ_c be the apparent Poisson's ratio as determined from the uncorrected strain gage readings, then

$$\mu_c = \frac{\varepsilon_{c2}}{\varepsilon_{c1}} \tag{25}$$

The error is

$$e = \frac{\mu_c-\mu}{\mu} \tag{26}$$

which from Equations 24 and 25 becomes

$$e = \frac{\dfrac{\varepsilon_{c2}}{\varepsilon_{c1}} - \dfrac{\varepsilon_{c2}-k\varepsilon_{c1}}{\varepsilon_{c1}-k\varepsilon_{c2}}}{\dfrac{\varepsilon_{c2}-k\varepsilon_{c1}}{\varepsilon_{c1}-k\varepsilon_{c2}}} . \tag{27}$$

This expression reduces to

$$e = \frac{k(\varepsilon_{c1}^2 - \varepsilon_{c2}^2)}{\varepsilon_{c1}(\varepsilon_{c2}-k\varepsilon_{c1})} . \tag{28}$$

But, from Equations 22 and 23,

$$\varepsilon_{c1} = \frac{\varepsilon_1 + k\varepsilon_2}{1-\mu_0 k} , \tag{29}$$

$$\varepsilon_{c2} = \frac{\varepsilon_2 + k\varepsilon_1}{1-\mu_0 k} . \tag{30}$$

By substitution in Equation 28 the error expression becomes

$$e = \frac{k\left[\left(\frac{\varepsilon_1 + k\varepsilon_2}{1-\mu_o k}\right)^2 - \left(\frac{\varepsilon_2 + k\varepsilon_1}{1-\mu_o k}\right)^2\right]}{\frac{\varepsilon_1 + k\varepsilon_2}{1-\mu_o k}\left[\left(\frac{\varepsilon_2 + k\varepsilon_1}{1-\mu_o k}\right) - k\left(\frac{\varepsilon_1 + k\varepsilon_2}{1-\mu_o k}\right)\right]} \tag{31}$$

which reduces to

$$e = \frac{k\left(\varepsilon_1^{\,2} - \varepsilon_2^{\,2}\right)}{\varepsilon_2\left(\varepsilon_1 + k\varepsilon_2\right)} \;. \tag{32}$$

In the case of uniaxial stress,

$$\varepsilon_2 = \mu\varepsilon_1 \;. \tag{33}$$

Then Equation 32 becomes

$$e = \frac{k\left(\varepsilon_1^{\,2} - \mu^2\varepsilon_1^{\,2}\right)}{-\mu\varepsilon_1\,(\varepsilon_1 - k\mu\varepsilon_1)} \tag{34}$$

$$= \frac{-k(1-\mu^2)}{\mu(1-k\mu)} \;.$$

Equation 34 is the general expression, in terms of k and μ, for the error in the determination of Poisson's ratio caused by neglecting the transverse sensitivity coefficient k. Figure 6 shows graphs of the percent error in calculated Poisson's ratio versus the transverse sensitivity coefficient, k_s, of the gage for values of μ of 0.28, 0.30 and 0.33. For reference purposes the transverse sensitivity coefficients of a few of the most commonly used SR-4 wire and foil type strain gages are marked on the graph. It is obvious that the error can be quite large in some cases and that the proper correction is required.

Figure 6 also reveals a simple rule of thumb for estimating the approximate error, ie., the error is approximately three times the transverse sensitivity coefficient but opposite in algebraic sign. For example, gages having k = +1 percent (+0.01) will give an error of approximately -3 percent in μ if uncorrected. This rule leads the simple approximate correction formula.

$$\mu \approx \frac{\mu_c}{1-3k} = \frac{1}{1-3k}\left(\frac{\varepsilon_{c2}}{\varepsilon_{c1}}\right) \tag{35}$$

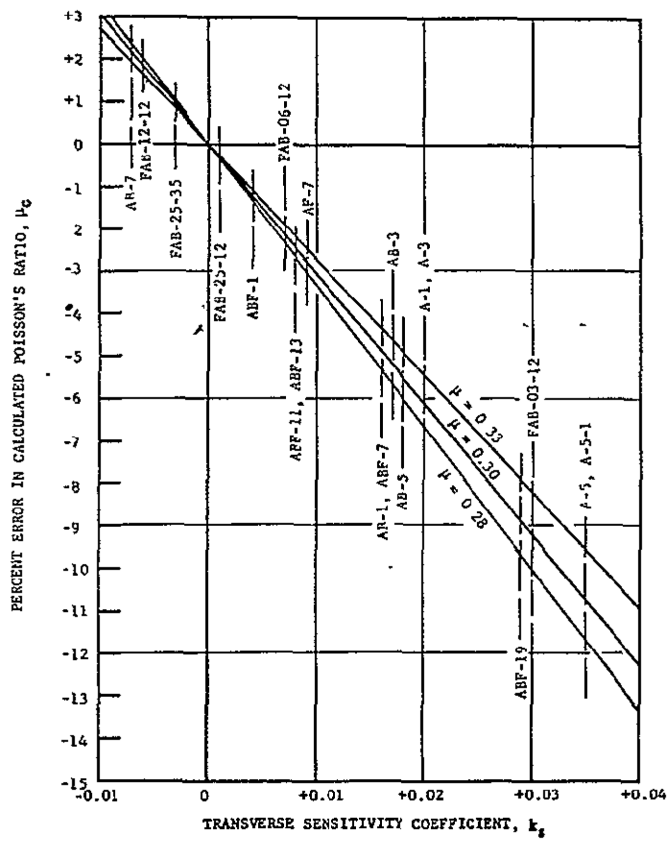

Figure 6 Error in determination of Poisson's ratio caused by neglecting the correction for strain gage transverse sensitivity.

Tables of the mechanical properties of materials frequently contain values for both E, the modulus of elasticity in tension and compression, and for G, the modulus of elasticity in shear or the modulus of rigidity. The relation between E and G is given, from the general theory of elasticity, as

$$G = \frac{E}{2(1+\mu)}.$$

Solving the above expression for μ, Poisson's ratio, gives

$$\mu = \frac{E-2G}{2G}$$

If Poisson's ratio is unknown, it would appear that it could be computed from this expression, using the given values of E and G. The use of this method is unacceptable, however, because of the magnification of errors that is inherent in the formula. The computed value of μ will be in error by approximately 5 percent for a 1 percent error in E, and by approximately 10 percent for a 1 percent error in G. It is thus evident that this method cannot be used for an accurate determination of Poisson's ratio.

REFERENCES

1. Williams, Sidney B., "The Dyadic Gage", Proceedings of the Society for Experimental Stress Analysis, Volume I, No. 2, 1944, pp. 43-55.

2. Williams, Sidney B., (to Curtis-Wright Corporation), "Strain Responsive Gauge", U. S. Patent 2,592,223, April 8, 1952.

3. Baumberger, R. and Hines, F., "Practical Reduction Formulas for Use on Bonded Wire Strain Gages in Two-Dimensional Stress Fields," Proceedings of the Society for Experimental Stress Analysis", Volume II, No. 1, 1944, pp. 113-127.

THE BOEING WIND TUNNEL FORCE MEASUREMENT PROGRAM

THE BOEING COMPANY
Wind Tunnel Laboratory
Seattle, Washington

APPENDIX B

THE BOEING WIND TUNNEL FORCE MEASUREMENT PROGRAM

T. M. Curry
The Boeing Company

The Boeing Wind Tunnel Laboratories Unit consists of five major wind tunnels ranging from subsonic and transonic through supersonic, hypersonic, and hypervelocity such as our 8-inch and 44-inch Hotshot tunnels. In addition we have three pilot tunnels, two shock tubes, and a hypervelocity ballistic range. Out of town tests are scheduled in government and contractors facilities on a more or less regular basis. With the exception of the shock tubes and the ballistics ranges we are running force tests in an average of about a dozen research facilities.

The Boeing Wind Tunnel Unit has some 90 multi-component internal sting balances currently in active scheduling. These designs represent many different approaches based on analysis and experience which are in general, tailored to the testing requirements. The identification charts of Supplement 1 show most of our balances graphically associated with the facility and type of vehicle for which they were designed. It is our philosophy to utilize those concepts of measurement which seem to best suit the situation, remembering that a successful balance represents many compromises. Thus the balances that Boeing develops show a high degree of variation in appearance and in the general principles utilized.

The development of multi-component strain gage balances for our wind tunnel tests falls in three separate categories:

1. Internal balance requirements based on long range forecasting for specific types of aircraft tests (i.e., missiles, airplanes, boost glide, etc.).
2. Requirements for internal balances based on specific tests for specific model configurations.
3. Requirements for special purpose balances for control surfaces, fins, nacelles, etc. for specific model configurations.

The first of these categories permits the most sophisticated analytical and fabrication techniques in that the long lead time (six months to a year) is anticipated. The second and third categories permit only one to four months of development and therefore, the most simplified techniques are justified.

All of our designs reflect not only the testing requirements but the facilities at our disposal for design, fabrication, heat treating, gaging, calibration and data reduction. We are fortunate in the emphasis that Boeing places on the value of Wind Tunnel testing which results in priority usage of existing company facilities and a cooperative outlook in helping us get the tools and manpower required to do the job right. High speed digital computing facilities are available to aid us in programmed computations for balance design criteria, stress analysis for generalized balance configurations, preparations of tables of section properties, force calibration data reduction, and wind tunnel test data reduction. Special machinery for the fabrication of balances, such as Eleroda and Japax electric discharge milling equipment has been installed in our balance development machine shop. This permits the construction of balance configurations, otherwise impossible, so that maximum utilization of material and space may be realized. Advantage is taken of our high quality metallurgical facilities and personnel at Boeing. Salt bath martempering is used on all of our steel balances with the advantages of extremely low warpage and surface scale during heat treat. This permits heat treating after finishing most of the surfaces on the balances.

Because of the size of the investment and cost of testing time it is of prime importance that the balance designs should reflect strong emphasis on dependability, reliability and utility. Considerable effort is made to minimize sources of random and unpredictable errors such as temperature effects and mechanical hysteresis. However, because of our ability to handle compensatable errors, such as interactions, we are only secondarily interested in minimizing them and then not at the expense of reliability. This is not to say that our design approach sacrifices accuracy but definitely emphasizes reliability because of the fine support that we have for calibration and data reduction.

Likewise, another design aim is to minimize the amount of compensation apparatus and extra equipment associated directly with the balance and model so that we may reduce the sources of human and mechanical error. This, too, has contributed to our reliance on rather sophisticated laboratory calibration techniques and off line digital data reduction programs for compensating predictable errors mathematically.

This philosophy has led us toward one piece balance designs whose outputs are directly proportional to the components to be measured. Some of our balance development techniques will be discussed in the following text.

1. Stress Cancellation Moment Transfer Technique The limited space available for the construction of internal balances poses especially severe problems in the design of the axial force element because of the other loads which must be supported, but not measured by this element. One of the problems is that the axial force element is that part of the balance structure which is characteristically, weakest to bending moments. Hence, in most of our compact (high loads-small space) designs the axial force element is located at the station about which moments are to be reduced, since statistically the maximum bending moments about that point are lowest (Figure 1a).

1(a)

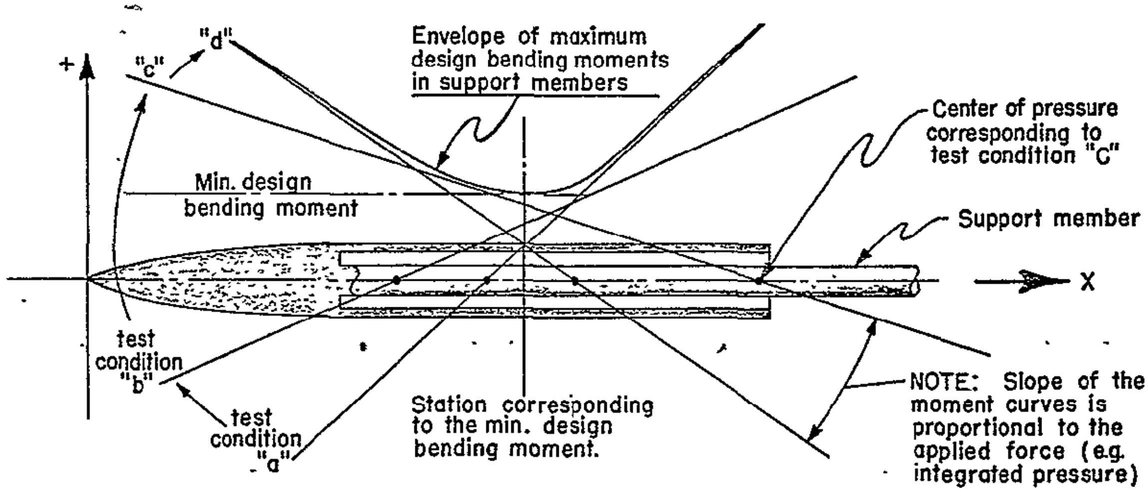

1(b)

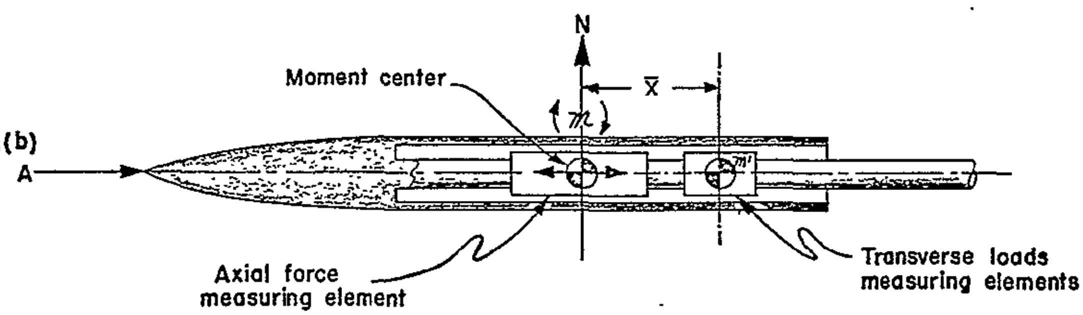

Figure 1.

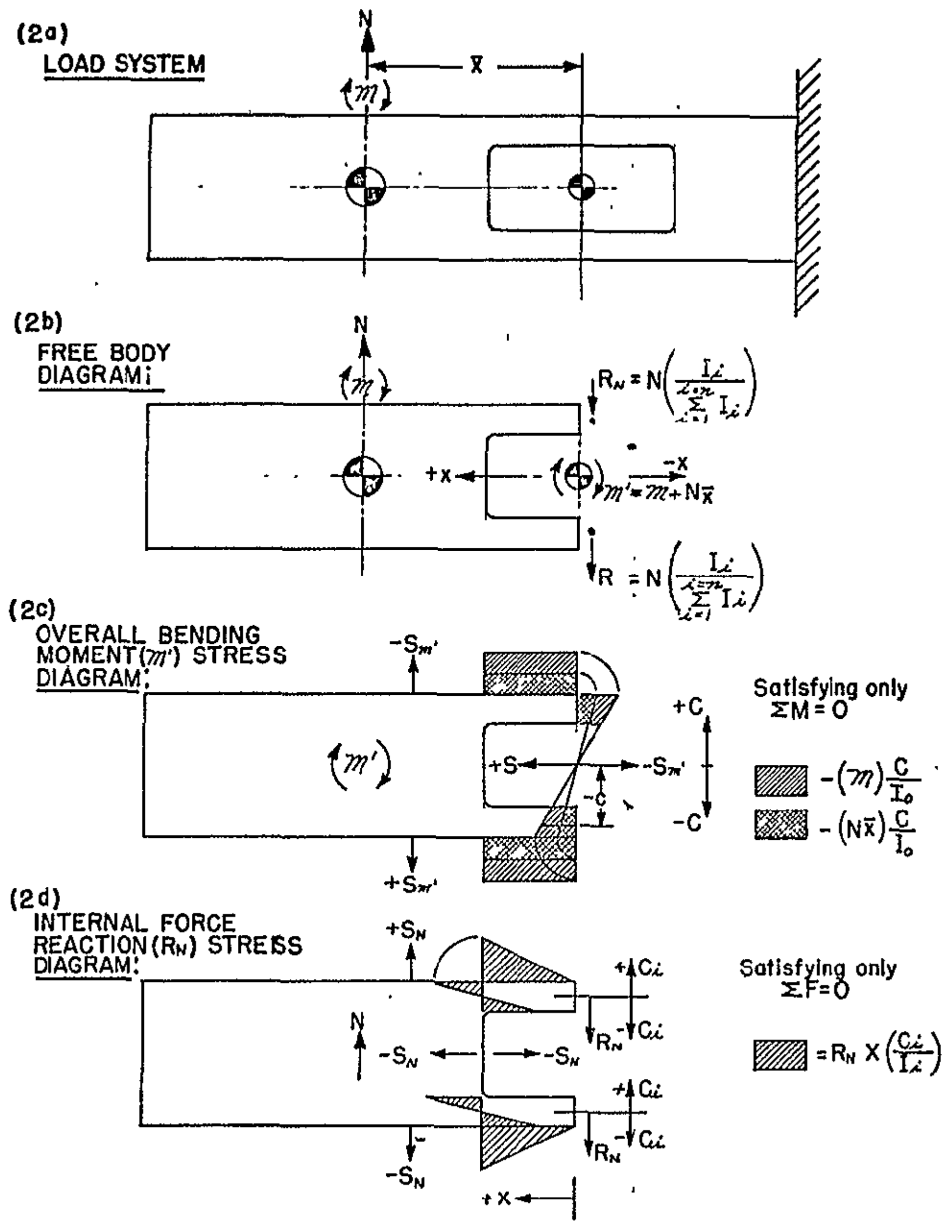

Figure 2.

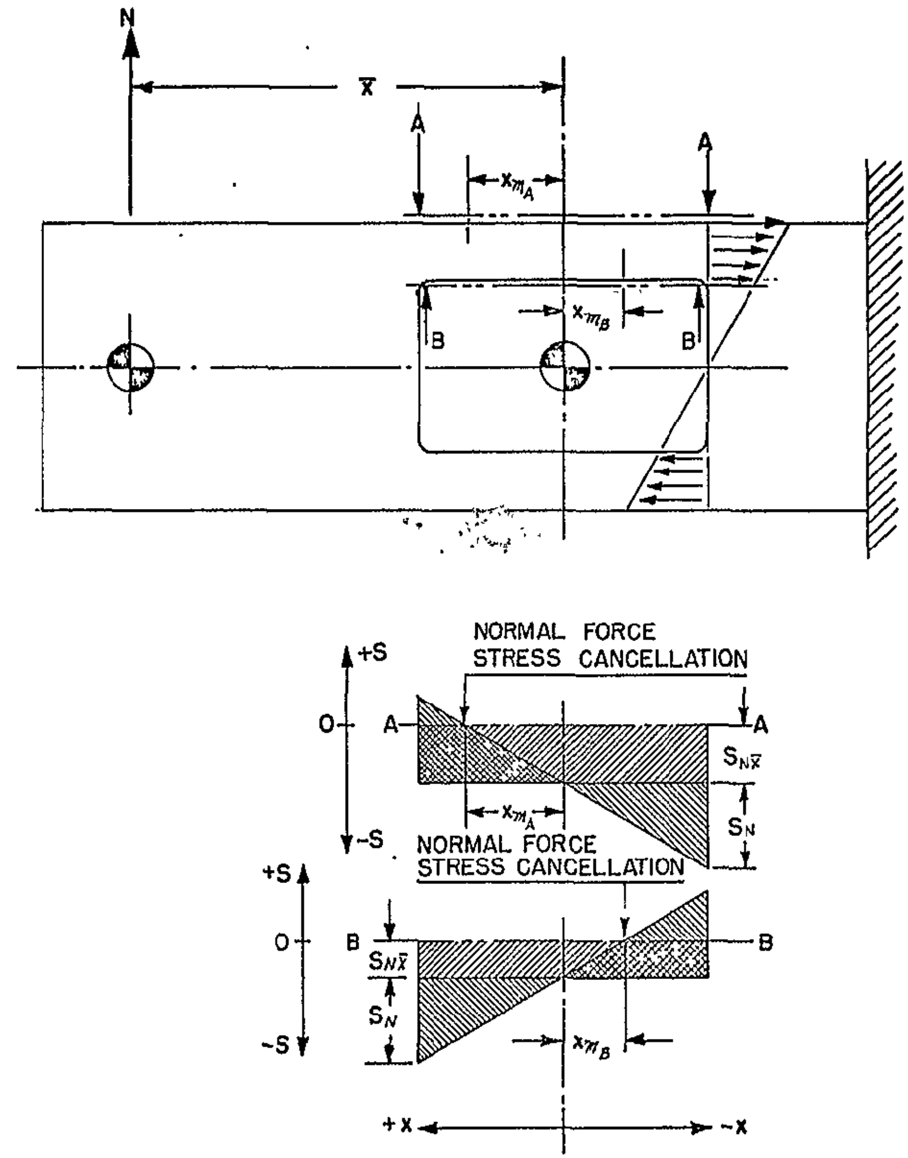

Figure 3.

In order to measure moments about the moment center with our typical five component cage which is located remotely from the moment center (Figure 1b), it has been necessary to transfer moments from the center of the cage either electrically through an anolog device or mathematically. The subject of the discussion in Supplement 2 is a parallel member cage on which advantage is taken of the fact that two sources of normal force (or side force) stress due to force applied at the moment center tend to cancel. (See Figure 2.) Points are picked on the structure at which the normal force stresses are zero. Hence, pitching moment gages may be handily mounted there, which are outside of the influence of the normal force; thus, they read moments about the moment center (see Figure 3) regardless of the magnitude of the normal force.

This technique has been developed for use in two component (normal force and pitching moment) and five component cages (normal and side forces, pitching, yawing, and rolling moments) of which our balances 3124A and 6132A and B (Figures 4 and 5, respectively) are typical examples. The analysis and mathematics of the design, which are given in Supplement 2, have been programmed for use in selecting balance configurations. Final stress analyses of the selected configurations, which have also been digitally programmed, appear in Supplement 3.

2. High Frequency Response Balances for Hypervelocity Hotshot Testing Extremely high Mach numbers and temperatures may be achieved for very short time durations in our "Hotshot" (arc discharge, hypervelocity) wind tunnels. Aerodynamic force balance designs for these facilities, otherwise enhanced by low q's and the relatively high temperature inertia of the model - balance structure, are fraught with instrument dynamics problems associated with the short time duration of the aerodynamic loads to be measured.

The technique of inertia compensating a force balance with accelerometer outputs can, if analysis is applied rigorously, provide true aerodynamic loads data. However, at the Boeing Hotshot facilities we have utilized another approach:

The output of the force transducer (essentially an undamped system) is comprised of aerodynamic loads and inertia loads. In order to filter out the inertia loads, either by curve fairing or with electronic filters, it is necessary to separate the structural natural frequencies from the frequency components of the aerodynamic forcing function by as large an order as possible. This approach minimizes the phase shift and amplitude distortion to the relatively lower aerodynamic frequencies in low pass electronic filters, or permits accurate curve fairing through the relatively higher inertial frequencies when using unfiltered traces.

The advantages of this approach are the comparatively simple model installation and data handling procedures. However, the problems in designing a model support system, including the support base, angle sector, sting, and internal balance, with sufficiently high natural frequencies are considerable. To these ends we have programmed sting frequency and amplitude parameters for digital computation in selecting suitable sting configurations.

The balance shown in Figures 6, 7 and 8 is a design which emphasizes high structural natural frequencies; hence, high response rates for the dynamic forcing functions which must be measured by the balance. Additional advantages are achieved by the compactness of the design and the relatively simple procedure required to fabricate this balance from one piece of metal. One piece construction eliminates problems caused by relative motions in discontinuous joints and the resulting dry friction which is undesirable in making dynamic measurements. Figure 8, not to scale, shows position of the gages on the balance structure required to measure the six components of the resultant force and moment.

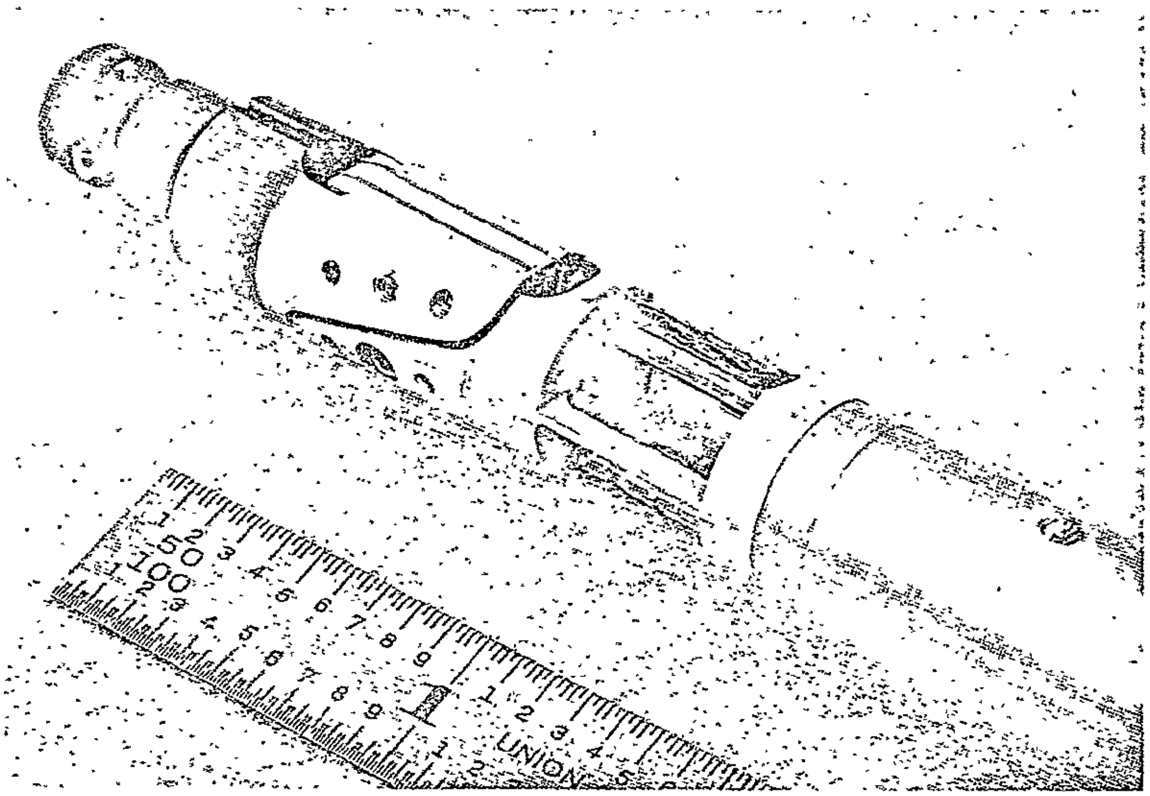

Figure 4.

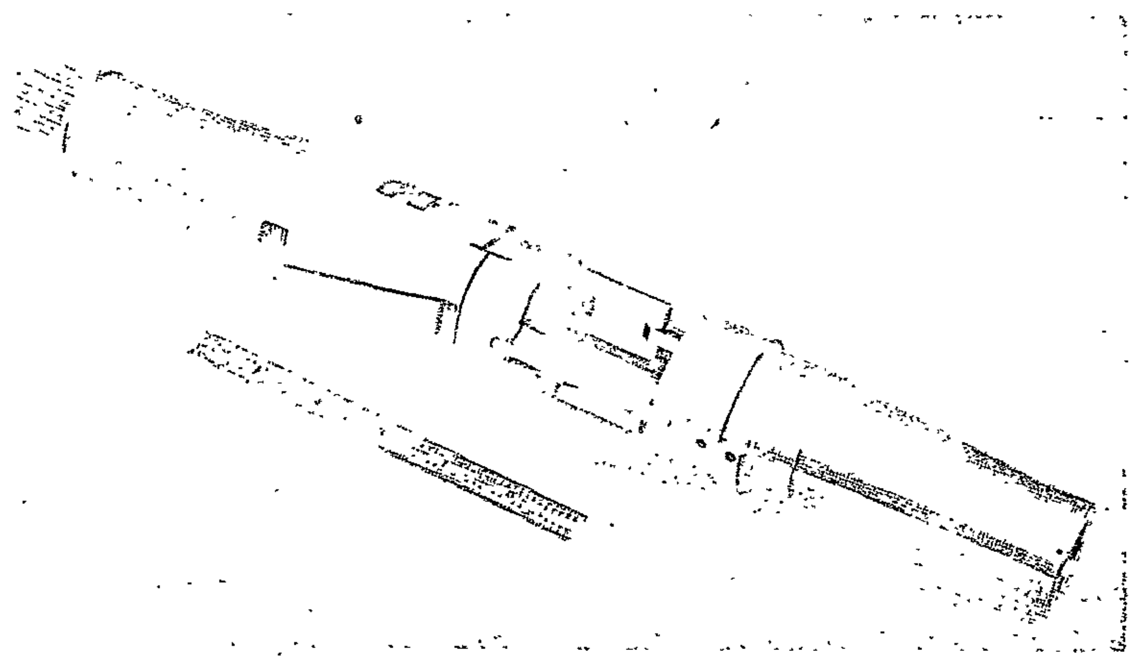

Figure 5.

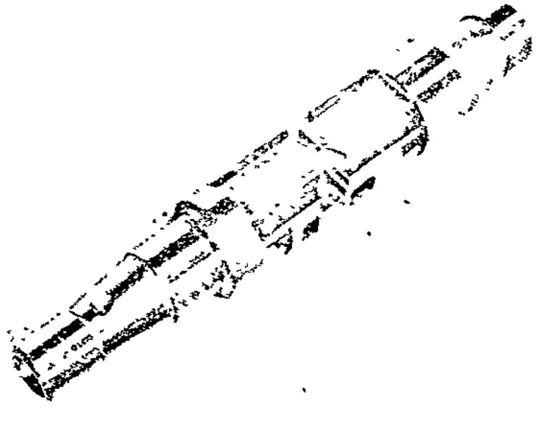

Figure 6.

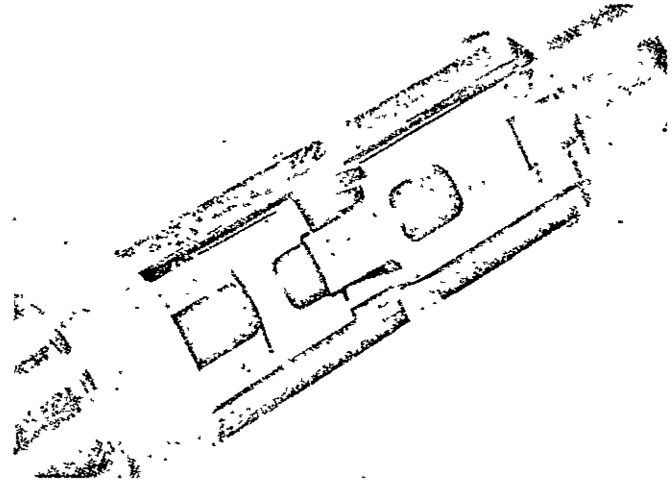

Figure 7.

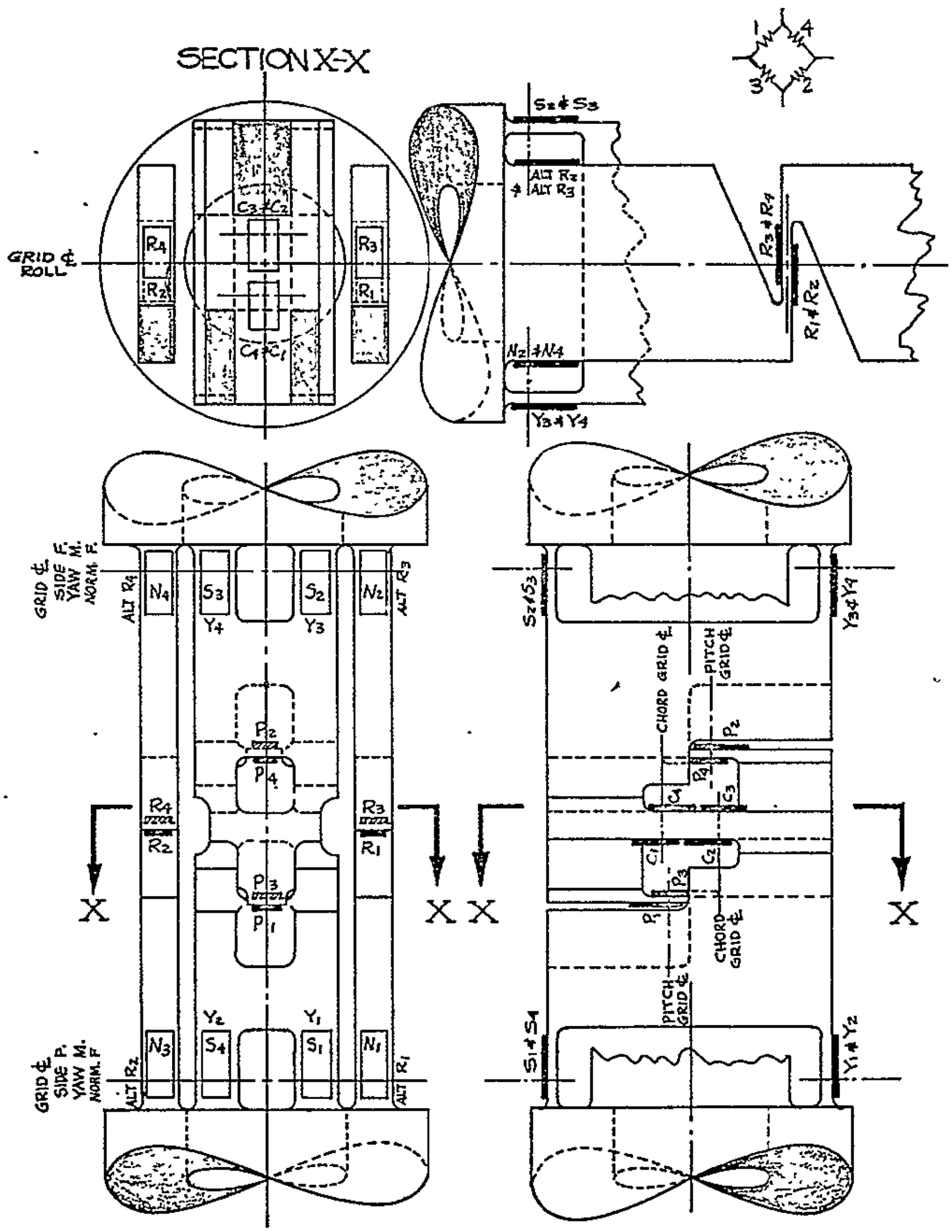

Figure 8.

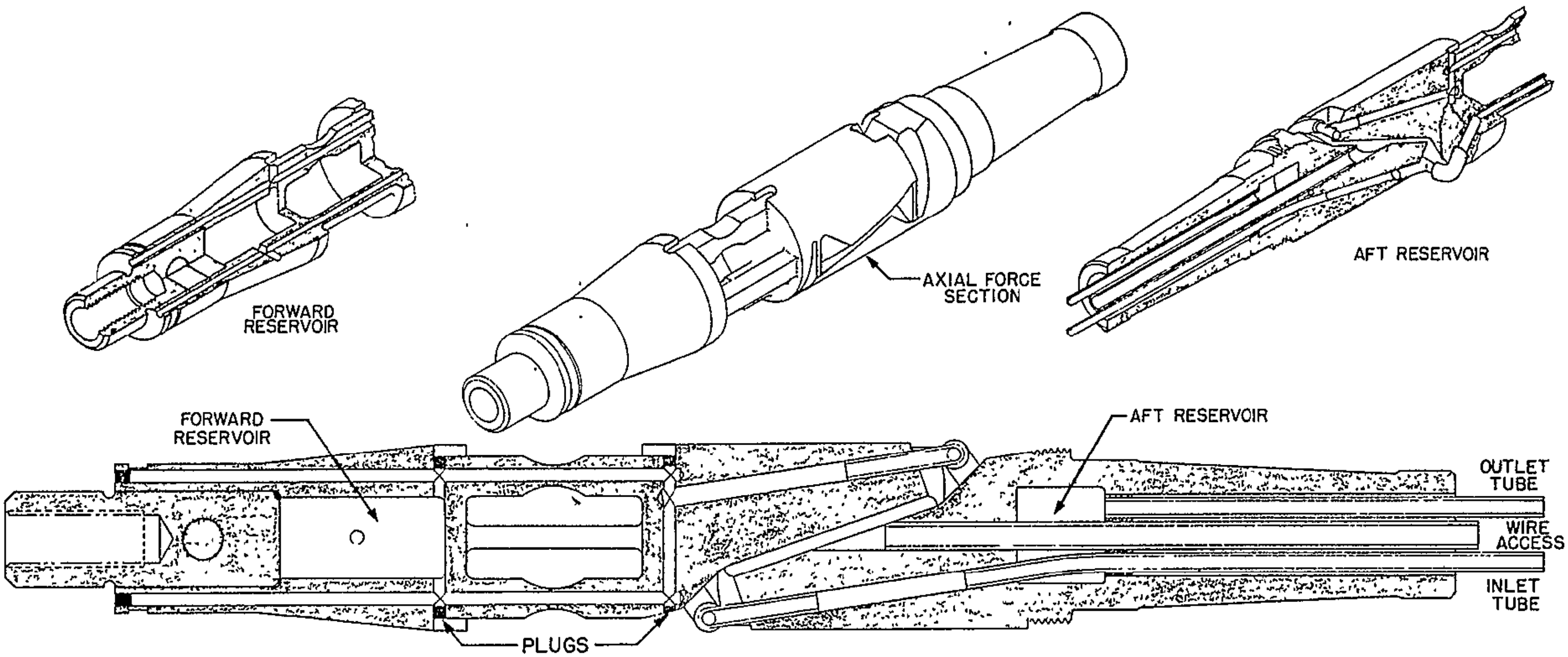
FORWARD RESERVOIR
AXIAL FORCE SECTION
AFT RESERVOIR
FORWARD RESERVOIR
AFT RESERVOIR
OUTLET TUBE
WIRE ACCESS
INLET TUBE
PLUGS

Figure 9.

In order to keep the balance configuration as stiff as possible, the measuring elements are designed so that as large a percentage as possible of the load components to be measured are supported by their respective measuring elements. The percentage of the loads not measured (but supported) by those elements is minimized by making the measuring elements as limber as possible to components of loading not being measured by them.

Thus, designing the measuring elements to the relatively high loads results in relatively thick bending sections. This gives more stiffness for a given measured bending strain level resulting in high element natural frequencies.

3. <u>Water Cooled Balance Designs</u> The development of high temperature commercial strain gages has not achieved the degree of reliability and accuracy that warrants their use on our wind tunnel force transducers (balances). We have, therefore, chosen the course of water cooling our balances. Some of our earlier attempts incorporated an inner body which acted as a reservoir to which were attached inlet and outlet tubes which spiraled around the balance and sting. Although this technique was successful, it was bulky and difficult to apply in our smaller models.

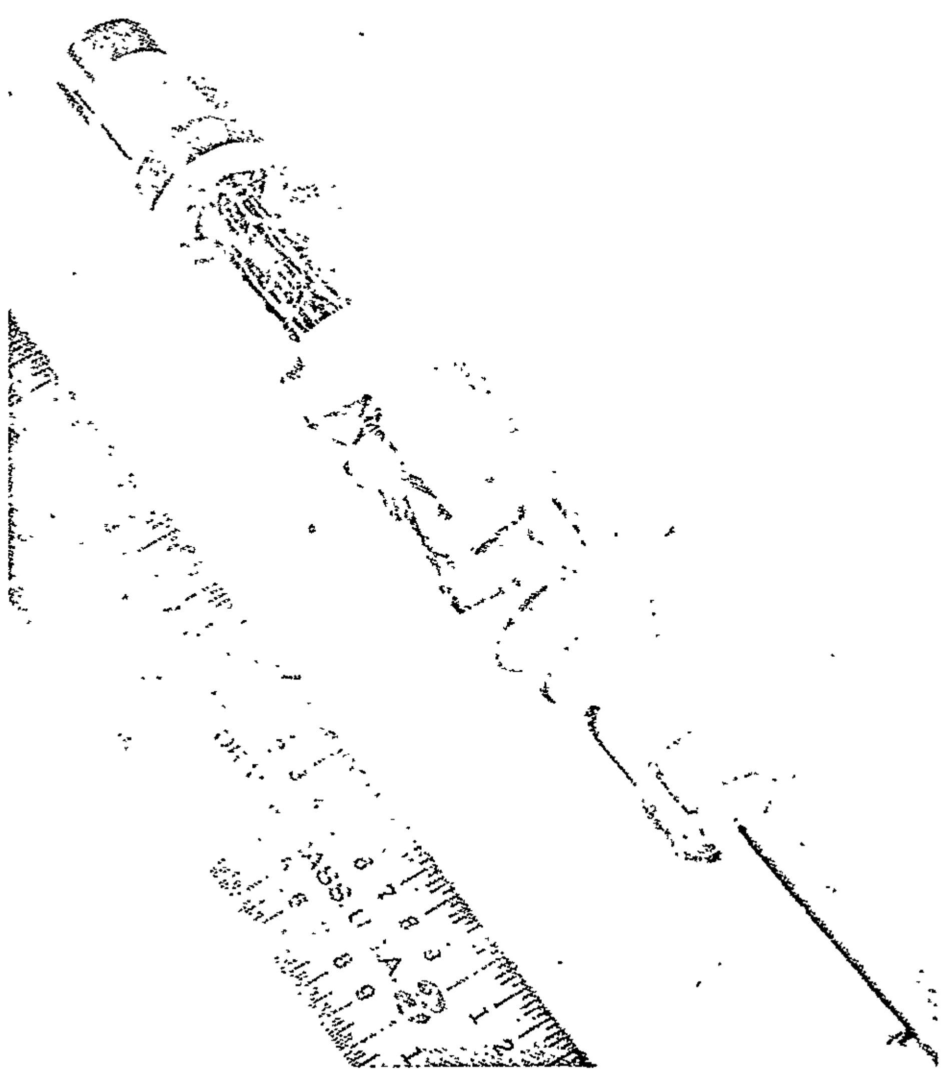

Figure 10. Balance number 5158-W

More recently we have been building one piece balances which are so drilled and bored that we achieve water cooled members in our moment cages with reservoirs in the forward model fitting and aft sting fitting. Figure 9 shows several views of our balance design 6148, a six component balance designed for hypersonic missile testing. This balance is .85 inch in diameter and has soft rubber jumper tubes bridging the axial force element. Fiberglass wool insulation is installed around the flexures and the entire actively strained portion of the balance is covered with an aluminum foil radiation shield to minimize the temperature gradients due to local conduction from ambient air and radiation from the model.

The smallest water cooled balance we have designed to date is a five component balance for hypersonic Dyna Soar testing which is .40 inch in diameter and about three inches long. This balance, which bears the number 5158, has an axial force range of only .4 pound and a normal force range of 3 pounds (Figure 10).

4. Force Calibration and Data Reduction System   Analysis of the deflection and initial displacement of balance axes in respect to model axes indicate that the equations of gage output of a typical strain gage balance component may be adequately expressed, qualitatively, as a polynomial of the second degree in twenty-seven (for a six-component balance) variables. These variables are the six primary variables of components; their squares; and their cross products.

Thus, the expression for the measured output (θ_M) in arbitrary counts, of a component may be given as follows:

$$(1)\quad \theta_M = K_1N + K_2S + K_3M + \text{——} K_7N^2 + K_8S^2 + K_9M^2 + \text{——} K_{25}NS + K_{26}NM + K_{27}SM$$

of which only one of the linear terms is the primary output of the balance component in question. The form of equation (1) is that which appears most logical to the calibrator wherein he sees an output which can be accounted for by an expression in terms of the external loads applied to the balance.

However, by transposing terms we can achieve an expression for predicting a load component being applied to the balance in terms of the output of that component in arbitrary counts and other load components being applied. Expression (2) below for reducing normal force illustrates this form of the gage output equation which is most useful in force testing.

$$(2)\quad N = \frac{\theta_N}{K_N} - \left(\frac{K_2}{K_N}\right)S + \left(\frac{K_3}{K_N}\right)M + \text{——} \left(\frac{K_7}{K_N}\right)N^2 + \left(\frac{K_8}{K_N}\right)S^2 + \text{——} \left(\frac{K_{25}}{K_N}\right)N.M + \left(\frac{K_{27}}{K_N}\right)S.M$$

The contents in the brackets are the interaction errors which are subtracted from the raw output term ($\frac{\theta_N}{K_N}$ in this case). The individual interaction sensitivity constants are ratioed to the primary component sensitivity constant (K_N in this case) and, thus, the interaction constants (parentheses) are seen to be not a function of instrument sensitivity. Thus, the values of the interaction constants may be determined from calibrations run in the laboratory, while wind tunnel force tests may be run on different, but compatible, readout installations.

Our standardized six-component calibration procedure consists of 35 primary (variable) loading routines and eight initial weight tare calibrations. The initial loadings are substituted in expressions of the form of equation (1) for the "zero" conditions, while the initial and applied loads are substituted for the loaded conditions. These equations are solved simultaneously to derive the constants of the form K_1 through K_{27} in expression (1). Of course, these constants are valid only for the calibration setup. However, by dividing by the appropriate sensitivity constants we achieve the interactions constants as used in wind tunnel force testing (see expression (2)). To aid in test monitoring the size of each term in percent of maximum component range with maximum balance loads applied is also computed.

These computations were originally programmed for the IBM-650 machine but are now performed on our Univac. Any combination of components up to a maximum of six may be computed since the form of the computation is identical for each component. Calibration data at present is plotted and manually faired. The faired values of the zeros and loaded end points and their corresponding loads (both initial and applied) are input to the machine.

These computations, though straightforward, would be tedious and time consuming if performed manually. Our calibration loadings absorb between two to six shifts elapsed time and are performed manually.

One of the more interesting phases of the calibration data reduction program are the methods of checking our data and computations. Using the derived coefficients of our gage output equations the machine program computs theoretical values of the end point meter deflections for each of our standardized calibration conditions. It then subtracts from these the values of the corresponding experimental (calibration) meter deflections. These differences, which we refer to as "random scatter and/or error", represent possible errors in calibration loading, curve fairing, reading the faired curves, data transcribing, and/or machine computation.

By far the most common sources of error are curve reading and data transcribing. These sources of error we hope to minimize soon with a new digitized force calibration readout system and programmed curve fairing.

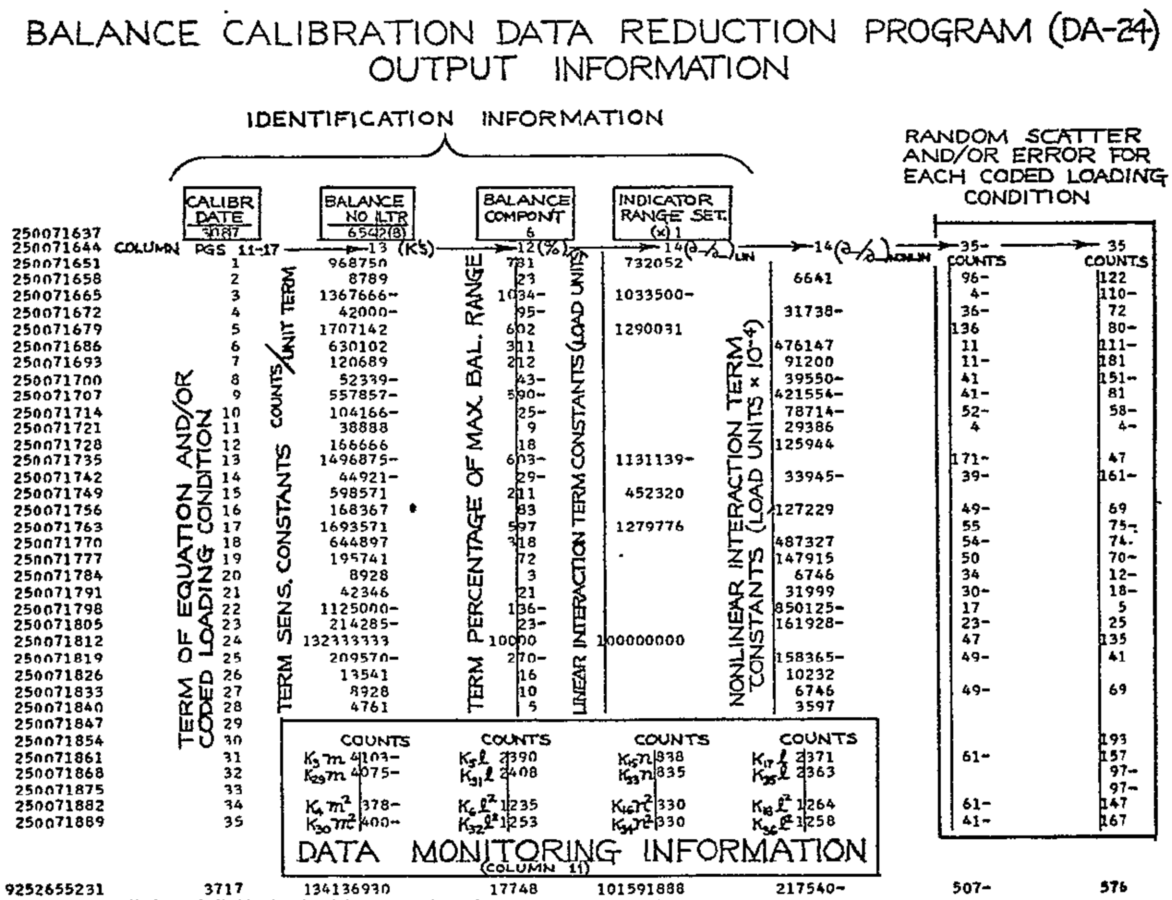

Number of digits to the right of the decimal for the following columns:

Column:

13	LINEAR TERMS:	Five more than the number of digits to the right of the decimal in the input meter readings.
	NONLINEAR TERMS:	Seven more than the number of digits to the right of the decimal in the input meter readings.
12		Two digits for all terms regardless of placement of input meter reading decimal.
14	LINEAR TERMS:	Eight digits regardless of placement of input meter reading decimal.
	NONLINEAR TERMS:	Ten digits regardless of placement of input meter reading decimal.
35&35-		Equal to the number of digits to the right of the decimal of the input meter readings.

Figure 11.

The "random scatter" computation, when coupled with the fact that we compare many of the constants which are computed by several completely independent methods, provides the information for engineering monitoring of the calibration. The presentation of the digital machine program is so arranged that to the experienced engineer or engineering aid errors are readily apparent and are then usually rapidly reconciled. Figure 11 is a sample of the machine output for a typical component (chord force in this case).

We have shown a cross section of the type of balances developed at the Boeing Wind Tunnel Laboratory for experimental force measurements in our wind tunnel facilities. These balances reflect our requirements for developmental as well as research testing. They also reflect the facilities available to us and the relative importance placed on wind tunnel testing by the Boeing Airplane Company.

Some of the detailed developments in our balance development program are discussed, while in the Supplements certain analyses are presented for those who may be interested in following more closely the reduction to hardware of the principles mentioned.

Our philosophy in the general applications of strain gage balances has been arrived at by experience, but remains fluid with the changing requirements and individual test requirements of wind tunnel testing.

REFERENCES

1. Samson, C.A., "Data Handling Practices in the Boeing Airplane Company Wind Tunnel Laboratory". Boeing Airplane Company, Seattle, Washington.

2. Curry, T. M., "Patent Application for Balance Design Number 6132". Boeing Airplane Company, Seattle, Washington.

3. Curry, T. M., "Patent Application for Balance Design Number 3143". Boeing Airplane Company, Seattle, Washington.

Supplement 1

THE BOEING COMPANY'S FORCE BALANCE TEST CAPABILITIES

AIRPLANE FORCE TEST CAPABILITIES

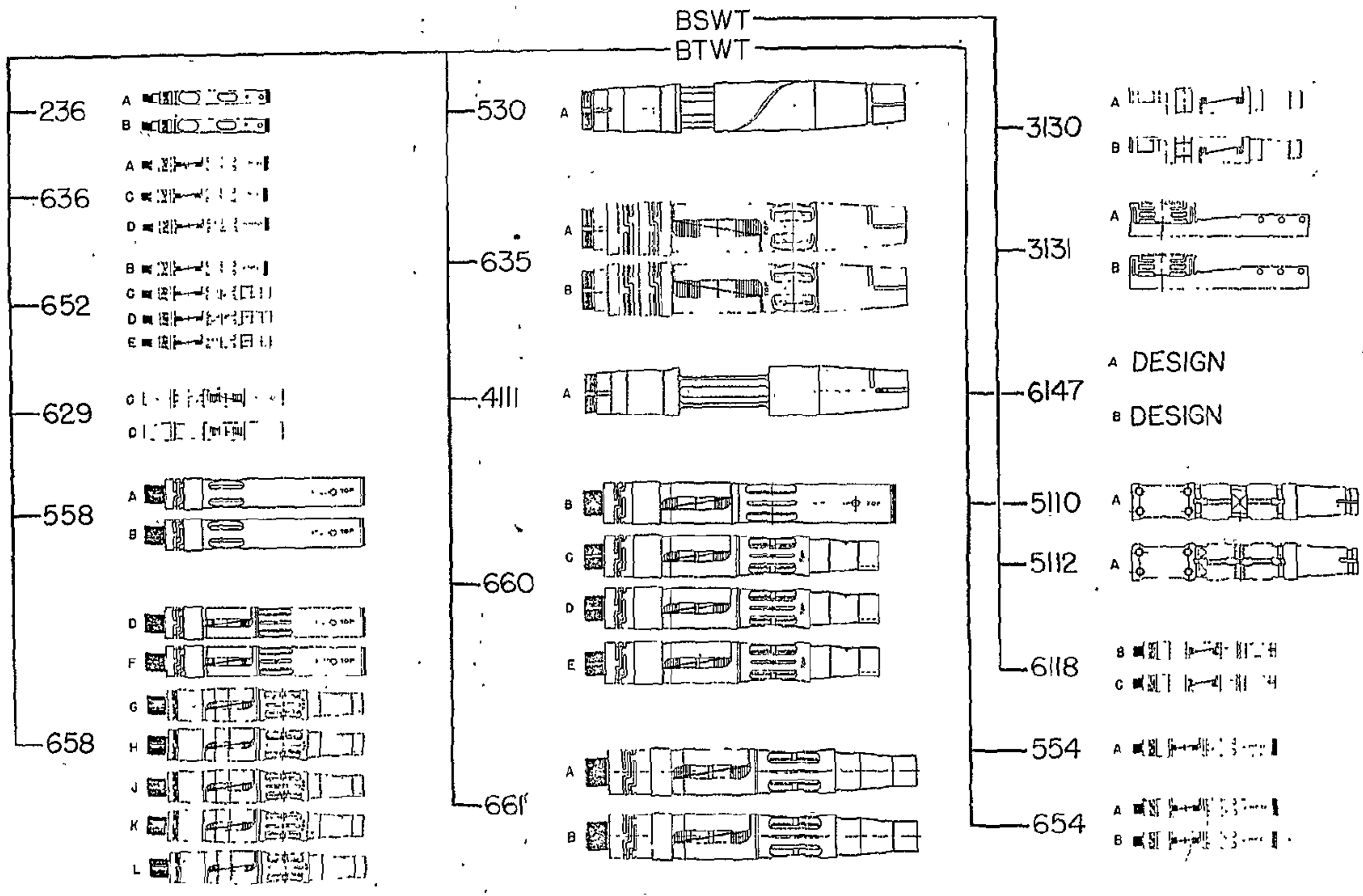

BOOST GLIDE FORCE TEST CAPABILITIES

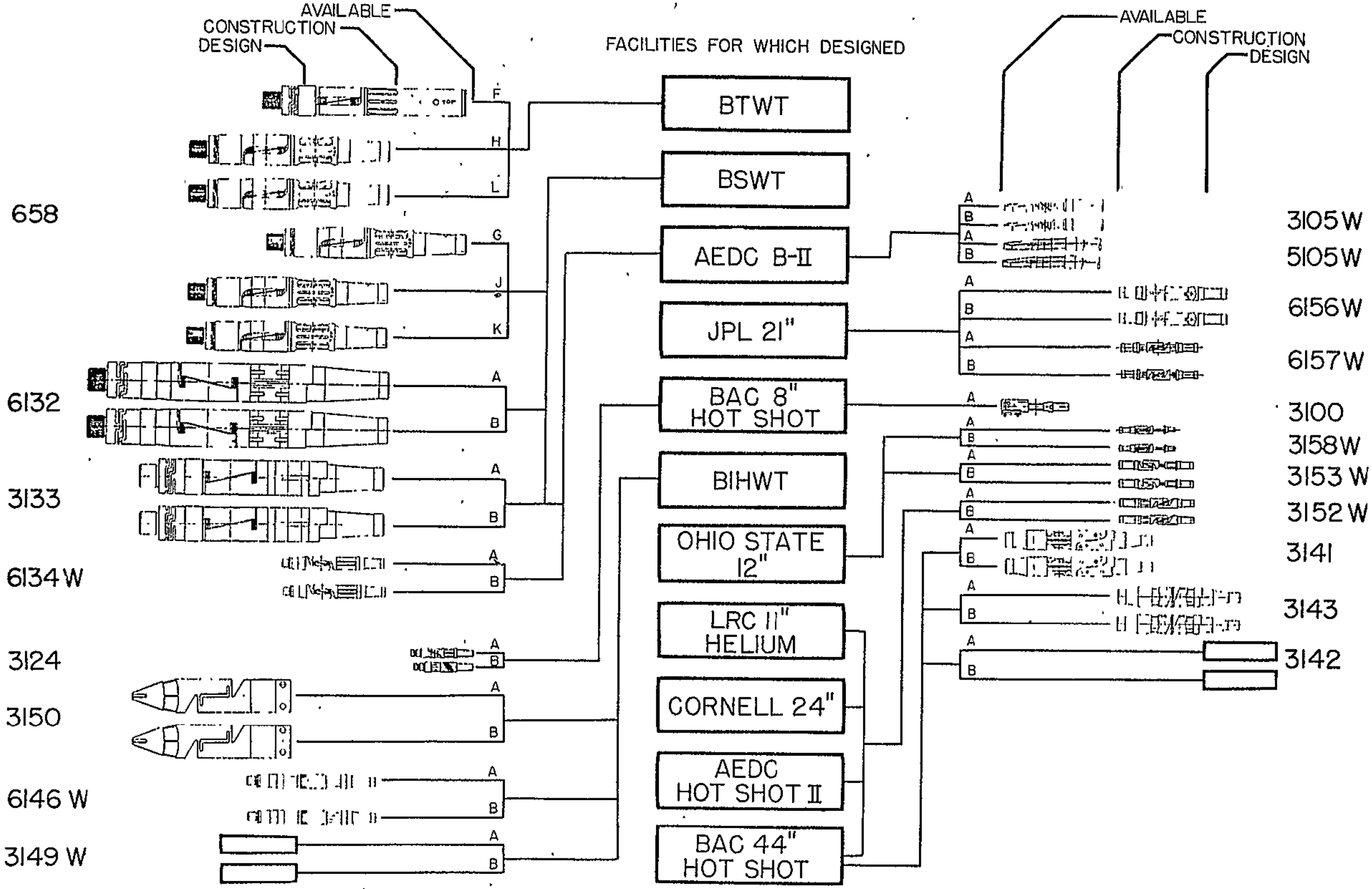

MISSILE FORCE TEST CAPABILITIES

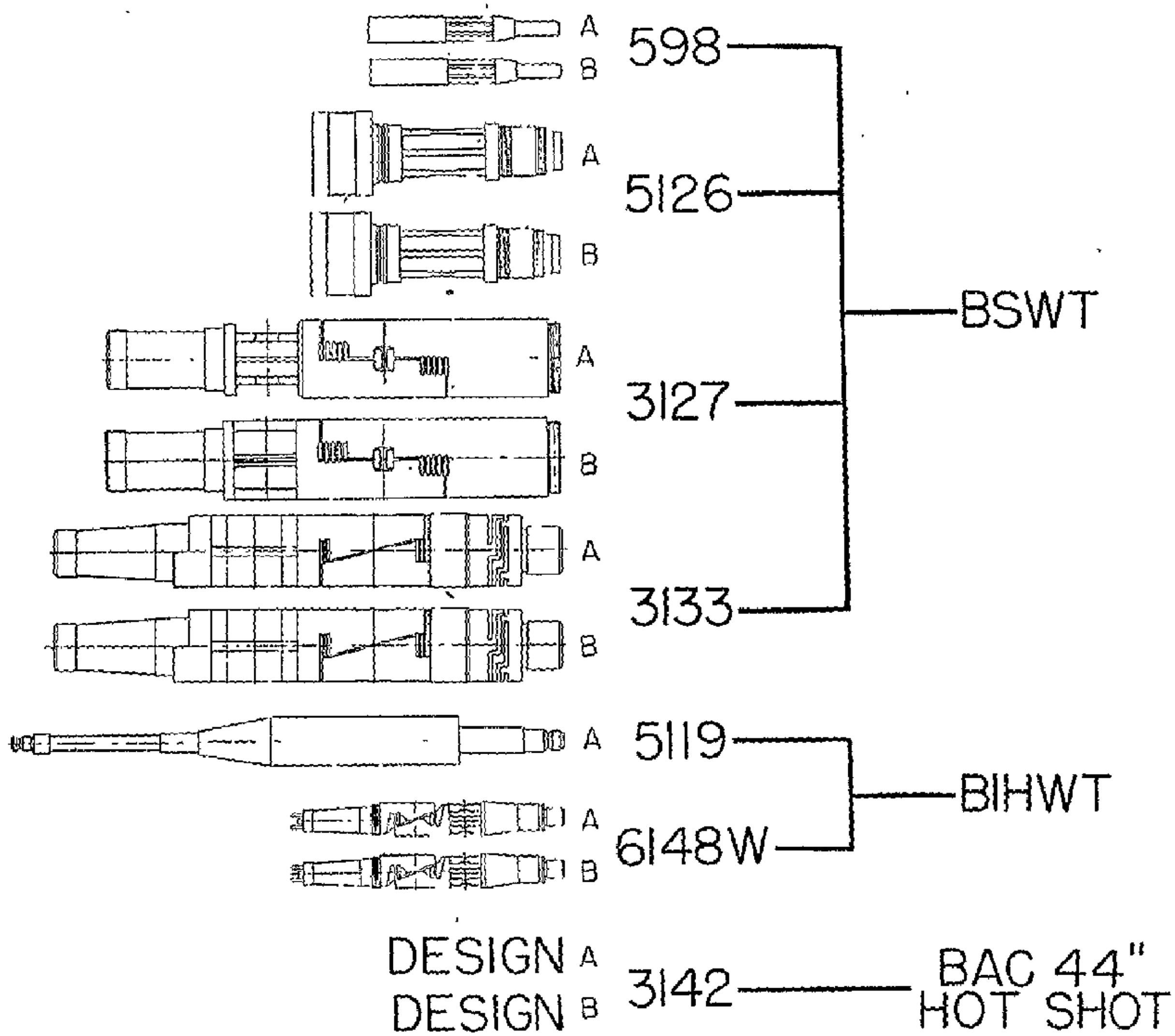

Supplement 2

MULTI-COMPONENT MOMENT TRANSFER CAGE

General Analysis:

In a system with any number (n) of parallel beams (a two-beam system shown in Figure 2 for simplicity) an overall bending moment m', about the group centroid at their axial center, produces an overall bending stress (see Figure 2C) on the system given as follows:

(1) $S_{m'} = -m' \frac{c}{I_o}$

where c is distance from group centroid to the fiber in question and I_o is the overall group section moment of inertia, about its own centroid.

Transposing equation (1) and substituting in (3) yields:

(2) $S_{m'} = -(m + N\bar{x}) \frac{c}{I_o} = -(m)\frac{c}{I_o} - (N)\bar{x} \frac{c}{I_o}$

From Figure 2C it is evident that the overall stress distribution due to moment along the individual beams is constant. Thus, gages located at any axial station (x) along the beam on the outer top and outer bottom surfaces are provided compressive and tensile stresses respectively, which may be used as a measure of the overall moment m' in a typical bridge circuit.

Now the stresses along the top and bottom outer surfaces caused by normal force reaction (R_N) are shown in Figure 2D to be proportional to the distance (x) from the center of this system of beams. Thus:

(3) $S_N = R_N(x) \frac{c_i}{I_i}$

but since

(4) $R_N = N \left(\frac{I_i}{\sum_{i=1}^{i=n} I_i} \right)$.

then

(5) $S_N = \frac{X c_i}{\sum_{i=1}^{i=n} I_i} (N)$

where c_i is the individual distance from centroid of individual beam to fiber in question, and I_i is individual beam moment of inertia about its own centroid.

Thus, by superposition

(6) $S_{total} = S_{m'} + S_N = -m(\frac{c}{I_o}) + N(\frac{xC_i}{\sum_{i=1}^{i=n} I_i} - \frac{\bar{x} C}{I_o})$

Hence, we can select configurations whereby the two terms in the right-hand most bracket of equation (6) cancel each other at some station (x) lying within the half length of the beams (see Figure 3). Thus, at this station the portion of the stress level which is proportional to Normal Force (N) is zero. Since we can locate our gages at any station (x) without affecting the moment sensitivity we can thereby readout moments about any point external to the center of the moment measuring structure by any distance ($\bar{x}$). Hence, the condition for normal force cancellation is as follows:

(7) $\frac{x C_i}{\sum_{i=1}^{i=n} I_i} = \frac{\bar{x} C}{I_o}$

which might be applied in the pitching moment plane or the yawing moment plane.

Frequently in the practical application of equation (7), in balance design, stress levels required for accurate measurements, as well as strength (stress levels) requirements afford situations in which it is impossible to satisfy equation (7) because the stress level caused by $\overline{x}C/I_0$ is too large[δ] in respect to that caused by

$$\frac{x\, C_i}{\sum_{i=1}^{i=n} I_i}$$

Thus, the following analysis shows a practical method of easily controlling the relative magnitude of these two terms in the selection of a working balance configuration.

δ It could never be too small since x may be varied to zero.

MOMENT TRANSFER
FIVE COMPONENT CAGE
DESIGN CRITERIA

TERMINOLOGY:

N' — EXTERNAL NORMAL FORCE (LBS).
S' — " SIDE " " .
ℓ' — " ROLLING MOMENT (INCH POUNDS).
m' — " PITCHING " " " .
n' — " YAWING " " " .
Q — INTERNAL HORIZONTAL BEAM REACTION. (LBS).
P — " VERTICAL " " " .
M — " BENDING MOMENT (INCH LBS).
D — MAXIMUM VERTICAL HEIGHT OF CAGE (INCHES).
D_S — " HORIZONTAL WIDTH " " " .
W_G — WIDTH OF GAGE.
X — FORE & AFT DISTANCE FROM CENTER OF CAGE (INCHES).
X_m — " " " " TO PITCHING MOMENT GAGES.
X_N — " " " " " NORMAL FORCE " .
X_ℓ — " " " " " ROLLING MOMENT " .
X_Q — DISTANCE FROM MOMENT CENTER TO PITCHING MOMENT GAGES (FORE & AFT).
$\bar{X}$ — MOMENT TRANSFER DISTANCE (MOMENT CENTER TO CAGE ℄).
H — HEIGHT OF BEAM ①.
B — WIDTH " " " .
h_1 — HEIGHT OF BEAM ② AT STATION 1.
h_2 — " " " " " " 2.
b OR $b_{②}$ — WIDTH " " ②.
ℓ_1 — DISTANCE FROM CAGE ℄ TO ETREMITY OF BEAM ②.
ℓ_2 — " " " " " STEP IN BEAM ②.
$I_{①Z}$ — MOMENT OF INERTIA OF BEAM ① ABOUT VERTICAL AXIS.
$I_{②Z}$ — " " " " " ② " " " .
$I_{①Y}$ — " " " " " ① " HORIZONTAL AXIS.
$I_{②Y}$ — " " " " " ② " " " .
$I_{③Y}$ — " " " " " ③ " " " .

$S_{N'}$ — DOUBLE CANTELIVER STRESS DUE TO NORMAL FORCE.
$S_{\ell'}$ — " " " " " ROLLING MOMENT.
$S_{S'}$ — " " " " " SIDE FORCE.
$S_{N'\bar{X}}$ — OVERALL SECTION BENDING STRESS DUE TO $N'\bar{X}$.
$S_{S'\bar{X}}$ — " " " " " " $S'\bar{X}$.

$A_{③}$ — CROSS SECTIONAL AREA OF BEAM ③.
$Y_{③}$ — TRANSVERSE (HORIZONTAL) DISTANCE FROM CAGE CROSS SECTIONAL ℄ TO THE ℄ OF THE BEAM ③ CROSS SECTION.

FIGURE 1.

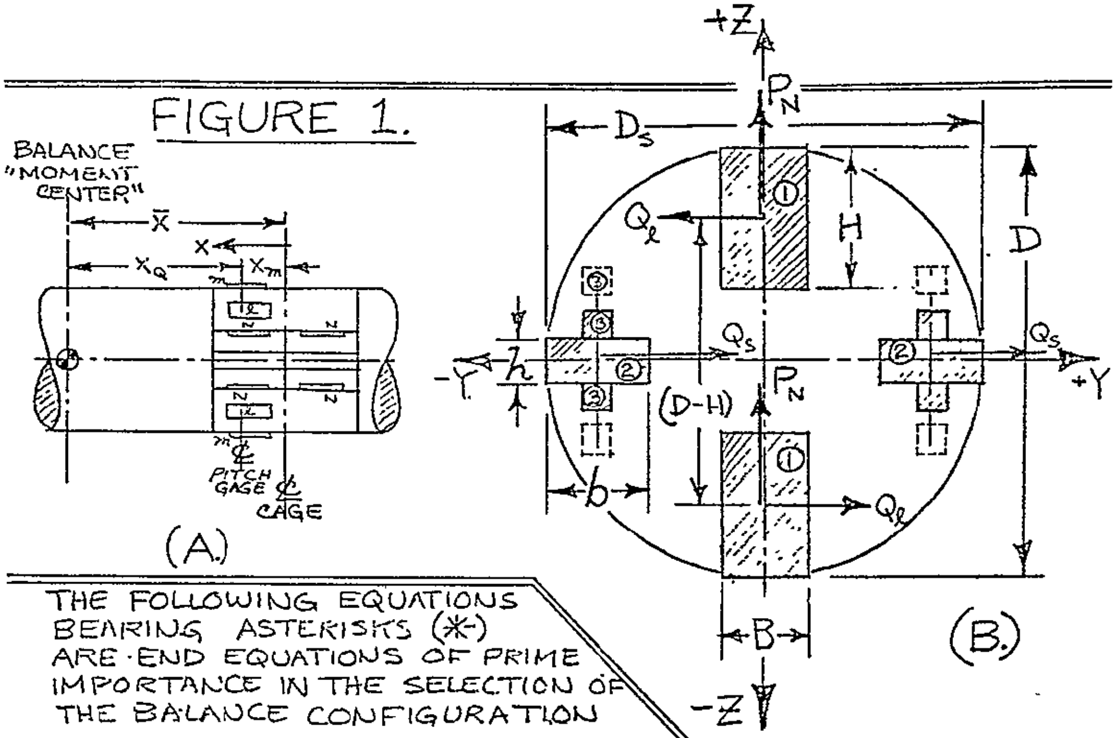

THE FOLLOWING EQUATIONS BEARING ASTERISKS (*) ARE END EQUATIONS OF PRIME IMPORTANCE IN THE SELECTION OF THE BALANCE CONFIGURATION

ROLL-NORMAL STRESS RELATIONSHIP:

(1) $Q_\ell \approx \frac{\ell'}{D-H}$ (MEASURED LEVEL OF ROLL STRESS NOT CRITICAL)

(2) $S_\ell = \frac{6M_\ell}{HB^2} \approx \frac{6\ell'}{(D-H)}\frac{X_\ell}{HB^2}$

(3) $S_{N'} = \frac{6M_N}{BH^2} = \frac{3N'X_N}{BH^2}$ HENCE $B = \frac{3N'X_N}{S_N H^2}$

IGNORING EFFECTS OF $I_{②Y}$ & $I_{③Y}$

(4) $S_\ell = S_{N'}(C_{S_\ell})$ WHERE C_{S_ℓ} = STRESS COEFFICIENT (ROLL)

(5) ∴ $\frac{2\ell X_\ell}{(D-H)\cancel{H}B^{\cancel{2}}} = \frac{N'X_N}{\cancel{B}H^{\cancel{2}}}\cdot C_{S_\ell}$ — SUBSTITUTING (2) & (3) IN (4).

(6) ∴ $B = \frac{2\ell}{C_S N}\left(\frac{X_\ell}{X_N}\right)\left(\frac{H}{D-H}\right)$

(7) FROM 3 $B = \frac{3N'X_N}{S_N H^2}$ *

(8) EQUATING (6) & (7) $\frac{2\ell'}{C_S N'}\left(\frac{X_\ell}{X_N}\right)\frac{H}{D-H} = \frac{3N'X_N}{S_N H^2}$

(9) $\frac{2\ell' S_N}{C_{S_\ell} N'^2}\left(\frac{X_\ell}{X_N}\right)H^3 = 3X_N(D-H)$

LET US ASSUME THAT $X_\ell/X_N = 1$ THUS LETTING C_{S_ℓ} ACCOUNT FOR THE LEVEL OF S_ℓ

(10) $\frac{2\ell S_N}{3C_{S_\ell}N^2}\frac{H^3}{(D-H)} = X_N$

PITCH – NORMAL – ROLL STRESS RELATIONSHIPS:

(11.) IGNORING I_Y OF BEAMS ② & ③; $I_{OVERALL_Y} = \frac{B}{12}\left[D^3-(D-2H)^3\right]$

(12) $I_{OY} = \frac{HB}{6}(3D^2-6HD+4H^2)$

(13) $S_{N'\bar{x}} = \frac{3D(X_Q+X_m)N'}{BH(3D^2-6HD+4H^2)}$ ∴ $S_m = S_{N\bar{x}}\left(\frac{m'}{N'\bar{X}}\right)$

TRANSFER IS ACHIEVED BY EQUATING $S_{N'2}$ & $S_{N'}$ [EQ'S (3) AND (13.)].

$$(14.) \quad \therefore \quad \frac{X_{N'}}{H^2}\left(\frac{3N'}{B}\right) = \frac{D(X_Q + X_m)}{H(3D^2 - 6HD + 4H^2)}\left(\frac{3N'}{B}\right)$$

LETTING $X_{N'} = X_m$:

$$(15.) \quad X_m = \frac{DH(X_Q + X_m)}{3D^2 - 6HD + 4H^2}$$

$$(16.) \quad X_m\left[1 - \frac{DH}{3D^2 - 6HD + 4H^2}\right] = \frac{DH(X_Q)}{3D^2 - 6HD + 4H^2}$$

$$(17.) \quad X_m\left[3D^2 - 7HD + 4H^2\right] = DH(X_Q)$$

$$(18.) \quad X_m = \frac{DH(X_Q)}{(3D - 4H)(D - H)} \quad *$$

EQUATING X_m & X_N SATISFIES STRESS CONDITIONS FOR TRANSFER, MEASURED STRESS LEVELS OF NORMAL & ROLL AS WELL AS ESTABLISHING MEASURED PITCH STRESS, THUS:

$$(19.) \quad \frac{DH(X_Q)}{(3D-4H)(D-H)} = \frac{2\ell' S_N}{3C_{S\ell}N^2}\,\frac{H^3}{(D-H)}$$

$$(20) \text{ HENCE } \quad \frac{C_S}{S_N} = \frac{2\ell'}{3N^2 X_Q D}\left(3DH^2 - 4H^3\right) \quad *$$

SAMPLE COMPUTATION SHEET "A":

$X_Q = 2.45$	S_N = 16 000 PSI						18,000 PSI			
H	C_S/S_N	X_m	B	C_S	S_ℓ	ASSUM. I_{Φ_Z}	B	C_S	S_ℓ	I_{Φ_Z}
ECN →	(20)	(18)	(3)	(21)	(22)	(23)	(3)	(21)	(22)	(23)
.700	.3215	.775	.427	.643	12870	.00456				
.725	.3347	.957	.492	.660	13200					
.750	.3440	1.045	.501	.688	13770					
.775	3555	1.143	.514	.711	14200					
		1.260	.532	.730						

SEE DATA SHEET "A" FOR PHASE I OF THE BALANCE CONFIGURATION SELECTION AS WELL AS THE EQUIVALENT AUTOMATIC DIGITAL PROGRAM (W-001) INPUT & OUTPUT SHEETS IN THE APPENDIX.

$$(21) \quad C_S = C_S/S_N \cdot (S_N) \quad *$$

$$(22) \quad S_\ell = C_S/S_N\,(S_N)^2 \quad *$$

$$(23) \quad I_{\Phi_Z} = \frac{1}{12} HB^3 \quad *$$

NOTE: SELECTING VALUES OF H & B ABOVE WE MAY CONVERT FROM A RECTANGULAR CROSS SECTION TO THE STRONGER[1] & STIFFER[2] OCTAGONAL CROSS SECTION WITH EQUAL $(C/I)_Z$ AND $(C/I)_Y$ BY UTILIZING THE REFERENCE NOMOGRAPHS.

TABULATE THE FOLLOWING:

$$(24) \quad C_Y = (H_{oct}) \times \frac{1}{2}$$

$$(25) \quad C_Z = (B_{oct}) \times \frac{1}{2}$$

$$(26) \quad I_{\Phi_Y} = (I/C)_Y \times C_Y$$

$$(27) \quad I_{\Phi_Z} = (I/C)_Z \times C_Z$$

THESE VALUES TO BE USED HENCEFORTH

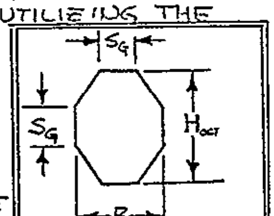

FIG. 2

$$(28) \quad A_m = (B_{oct})(H_{oct}) - \frac{1}{2}(H_{oct} - S_G)(B_{oct} - S_G)$$

NOTE 1. STRONGER BY VIRTUE OF THE FACT THAT IN THE OCTAGON THE MAXIMUM TRANSVERSE STRESSES DO NOT COMBINE DIRECTLY IN THE CORNERS AS IN THE RECTANGLE.

NOTE 2. STIFFER BY VIRTUE OF HIGHER VALUES OF I SINCE H & B WILL BE LARGER ON THE OCTAGON FOR EQUAL VALUES OF (C/I).

SIDE FORCE – YAW STRESS RELATIONSHIP:

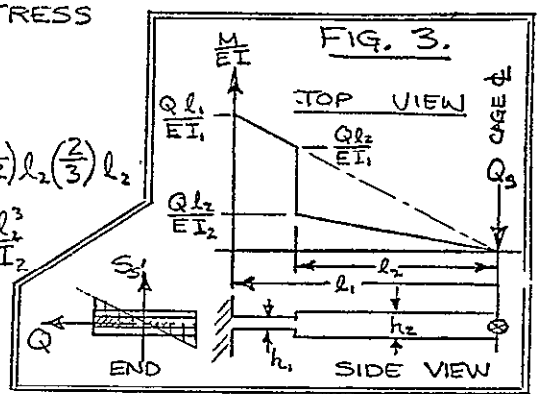

(29) $$\Delta_{STIFF} = \frac{Q\ell_1}{EI_1}\left(\frac{1}{2}\right)\ell_1\left(\frac{2}{3}\right)\ell_1 - \left[\frac{Q\ell_2}{EI_1} - \frac{Q\ell_2}{EI_2}\right]\left(\frac{1}{2}\right)\ell_2\left(\frac{2}{3}\right)\ell_2$$

(30) $$\Delta_{STIFF} = \frac{Q\ell_1^3}{3EI_1} - \frac{Q\ell_2^3}{3EI_1} + \frac{Q\ell_2^3}{3EI_2}$$

(31) $$\bar{\Delta}_{LIMBER} = \frac{Q\ell_1^3}{3EI_1}$$

(32) $$\frac{\Delta_{STIFF}}{\Delta_{LIMBER}} = \frac{\frac{\ell_1^3}{I_1} - \frac{\ell_2^3}{I_1} + \frac{\ell_2^3}{I_2}}{\frac{\ell_1^3}{I_1}} = 1 - \left(\frac{\ell_2}{\ell_1}\right)^3 + \left(\frac{\ell_2}{\ell_1}\right)^3\left(\frac{I_1}{I_2}\right)$$
$$= 1 + \left(\frac{\ell_2}{\ell_1}\right)^3\left(\frac{\cancel{\frac{1}{12}}h_1\cancel{b^3}}{\cancel{\frac{1}{12}}h_2\cancel{b^3}} - 1\right) = 1 + \left(\frac{\ell_2}{\ell_1}\right)^3\frac{h_1 - h_2}{h_2}$$

(33) $$\frac{\Delta_{STIFF}}{\Delta_{LIMBER}} = f = 1 - \left(\frac{\ell_2}{\ell_1}\right)^3\left(\frac{h_2 - h_1}{h_2}\right)$$

IGNORING EFFECTS OF $I_{③z}$

(34) $$\Delta_{STIFF} = f \cdot \Delta_{LIMBER} \Rightarrow \frac{Q_{②s}\cancel{\ell_1^3}}{\cancel{3E}I_{②z}}\left[1 - \left(\frac{\ell_2}{\ell_1}\right)^3\left(\frac{h_2 - h_1}{h_2}\right)\right] \Rightarrow \frac{Q_{①s}\cancel{\ell_1^3}}{\cancel{3E}I_{①z}}$$

(35) $$\therefore \frac{Q_{②s}}{I_{②z}} \cdot f = \frac{Q_{①s}}{I_{①z}}$$

(36.) $$Q_{①s} = Q_{②s}\, f\left(\frac{I_{①z}}{I_{②z}}\right)$$

(37) $$Q_{①s} + Q_{②s} = \frac{S'}{2} \Rightarrow Q_{②s}\left[1 + f \cdot \frac{I_{①z}}{I_{②z}}\right]$$

(38) $$Q_{②s} = \frac{S'}{2\left[1 + f \cdot \frac{I_{①z}}{I_{②z}}\right]} = \frac{S' I_{②z}}{2(I_{②z} + f \cdot I_{①z})}$$

WHEN YAW GAGE IS MOUNTED ON END FACE OF BEAM ② THEN $W_G = 0$

(39) $$S_{s'} = \frac{S' x_s (b_② - W_G)}{4(I_{②z} + f \cdot I_{①z})} \quad ; \therefore \quad I_{②z} + f \cdot I_{①z} = \frac{S' x_s (b_② - W_G)}{4 S_{s'}}$$

(40) $$I_{②z} = \frac{1}{12} h_1 b_②^3 = \frac{S' x_s (b_② - W_G)}{4 S_{s'}} - f \cdot I_{①z}$$

AND THUS $S_{x'} = S_{s'x}\left(\frac{x'}{s'x}\right)$

(41) $$h_1 = \frac{3 S' x_s (b_② - W_G)}{S_{s'} b_②^3} - \frac{I_{①z}(12)}{b_②^3} \cdot f$$

(42) $$h_1 = \frac{3 S' x_s (b_② - W_G)}{S_{s'} b_②^3} - \frac{I_{①z}(12)}{b_②^3} + \frac{I_{①z}(12)}{b_②^3}\left(\frac{\ell_2}{\ell_1}\right)^3 - \frac{I_{①z}(12)}{b_②^3}\left(\frac{\ell_2}{\ell_1}\right)^3\left(\frac{h_1}{h_2}\right)$$

(43) $$h_1\left[1 + \frac{I_{①z}(12)}{h_2 b_②^3}\left(\frac{\ell_2}{\ell_1}\right)^3\right] = \frac{3 S' x_s (b_② - W_G)}{S_{s'} b_②^3} - \frac{I_{①z}(12)}{b_②^3}\left[1 - \left(\frac{\ell_2}{\ell_1}\right)^3\right]$$

$$(44)\quad h_1 = \frac{\dfrac{3S'X_s(b_{\textcircled{2}}-W_G)}{S_{s'}\,b_{\textcircled{2}}^3} - \dfrac{I_{\textcircled{1}z}(12)}{b_{\textcircled{2}}^3}\left[1-\left(\dfrac{\ell_2}{\ell_1}\right)^3\right]}{1+\dfrac{I_{\textcircled{1}z}(12)}{h_2\,b_{\textcircled{2}}^3}\left(\dfrac{\ell_2}{\ell_1}\right)^3} \quad *$$

--- WHERE EVERYTHING IN THE RIGHT OF THE EQUATION IS KNOWN FOR GIVEN VALUES OF X_s, $b_{\textcircled{2}}$ AND $h_{\textcircled{2}}$.

$$(45)\quad I_{(\text{OVERALL})z} = \frac{h_1 b_{\textcircled{2}}}{6}\left[3D_s^2 - 6b_{\textcircled{2}}D_s + 4b_{\textcircled{2}}^2\right] + 2I_{\textcircled{1}z} + 4A_{\textcircled{3}}Y_{\textcircled{3}}^2$$

$$(46)\quad \text{SINCE } Y_3 = \frac{D-b}{2}$$ REQUIRED WHEN BEAM ③ ABUTS BEAM NO. ② INTEGRALLY ON A COMMON ℄.

IN ORDER TO SATISFY THE CONDITION FOR CANCELLATION

$$(47)\quad S_{s'\bar{x}} = S_{s'} = \frac{S'\bar{x}\left(D_s/2 - W_G/2\right)}{\frac{h_1 b_{\textcircled{2}}}{6}\left(3D_s^2 - 6b_{\textcircled{2}}D_s + 4b_{\textcircled{2}}^2\right) + 2I_{\textcircled{1}z} + A_{\textcircled{3}}(D_s - b_{\textcircled{2}})^2}$$

$$(48)\quad A_{\textcircled{3}}(D_s - b_{\textcircled{2}})^2 + \frac{h_1 b_{\textcircled{2}}}{6}\left(3D_s^2 - 6b_{\textcircled{2}}D_s + 4b_{\textcircled{2}}^2\right) + 2I_{\textcircled{1}z} = \frac{S'\bar{x}\,(D_s - W_G)}{2S_{s'}}$$

$$(49)\quad A_{\textcircled{3}} = \frac{S'\bar{x}\,(D_s - W_G)}{2S_{s'}(D_s - b_{\textcircled{2}})^2} - \frac{h_1 b_{\textcircled{2}}}{6(D - b_{\textcircled{2}})^2}\left(3D_s^2 - 6b_{\textcircled{2}}D_s + 4b_{\textcircled{2}}^2\right) - \frac{2I_{\textcircled{1}z}}{(D_s - b_{\textcircled{3}})^2} \quad *$$

UTILIZING DATA SHEET "B" COMPUTE h_1 AND $A_{\textcircled{3}}$ FROM EQUATIONS (44) AND (49) ABOVE

$$(50)\quad I_{\textcircled{2}Y} = b_{\textcircled{2}}h_{\textcircled{2}}^3/12$$

$$(51)\quad I_{\textcircled{3}Y} = b_{\textcircled{3}}h_{\textcircled{3}}^3/12$$

$$(52)\quad A_{\textcircled{3}} = b_{\textcircled{3}}h_{\textcircled{3}}$$

$$(53)\quad Z_{\textcircled{3}} = \frac{h_{\textcircled{2}} + h_{\textcircled{3}}}{2}$$ IF BEAMS ② & ③ ARE INTEGRAL

VALUES OF $I_{\textcircled{1}Y}$ AND $A_{\textcircled{1}}$ MAY BE DETERMINED FROM EQUATIONS (26) AN (28)

$$(54)\quad S_{N'} = \frac{\cancel{I_{\textcircled{1}X}}\,N'X_m}{2I_{\textcircled{1}Y} + 2I_{\textcircled{2}Y} + 4\left(I_{\textcircled{3}Y} + A_{\textcircled{3}}Z_{\textcircled{3}}^2\right)} \times \frac{H}{2\cancel{I_{\textcircled{1}X}}}$$

$$S_{N'} = \frac{N'X_m H}{4\left[I_{\textcircled{1}Y} + I_{\textcircled{2}Y} + 2\left(I_{\textcircled{3}Y} + A_{\textcircled{3}}Z_{\textcircled{3}}^2\right)\right]}$$

IF BEAMS ② & ③ ARE NOT INTEGRAL OMIT THIS TERM

$$(55)\quad S_{N'\bar{x}} = \frac{N'\bar{x}\;D/2}{2\left[I_{\textcircled{1}Y} + \frac{A_{\textcircled{1}}}{4}(D-H)^2 + 2\left(I_{\textcircled{3}Y} + A_{\textcircled{3}}Z_{\textcircled{3}}^2\right) + I_{\textcircled{2}Y}\right]} \quad *$$

EQUATING (54) & (55) TO SATISFY TRANSFER

$$(56)\quad \frac{\cancel{N'}X_m H}{\cancel{4}\left[I_{\textcircled{1}Y} + I_{\textcircled{2}Y} + 2\left(I_{\textcircled{3}Y} + A_{\textcircled{3}}Z_{\textcircled{3}}^2\right)\right]} = \frac{\cancel{N'}\bar{x}\;D}{\cancel{4}\left[I_{\textcircled{1}Y} + \frac{A_{\textcircled{1}}}{4}(D-H)^2 + 2\left(I_{\textcircled{3}Y} + A_{\textcircled{3}}Z_{\textcircled{3}}^2\right)\right]}$$

SOLVING FOR A NEW VALUE OF X_m FOR FINAL CONFIGURATION:

$$(57)\quad X_m = \frac{\bar{x}D}{H}\cdot\frac{I_{\textcircled{1}Y} + I_{\textcircled{2}Y} + 2\left(I_{\textcircled{3}Y} + A_{\textcircled{3}}Z_{\textcircled{3}}^2\right)}{I_{\textcircled{1}Y} + \frac{A_{\textcircled{1}}}{4}(D-H)^2 + I_{\textcircled{2}Y} + 2\left(I_{\textcircled{3}Y} + A_{\textcircled{3}}Z_{\textcircled{3}}^2\right)} \quad *$$

$\boxed{\text{IF BEAMS ② \& ③ ARE NOT INTEGRAL OMIT THIS TERM.}}$

OUR SELECTION OF A FIVE COMPONENT MOMENT TRANSFER TYPE CAGE HAS BEEN COMPLETED & IS NOW READY FOR A DETAILED STRESS ANALYSIS PER AVAILABLE DIGITAL PROGRAM.

Supplement 3

GENERAL STRESS ANALYSIS FOR A PRISMATIC MULTIPLE PARALLEL MEMBER STRAIN GAGE BALANCE CONFIGURATION

GENERAL STRESS ANALYSIS FOR A PRISMATIC MULTIPLE PARALLEL MEMBER STRAIN GAGE BALANCE CONFIGURATION.

FIGURE I

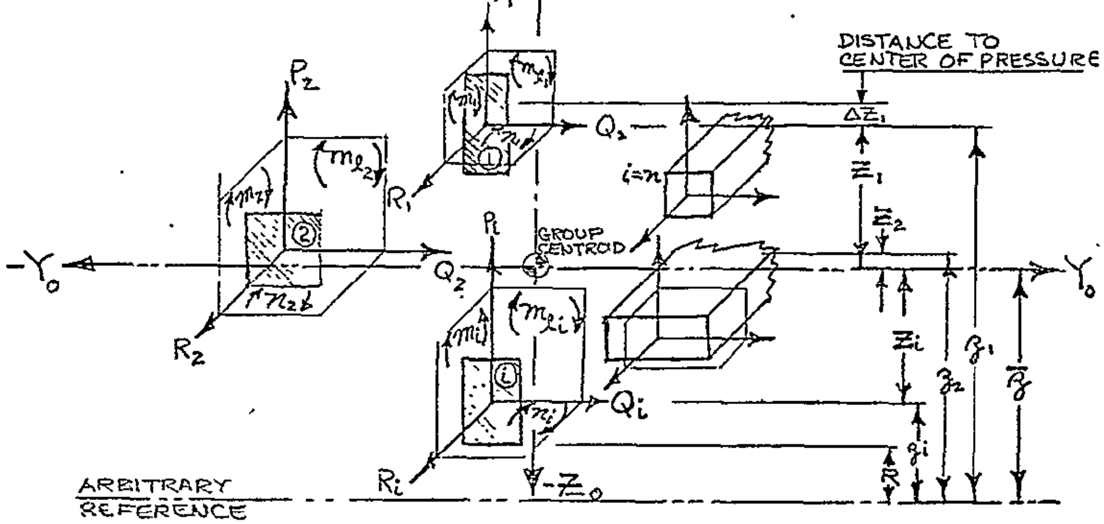

NORMAL FORCE (SIDE FORCE) RELATIONSHIPS:

VERTICAL DEFLECTION $\Delta = \Delta_1 = \Delta_2 = \cdots \Delta_n$

(1) $\therefore \dfrac{P_1 l_1^3}{3EI_{1_Y}} = \dfrac{P_2 l_2^3}{3EI_{2_Y}} = \text{------} \dfrac{P_i l_i^3}{3EI_{i_Y}}$

(2) $P_2 = P_1 \dfrac{I_{2Y}}{I_{1Y}} \left(\dfrac{l_1}{l_2}\right)^3$

(3) $P_3 = P_1 \dfrac{I_{3Y}}{I_{1Y}} \left(\dfrac{l_1}{l_3}\right)^3$

(4) $P_i = P_1 \dfrac{I_{iY}}{I_{1Y}} \left(\dfrac{l_1}{l_i}\right)^3$

(5) $N' = P_{1_{N'}} \sum_{i=1}^{i=n} \left[\left(\dfrac{I_{iY}}{I_{1Y}}\right)\left(\dfrac{l_1}{l_i}\right)^3\right] = \dfrac{P_{1N'} l_1^3}{I_{1Y}} \sum_{i=1}^{i=n} \left(\dfrac{I_{iY}}{l_i^3}\right)$

(6) $P_{1_{N'}} = N' \dfrac{I_{1Y}}{l_1^3 \sum_{i=1}^{i=n} \dfrac{I_{iY}}{l_i^3}}$ (TABULATE FOR $i = 1 \rightarrow n$)

BY INSPECTION:

(7) $Q_{i_{S'}} = S' \dfrac{I_{iz}}{l_i^3 \sum_{i=1}^{i=n} \dfrac{I_{iz}}{l_i}}$ (TABULATE FOR $i = 1 \rightarrow n$)

PITCHING MOMENT (YAWING MOMENT) STRESS RELATIONSHIPS:

FIG II

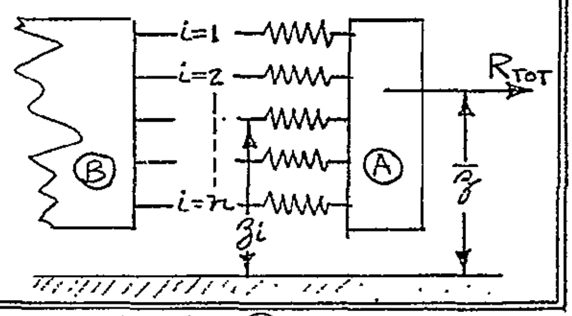

(8) $\Sigma M = 0$

(9) $\Sigma(R_i z_i) - \bar{z}(\Sigma R_i) = 0$

(10) $\therefore\ \bar{z} = \dfrac{\sum_{i=1}^{i=n}(R_i z_i)}{\sum_{i=1}^{i=n} R_i}$

FOR PARALLEL MOTION OF BLOCK (A) IN RESPECT TO BLOCK (B) WE GET:

(11) HORIZONTAL DEFLECTION $(\Delta) = \Delta_1 = \Delta_2 = \Delta_3 = \cdots \Delta_n$

HENCE

(12) $\dfrac{R_1 \ell_1}{EA_1} = \dfrac{R_2 \ell_2}{EA_2} = \cdots\ \dfrac{R_n \ell_n}{EA_n}$

THUS

(13) $R_i = R_1 \dfrac{\ell_1}{A_1}\left(\dfrac{A_i}{\ell_i}\right)$

SUBSTITUTING (13) IN (10) YIELDS:

(14) $\bar{z} = \dfrac{\Sigma\left[R_1\left(\frac{\ell_1}{A_1}\right)\left(\frac{A_i}{\ell_i}\right)z_i\right]}{\Sigma\left[R_1\left(\frac{\ell_1}{A_1}\right)\left(\frac{A_i}{\ell_i}\right)\right]} = \dfrac{\sum_{i=1}^{i=n}\left(\frac{A_i}{\ell_i}\right)z_i}{\sum_{i=1}^{i=n}\left(\frac{A_i}{\ell_i}\right)}$

(15) $Z_i = z_i - \bar{z}$

BY INSPECTION:

(16) $\bar{y} = \dfrac{\sum_{i=1}^{i=n}\left(\frac{A_i}{\ell_i}\right)z_i}{\sum_{i=1}^{i=n}\left(\frac{A_i}{\ell_i}\right)}$

(17) $\overline{Y_i} = Y_i + \Delta Y_i$

FIG III

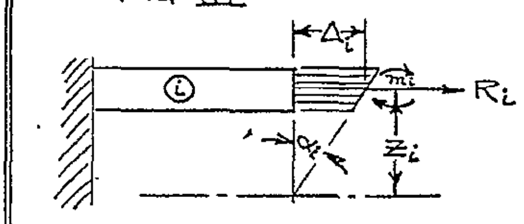

MOMENT AREA METHOD (FIG III) YIELDS:

(18) $\dfrac{m_i \ell_i}{I_i E} = \alpha_i$ — (ANGULAR DEFLECTION)

(19) $\dfrac{R_i \ell_i}{A_i E} = \Delta_i$ — (HORIZONTAL DISPLACEMENT)

(20) $\alpha_i = \Delta_i / Z_i$

(21) $\therefore\ \dfrac{m_i \cancel{\ell_i}}{\cancel{E} I_{Y_i}} = \dfrac{R_i \cancel{\ell_i}}{A_i \cancel{E} Z_i}$

(22) $m_i = R_i \dfrac{I_{Y_i}}{A_i Z_i}$

$$(23)\quad \alpha_1 = \alpha_2 = \alpha_i ---- = \alpha_n$$

$$(24)\quad \frac{m_1 l_i}{I_{Y_1}} = \frac{m_2 l_2}{I_{Y_2}} = \frac{m_i l_i}{I_{Y_i}} ---- = \frac{m_n l_n}{I_{Y_n}}$$

SUBSTITUTING (22) IN (24) YIELDS

$$(25)\quad \frac{R_1 l_1}{Z_1 A_1} = \frac{R_2 l_2}{Z_2 A_2} = \frac{R_i l_i}{Z_i A_i} = ---- \frac{R_n l_n}{Z_n A_n}$$

HENCE:

$$(26)\quad R_2 = R_1 \frac{Z_2 A_2 l_1}{Z_1 A_1 l_2}$$

AND

$$(27)\quad R_i = R_1 \frac{Z_i A_i l_1}{Z_1 A_1 l_i}$$

Σ INTERNAL MOMENTS = EXTERNAL MOMENT:

$$(28)\quad \sum_{i=1}^{i=n} R_i \left(\frac{I_{iY}}{A_i Z_i} + Z_i \right) = m'$$

SUBSTITUTING (27) IN (28) YIELDS:

$$(29)\quad \sum_{i=1}^{i=n} R_1 \left(\frac{Z_i A_i l_i}{Z_1 A_1 l_i} \right) \left(\frac{I_{iY}}{A_i Z_i} + Z_i \right) = m'$$

$$(30)\quad \sum_{i=1}^{i=n} R_1 \left(\frac{I_{iY} l_1}{Z_1 A_1 l_i} + \frac{Z_i^2 A_i l_1}{Z_1 A_1 l_i} \right) = m'$$

$$(31)\quad \therefore\ R_{1_{m'}} = \frac{m' Z_1 A_1}{\left[\sum_{i=1}^{i=n} \left(\frac{I_{iY}}{l_i} + \frac{Z_i^2 A_i}{l_i} \right) \right] l_1}$$

SUBSTITUTING (31) IN (27) YIELDS:

$$(32)\quad R_{i_{m'}} = \frac{m' Z_i A_i}{l_i \sum_{i=1}^{i=n} \left(\frac{I_{iY}}{l_i} + \frac{Z_i^2 A_i}{l_i} \right)}$$

BY INSPECTION

$$(33)\quad R_{i_{n'}} = \frac{n' Y_i A_i}{l_i \sum_{i=1}^{i=n} \left(\frac{I_{iz}}{l_i} + \frac{Z_i^2 A_i}{l_i} \right)}$$

ROLLING MOMENT STRESS RELATIONSHIPS:

$$(34)\quad \phi_{l'_1} = \phi_{l'_2} = \phi_{l'_i} = --- \phi_{l'_n}$$

$$(35)\quad \therefore \frac{\epsilon_{l'_1}}{\sqrt{Z_1^2 + Y_1^2}} = \frac{\epsilon_{l'_2}}{\sqrt{Z_2^2 + Y_2^2}} = \frac{\epsilon_{l'_i}}{\sqrt{Z_i^2 + Y_i^2}} = --- \frac{\epsilon_{l'_n}}{\sqrt{Z_n^2 + Y_n^2}}$$

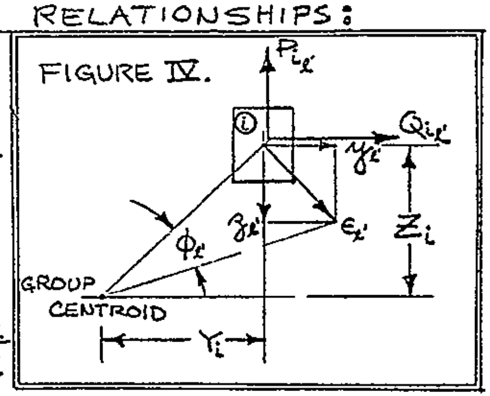

FIGURE IV.

FROM FIG IV

$$(36)\quad \frac{y_{l'_i}}{Z_i} = \frac{z_{l'_i}}{Y_i};\ \therefore\ z_{l'_i} = y_{l'_i} \frac{Y_i}{Z_i}$$

ALSO FROM FIG IV

$$(37)\quad \epsilon_{l'_i} = \sqrt{y_{l'_i}^2 + z_{l'_i}^2} = \sqrt{y_{l'_i}^2\left[1 + \left(\frac{Y_i}{Z_i}\right)^2\right]} = \frac{y_{l'_i}}{Z_i} \sqrt{Y_i^2 + Z_i^2}$$

SUBSTITUTING IN (35) YIELDS:

(38) $$\frac{y_{l_1'}}{Z_1} = \frac{y_{l_2'}}{Z_2} = \frac{y_{l_i'}}{Z_i} = \text{------} \frac{y_{l_n'}}{Z_n}$$

AND

(39) $$\frac{z_{l_1'}}{Y_1} = \frac{z_{l_2'}}{Y_2} = \frac{z_{l_i'}}{Y_i} = \text{------} \frac{z_{l_n'}}{Y_n}$$

THUS

(40) $$y_{l_i'} = y_{l_1'} \frac{Z_i}{Z_1}$$

AND

(41) $$z_{l_i'} = z_{l_1'} \frac{Y_i}{Y_1}$$

FROM (36) WE GET (42)

(42) $$z_{l_i'} = y_{l_i} \frac{Y_i}{Z_i}$$

(43) $$z_{l_i'} = \frac{P_{l_i'} l_i^3}{3EI_{Y_i}}$$

(44) $$y_{l_i'} = \frac{Q_{l_i'} l_i^3}{3EI_{Z_i}}$$

SUBSTITUTING (43) & (44) IN (42) YIELDS

(45) $$\frac{P_{l_i'} l_i^3}{3EI_{Y_i}} = \frac{Q_{l_i'} l_i^3}{3EI_{Z_i}} \frac{Y_i}{Z_i}$$

(46) $$\therefore P_{l_i'} = Q_{l_i'} \frac{I_{Y_i}}{I_{Z_i}} \frac{Y_i}{Z_i} \qquad \text{OR} \qquad Q_{l_i'} = P_{l_i'} \frac{I_{Z_i}}{I_{Y_i}} \frac{Z_i}{Y_i}$$

FROM EQUATION (40), SUBSTITUTING EQ (44) YIELDS:

(47) $$y_{l_2'} = y_{l_1'} \frac{Z_2}{Z_1} \implies \frac{Q_{l_2'} l_2^3}{3EI_{Z_2}} = \frac{Q_{l_1'} l_1^3}{3EI_{Z_1}} \frac{Z_2}{Z_1}$$

(48) $$y_{l_3'} = y_{l_1'} \frac{Z_3}{Z_1} \implies \frac{Q_{l_3'} l_3^3}{3EI_{Z_3}} = \frac{Q_{l_1'} l_1^3}{3EI_{Z_1}} \frac{Z_3}{Z_1},$$

(49) $$y_{l_i'} = y_{l_1'} \frac{Z_i}{Z_1} \implies \frac{Q_{l_i'} l_i^3}{3EI_{Z_i}} = \frac{Q_{l_1'} l_1^3}{3EI_{Z_1}} \frac{Z_i}{Z_1}$$

THUS AND BY INSPECTION

(50) $$Q_{l_2'} = Q_{l_1'} \frac{I_{Z_2}}{I_{Z_1}} \left(\frac{l_1}{l_2}\right)^3 \frac{Z_2}{Z_1} \qquad P_{l_2'} = P_{l_1'} \frac{I_{Y_2}}{I_{Y_1}} \left(\frac{l_1}{l_2}\right)^3 \frac{Y_2}{Y_1}$$

(51) $$Q_{l_3'} = Q_{l_1'} \frac{I_{Z_3}}{I_{Z_1}} \left(\frac{l_1}{l_3}\right)^3 \frac{Z_3}{Z_1} \qquad P_{l_3'} = P_{l_1'} \frac{I_{Y_3}}{I_{Y_1}} \left(\frac{l_1}{l_3}\right)^3 \frac{Y_3}{Y_1}$$

(52) $$Q_{l_i'} = Q_{l_1'} \frac{I_{Z_i}}{I_{Z_1}} \left(\frac{l_1}{l_i}\right)^3 \frac{Z_i}{Z_1} \qquad P_{l_i'} = P_{l_1'} \frac{I_{Y_i}}{I_{Y_1}} \left(\frac{l_1}{l_i}\right)^3 \frac{Y_i}{Y_1}$$

Σ INTERNAL MOMENTS EQUAL THE EXTERNAL MOMENT:

(53) $$P_{l_1'}Y_1 + P_{l_2'}Y_2 + P_{l_i'}Y_i + \text{---} P_{l_n'}Y_n + Q_{l_1'}Z_1 + Q_{l_2'}Z_2 + Q_{l_i'}Z_i + \text{-----}$$

$$\text{---} Q_{l_n'}Z_n + \sum_{i=1}^{i=n} l_i' = l'.$$

SUBSTITUTING (50), (51) & (52):

(54) $$\frac{P_{l_1'} l_1^3}{I_{Y_1} Y_1} \times \left[\sum_{i=1}^{i=n} \left(\frac{I_{Y_i} Y_i^2}{l_i^3}\right)\right] + \frac{Q_{l_1'} l_1^3}{I_{Z_1} Z_1} \left[\sum_{i=1}^{i=n} \left(\frac{I_{Z_i} Z_i^2}{l_i^3}\right)\right] + \sum_{i=1}^{i=n} l_i' = l'$$

FROM (46) & (54)

$$(55)\quad \frac{P_{\ell'_1}\ell_1^3}{I_{Y_1}Y_1}\left[\sum_{i=1}^{i=n}\left(\frac{I_{Y_i}Y_i^2}{\ell_i^3}\right)+\sum_{i=1}^{i=n}\left(\frac{I_{Z_i}Z_i^2}{\ell_i^3}\right)\right]+\sum_{i=1}^{i=n}\ell'_i=\ell'$$

$$(56)\quad P_{\ell'_1}=\frac{I_{Y_1}Y_1\left(\ell'-\sum_{i=1}^{i=n}\ell'_i\right)}{\ell_1^3\sum_{i=1}^{i=n}\left[\frac{I_{Y_i}Y_i^2}{\ell_i^3}+\frac{I_{Z_i}Z_i^2}{\ell_i^3}\right]}$$

INDIVIDUAL BEAM TORSIONAL STIFFNESS:

$$(57)\quad \theta=\frac{\ell'_i\ell_i}{K_iG}=\frac{\sqrt{\mathfrak{z}_i^2+y_i^2}}{\sqrt{Z_i^2+Y_i^2}}$$

& FROM EQ (36) WE GET $y=\frac{\mathfrak{z}}{Y}Z$

$$(58)\quad \therefore\ \frac{\ell'_i\ell_i}{K_iG}=\frac{\mathfrak{z}_i\sqrt{1+(Z_i/Y_i)^2}}{\sqrt{Z_i^2+Y_i^2}}=\frac{\mathfrak{z}_i}{Y_i}$$

$$(59)\quad \therefore\ \ell'_i=\frac{\mathfrak{z}_iK_iG}{Y_i\ell_i}$$

BUT FROM EQ (43) WE GET

$$(60)\quad \ell'_i=\frac{P_{\ell'_i}\ell_i^3}{3EI_{Y_i}}\times\frac{K_iG}{Y_i\ell_i}=\frac{P_{\ell'_i}\ell_i^2}{3EI_{Y_i}}\times\frac{K_iG}{Y_i}$$

SUBSTITUTING (52) IN (60) YIELDS:

$$(61)\quad \ell'_i=\frac{P_{\ell'_1}\ell_i^2}{3E\cancel{I_{Y_i}}}\,\frac{K_iG}{\cancel{Y_i}}\,\frac{\cancel{I_{Y_i}}}{I_{Y_1}}\left(\frac{\ell_1}{\ell_i}\right)^3\frac{\cancel{Y_i}}{Y_1}=P_{\ell'_1}\frac{\ell_1^3K_iG}{3EI_{Y_1}Y_1\ell_i}=\frac{Q_{\ell'_1}K_iG\ell_1^3}{3EI_{Z_1}Z_1\ell_i}$$

SUBSTITUTING (61) IN (56) YIELDS

$$(62)\quad P_{\ell'_1}\ell_1^3\left\{\sum_{i=1}^{i=n}\left[\frac{I_{Y_i}}{I_{Y_1}\ell_i^3}\left(\frac{Y_i^2}{Y_1}\right)+\frac{I_{Z_i}}{I_{Y_1}\ell_i^3}\left(\frac{Z_i^2}{Y_1}\right)\right]\right\}=\ell'-\sum_{i=1}^{i=n}\left[P_{\ell'_1}\frac{\ell_1^3K_iG}{\ell_i3EI_{Y_1}Y_1}\right]$$

THUS

$$(63)\quad P_{\ell'_1}=\frac{I_{Y_1}Y_1\ell'}{\sum_{i=1}^{i=n}\left[\frac{I_{Y_i}Y_i^2\ell_1^3}{\ell_i^3}+\frac{I_{Z_i}Z_i^2\ell_1^3}{\ell_i^3}+\frac{\ell_1^3K_iG}{\ell_i3E}\right]}$$

FROM EQ (46)' WE GET:

$$(64)\quad Q_{\ell'_1}=\frac{I_{Z_1}Z_1\ell'}{\sum_{i=1}^{i=n}\left[\frac{I_{Z_i}Z_i^2\ell_1^3}{\ell_i^3}+\frac{I_{Y_i}Y_i^2\ell_1^3}{\ell_i^3}+\frac{\ell_1^3K_iG}{\ell_i3E}\right]}$$

[SAME DENOMINATOR AS IN (63)].

INTERMEDIATE SUMMARY OF INTERNAL LOADS:

TABULATE FOR VALUES OF $i=1\rightarrow n$.

CASE I WHEN ROLL IS MEASURED ON BEAMS WITH LARGE Z THEN THIS BEAM SHOULD BE THAT ONE CORRESPONDING TO $i=1$. COMPUTE ROLL LOADS AS FOLLOWS:

$$(65)\quad Q_{1_{\ell'}}=\frac{I_{Z_1}Z_1\ell'}{\sum_{i=1}^{i=n}\left[\frac{I_{Z_i}Z_i^2\ell_1^3}{\ell_i^3}+\frac{I_{Y_i}Y_i^2\ell_1^3}{\ell_i^3}+\frac{\ell_1^3K_iG}{\ell_i3E}\right]}$$

REFERENCE EQUATION (64)

$$(66)\quad Q_{i_{\ell'}}=Q_{\ell'_1}\left(\frac{I_{Z_i}}{I_{Z_1}}\right)\left(\frac{Z_i}{Z_1}\right)\left(\frac{\ell_1}{\ell_i}\right)^3 \qquad (52)$$

PROGRAM THIS ($P_{\ell'_1}$ MAY BE ZERO)

$$(67)\quad P_{1_{\ell'}}=Q_{\ell'_1}\left(\frac{I_{Y_1}}{I_{Z_1}}\right)\left(\frac{Y_1}{Z_1}\right) \qquad (46)$$

DO NOT PROGRAM THIS

$$(69)\quad P_{i_{\ell'}}=P_{\ell'_1}\left(\frac{I_{Y_i}}{I_{Y_1}}\right)\left(\frac{Y_i}{Y_1}\right)\left(\frac{\ell_1}{\ell_i}\right)^3=Q_{1_{\ell'}}\left(\frac{I_{Y_i}}{I_{Z_1}}\right)\left(\frac{Y_i}{Z_1}\right)\left(\frac{\ell_1}{\ell_i}\right)^3 \qquad (52)$$

$$(68.5)\quad \ell'_{i_{\ell'}}=\frac{Q_{1_{\ell'}}K_iG\ell_1^3}{3EI_{Z_1}Z_1\ell_i}$$

CASE II WHEN ROLL IS MEASURED ON BEAMS WITH LARGE Y THEN THIS BEAM SHOULD BE THAT ONE CORRESPONDING TO $i = 1$. COMPUTE ROLL LOADS AS FOLLOWS:

$$(69)\quad P_{1_{\ell'}} = \frac{I_{Y_1} Y_1 \ell'}{\sum_{i=1}^{i=n}\left[\frac{I_{Z_i} Z_i^2 \ell_1^3}{\ell_i^3} + \frac{I_{Y_i} Y_i^2 \ell_1^3}{\ell_i^3} + \frac{\ell_1^3 K_i G}{\ell_i 3E}\right]} \qquad (63)$$

$$(70)\quad P_{i_{\ell'}} = P_{\ell'_1}\left(\frac{I_{Y_i}}{I_{Y_1}}\right)\left(\frac{Y_i}{Y_1}\right)\left(\frac{\ell_1}{\ell_i}\right)^3 \qquad (52)$$

PROGRAM THIS ($Q_{\ell'_1}$ MAY BE ZERO)

DO NOT PROGRAM THIS

$$(71)\quad Q_{1_{\ell'}} = P_{\ell'_1}\left(\frac{I_{Z_1}}{I_{Y_1}}\right)\left(\frac{Z_1}{Y_1}\right) \qquad (46)$$

$$(72)\quad Q_{i_{\ell'}} = Q_{\ell'_1}\left(\frac{I_{Z_i}}{I_{Z_1}}\right)\left(\frac{Z_i}{Z_1}\right)\left(\frac{\ell_1}{\ell_i}\right)^3 = P_{\ell'_1}\left(\frac{I_{Z_i}}{I_{Y_1}}\right)\left(\frac{Z_i}{Y_1}\right)\left(\frac{\ell_1}{\ell_i}\right)^3 \qquad (52)$$

$$(72.5)\quad \ell'_{i_{\ell'}} = P_{1_{\ell'}}\frac{K_i G \ell_1^3}{3E I_{Y_1} Y_1 \ell_i}$$

THE FOLLOWING ARE THE SAME FOR BOTH CASE I AND CASE II:

$$(73)\quad P_{i_{N'}} = N'\frac{I_{Y_i}}{\ell_i^3 \sum_{i=1}^{i=n}\frac{I_{Y_i}}{\ell_i^3}} \qquad (6)$$

$$(74)\quad Q_{i_{S'}} = S'\frac{I_{Z_i}}{\ell_i^3 \sum_{i=1}^{i=n}\frac{I_{Z_i}}{\ell_i^3}} \qquad (7)$$

$$(75)\quad R_{i_{m'}} = m'\frac{Z_i A_i}{\ell_i \sum_{i=1}^{i=n}\left(\frac{I_{Y_i}}{\ell_i} + \frac{Z_i^2 A_i}{\ell_i}\right)} \qquad \text{REF EQ. } (32)$$

$$(76)\quad R_{i_{N'\bar{X}}} = \frac{N'\bar{X}}{m'} R_{m'_i}$$

$$(77)\quad R_{i_{n'}} = n'\frac{Y_i A_i}{\ell_i \sum_{i=1}^{i=n}\left(\frac{I_{Z_i}}{\ell_i} + \frac{Y_i^2 A_i}{\ell_i}\right)} \qquad (33)$$

$$(78)\quad R_{i_{S'\bar{X}}} = \frac{S'\bar{X}}{n'} R_{n'_i}$$

$$(79)\quad m'_{i_{m'}} = R_{i_{m'}}\frac{I_{Y_i}}{A_i Z_i} = \frac{m' I_{Y_i}}{\ell_i \sum_{i=1}^{i=n}\left(\frac{I_{Y_i}}{\ell_i} + \frac{Z_i^2 A_i}{\ell_i}\right)} \qquad (22)$$

THIS WORKS FOR ALL VALUES OF n FROM 1 TO ∞. TO BE PROGRAMMED

$$(80)\quad m'_{i_{N'\bar{X}}} = \frac{N'\bar{X}}{m'} m'_{i_{m'}}$$

$$(81)\quad n'_{i_{n'}} = R_{i_{n'}}\frac{I_{Z_i}}{A_i Y_i} = \frac{n' I_{Z_i}}{\ell_i \sum_{i=1}^{i=n}\left(\frac{I_{Z_i}}{\ell_i} + \frac{Y_i^2 A_i}{\ell_i}\right)} \qquad (22)$$

$$(82)\quad n'_{i_{S'\bar{X}}} = \frac{S'\bar{X}}{n'} n'_{i_{n'}}$$

STRESS COMPUTATIONS:

SAFETY (BREAKING) STRESSES

TENSILE:

$$(83)\quad S_{T_i} = \left(P_{i_{\ell'}} + P_{i_{N'}}\right)\frac{X_i C_{Z_i}}{I_{Y_i}} + \left(Q_{i_{\ell'}} + Q_{i_{S'}}\right)\frac{X_i C_{Y_i}}{I_{Z_i}} + \left(m'_{i_{m'}} + m'_{i_{N'\bar{X}}}\right)\frac{C_{Z_i}}{I_{Y_i}} + \left(n'_{i_{n'}} + n'_{i_{S'\bar{X}}}\right)\frac{C_{Y_i}}{I_{Z_i}} + \left(R_{i_{m'}} + R_{i_{N'\bar{X}}} + R_{i_{n'}} + R_{i_{S'\bar{X}}}\right)\frac{1}{A_i} + C'\frac{1}{\sum_{i=1}^{i=n} A_i}$$

(84) SHEAR $S_{S_i} = \frac{\sqrt{(P_{i\ell'} + P_{iN'})^2 + (Q_{i\ell'} + Q_{is'})^2}}{A_i}$.

(84a) $S_{S_{i\,TOTAL}} = S_{S_i} + \frac{\ell_{i\ell'} C_i}{K_i}$

THIS IS FOR MAX SHEAR & USUALLY DOES NOT OCCUR AT SAME PLACE AS MAX BENDING STRESS. NOT TO BE PROGRAMMED.

$C_i = P_i$ FOR A CIRCLE

$= .676 Q_i$ FOR A SQUARE

REF ROARK FOR OTHER VALUES OF C_i

COMBINED EFFECTIVE STRESSES:

(85) $S_{T_i\,(COMB.)} = \frac{1}{2} S_{T_i} + \sqrt{\left(\frac{1}{2} S_{T_i}\right)^2 + S_{S_i}^2}$

(86) $S_{S_i\,(COMB.)} = \sqrt{\left(\frac{1}{2} S_{T_i}\right)^2 + S_{S_i}^2}$

FACTORS OF SAFETY

(87) $\overline{F.S.}_{T_i} = \frac{S_{T_i(COMB)}}{S_{T(ULT.)_i}}$

(89) $\overline{F.S.}_{S_i} = \frac{S_{S_i(COMB)}}{S_{S(ULT)_i}}$

INDIVIDUAL COMPONENT (MEASURED) TENSILE STRESSES:

(90) $S_{\ell' Q_i} = Q_{i\ell'} \frac{X_i C_{Y_i}}{I_{Z_i}}$

(91) $S_{\ell' P_i} = P_{i\ell'} \frac{X_i C_{Z_i}}{I_{Y_i}}$

(92) $S_{N'_i} = P_{iN'} \frac{X_i C_{Z_i}}{I_{Y_i}}$

(93) $S_{N'\bar{x}_i} = R_{iN'\bar{x}} \left(\frac{1}{A_i}\right) + m'_{iN'\bar{x}} \left(\frac{C_{Z_i}}{I_{Y_i}}\right)$

(94) $S_{m'_i} = R_{im'} \left(\frac{1}{A_i}\right) + m'_{im'} \left(\frac{C_{Z_i}}{I_{Y_i}}\right)$

(95) $S_{s'_i} \doteq Q_{is'} \frac{X_i C_{Y_i}}{I_{Z_i}}$

(96) $S_{s'\bar{x}_i} = R_{is'\bar{x}} \left(\frac{1}{A_i}\right) \pm n'_{is'\bar{x}} \left(\frac{C_{Y_i}}{I_{Z_i}}\right)$

(97) $S_{n'_i} = R_{in'} \left(\frac{1}{A_i}\right) \pm n'_{in'} \left(\frac{C_{Y_i}}{I_{Z_i}}\right)$

FIGURE V

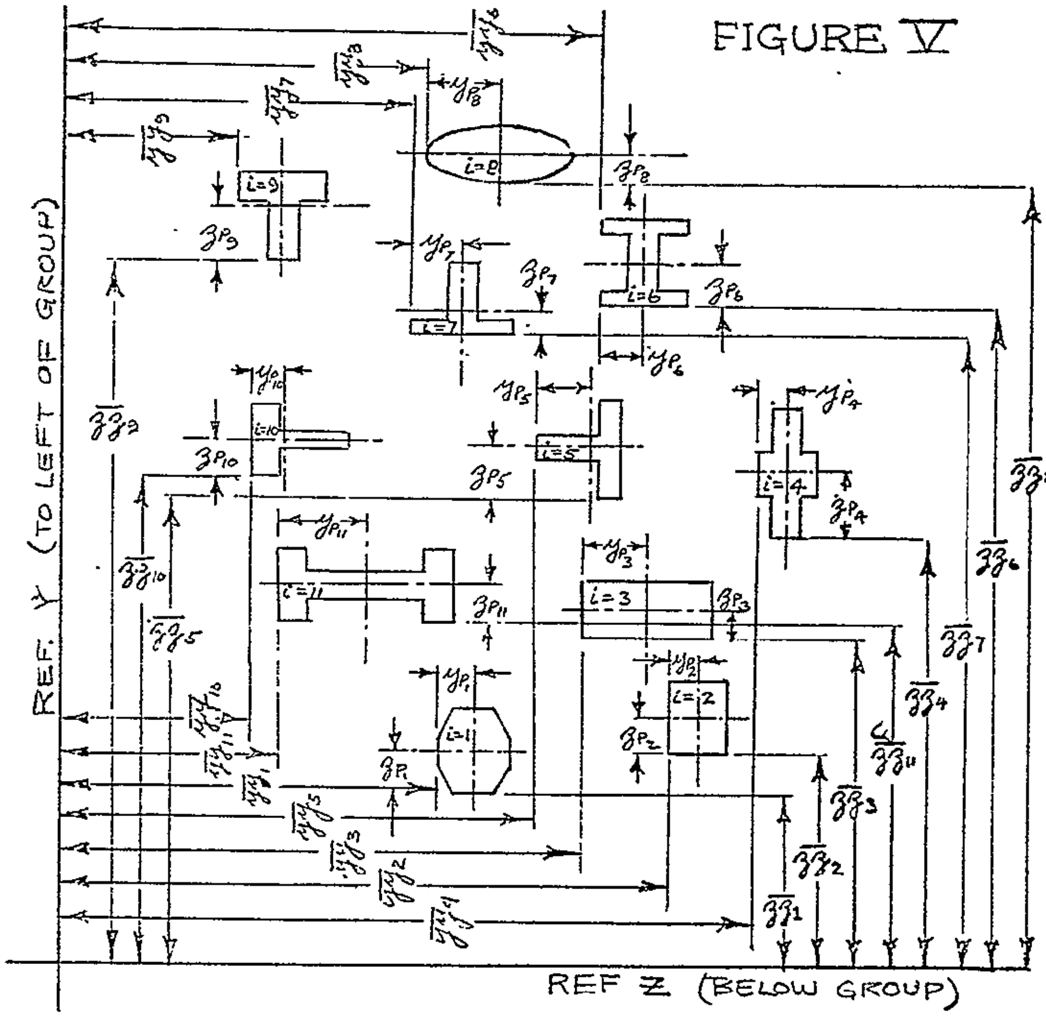

BY INSPECTING FIGURES I AND V IT IS EVIDENT THAT

(98) $z_i = \overline{zz}_i + z_{P_i}$. WHERE $\overline{zz}_i$ AND z_{P_i} ARE BOTH ITEMS OF INPUT.

AND

(99) $y_i = \overline{yy}_i + y_{P_i}$ WHERE $\overline{yy}_i$ AND y_{P_i} ARE BOTH ITEMS OF INPUT.

THUS:

REFERENCE EQUATION

(100) $$\bar{z} = \frac{\sum_{i=1}^{i=n} \frac{A_i}{l_i} z_i}{\sum_{i=1}^{i=n} \frac{A_i}{l_i}}$$ (14)

AND

(101) $$Z_i = z_i - \bar{z}$$ (15)

AND THUS

(102) $$\bar{y} = \frac{\sum_{i=1}^{i=n} \frac{A_i}{l_i} y_i}{\sum_{i=1}^{i=n} \frac{A_i}{l_i}}$$ (16)

AND

(103) $$Y_i = y_i - \bar{y}$$ (17)

CONFIGURATION 1.
VERTICAL RECTANGLE ($H_i > B_i$)

FIG VI

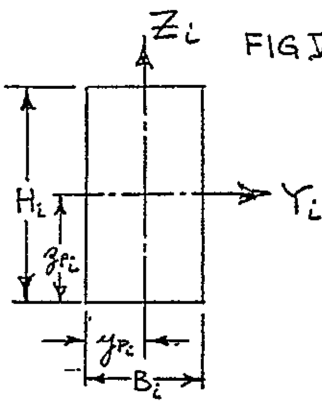

(104) $I_{Y_i} = \frac{1}{12} B_i H_i$

(105) $I_{Z_i} = \frac{1}{12} H_i B_i^3$

(106) $A_i = A_i B_i$

(107) $y_{P_i} = B/2$

(108) $z_{P_i} = H/2$

(109) $K_i = H_i B_i^3 \left[\frac{1}{3} - 0.21 \frac{B_i}{H_i}\left(1 - \frac{B_i^4}{12 H_i^4}\right)\right]$ --- ROURKE

CONFIGURATION 2.
HORIZONTAL RECTANGLE ($H_i < B_i$)

(110) $I_{Y_i} = \frac{1}{12} B_i H_i^3$

(111) $I_{Z_i} = \frac{1}{12} H_i B_i^3$

(112) $A_i = H_i B_i$

(113) $y_{P_i} = B_i/2$

(114) $z_{P_i} = H_i/2$

(115) $K_i = B_i H_i^3 \left[\frac{1}{3} - 0.21 \frac{H_i}{B_i}\left(1 - \frac{H_i^4}{12 B_i^4}\right)\right]$

CONFIGURATION 3
OCTOGON

FIG VII

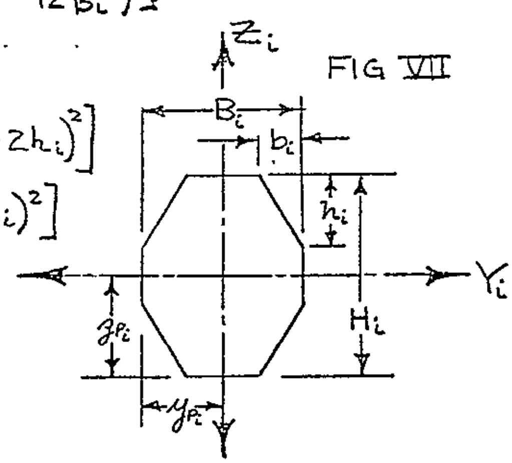

(116) $I_{Y_i} = \frac{1}{12} B_i H_i^3 - \left[\frac{1}{9} b_i h_i^3 - \frac{b_i h_i}{18}(3H_i - 2h_i)^2\right]$

(117) $I_{Z_i} = \frac{1}{12} H_i B_i^3 - \left[\frac{1}{9} h_i b_i^3 - \frac{b_i h_i}{18}(3B_i - 2b_i)^2\right]$

(118) $A_i = H_i B_i - 2h_i b_i$

(119) $z_{P_i} = H_i/2$

(120) $y_{P_i} = B_i/2$

(121) $K_i = \frac{A^4}{40(I_{Y_i} + I_{Z_i})}$ ---- ROURKE

CONFIGURATION 4
CRUCIFORM

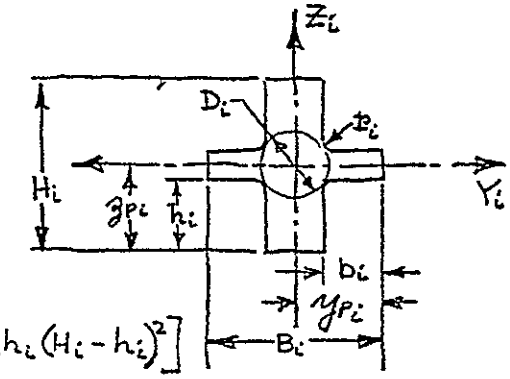

(122) $I_{Y_i} = \frac{1}{12} B_i H_i^3 - \left[\frac{1}{3} b_i h_i^3 + b_i h_i (H_i - h_i)^2\right]$

(123) $I_{Z_i} = \frac{1}{12} H_i B_i^3 - \left[\frac{1}{3} h_i b_i^3 + b_i h_i (B_i - b_i)^2\right]$

(124) $A_i = B_i H_i - 4 b_i h_i$

(125) $z_{pi} = H_i/2$

(126) $y_{pi} = B_i/2$

(127) $K \doteq \frac{\pi D^4}{32}$

CONFIGURATION 5
UPRIGHT I - BEAM

FIG IX

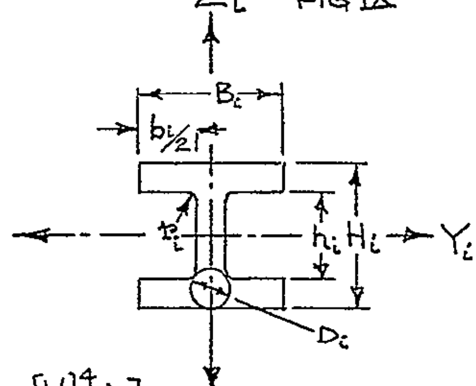

LET $b' = \frac{H_i - h_i}{2}$

$c' = h_i$

$d' = (B_i - b_i)$

$a' = B_i$

$K_i = 2K_1 + K_2 + 2\alpha D_i^4$

WHERE:

$K_1 = a'(b')^3 \left[\frac{1}{3} - 0.21 \frac{b'}{a'}\left(1 - \frac{[b']^4}{12[a']^4}\right)\right]$

OR

$K_1 = B(b')^3 \left[\frac{1}{3} - 0.21 \frac{b'}{B}\left(1 - \frac{[b']^4}{12 B^4}\right)\right]$

AND WHERE

$K_2 = \frac{1}{3} h (d')^3$

TEST:

IF $b' < d'$ THEN $t = b'$ AND $t_1 = d'$

IF $b' > d'$ THEN $t = d'$ AND $t_1 = b'$

THEN

$\alpha = \frac{t}{t_1}\left(0.15 + 0.10 \frac{r}{b'}\right)$

$I_{Y_i} = \frac{1}{12}\left(B_i H_i^3 - b_i h_i^3\right)$

$I_{Z_i} = \frac{1}{12}\left(H_i B_i^3\right) - 2\left[\frac{1}{96} h_i b_i^3 + \frac{b_i h_i}{32}(2B_i - b_i)^2\right]$

$A = B_i H_i - b_i h_i$

$y_{P_i} = B_i/2$

$z_{P_i} = H_i/2$

CONFIGURATION 6
HORIZONTAL I- BEAM

FIG X

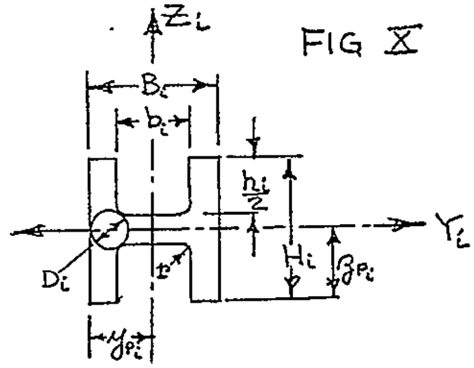

LET $b' = \frac{B_i - b_i}{2}$

$c' = b_i$

$d' = H_i - h_i$

$a' = H_i$

$K = 2K_1 + K_2 + 2\alpha D_i^4$

WHERE $K_1 = H_i (b')^3 \left[\frac{1}{3} - 0.21 \frac{b'}{H_i}\left(1 - \frac{[b']^4}{12 H_i^4}\right)\right]$

AND WHERE

$$K_2 = \frac{1}{3} b_i (d')^3$$

TEST:
IF $b' < d'$ THEN $t = b'$ AND $t_1 = d'$
IF $b' > d'$ THEN $t = d'$ AND $t_1 = b'$

$I_{Y_i} = \frac{1}{12}(B_i H_i^3) - 2\left[\frac{1}{96} b_i h_i^3 + \frac{h_i b_i}{32}(2H_i - h_i)^2\right]$

$I_{Z_i} = \frac{1}{12}\left[H_i B_i^3 - h_i b_i^3\right]$

$A_i = B_i H_i - b_i h_i$

$y_{P_i} = B_i/2$

$z_{P_i} = H_i/2$

CONFIGURATIONS 7 AND 8. :
UPRIGHT (SHOWN) AND INVERTED T-SECTIONS' RESPECTIVELY:

FOR BOTH CONFIGURATIONS 7 & 8:

FIG XI

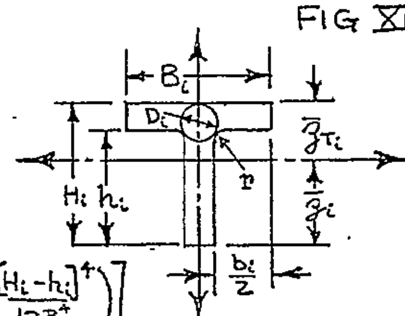

LET

$b' = H_i - h_i$

$d' = B_i - b_i$

$K_i = K_1 + K_2 + \alpha D_i^4$

WHERE

$K_1 = B_i (H_i - h_i)^3 \left[\frac{1}{3} - 0.21 \frac{H_i - h_i}{B_i}\left(1 - \frac{[H_i - h_i]^4}{12 B_i^4}\right)\right]$

$K_2 = h_i (B_i - b_i)^3 \left[\frac{1}{3} - 0.105 \frac{B_i - b_i}{h_i}\left(1 - \frac{[B_i - b_i]^4}{192 h_i^4}\right)\right]$

TEST:
IF $b' < d'$ THEN $t = b'$ AND $t_1 = d'$
IF $b' > d'$ THEN $t = d'$ AND $t_1 = b'$

THEN

$$\alpha = \frac{t}{t_1}\left(0.15 + 0.10\frac{r}{b'}\right)$$

$$\bar{z}_i = H_i - \frac{1}{2}\frac{(B_i - b_i)H_i^2 + b_i(H_i - h_i)}{(B_i - b_i)H_i + \frac{b_i}{2}(H_i - h_i)}$$

$$\bar{z}_{T_i} = H_i - \bar{z}_i$$

$$I_{Y_i} = \frac{1}{3}\left[B_i \bar{z}_{T_i}^3 - b_i(h_i - \bar{z}_i)^3 + (B_i - b_i)\bar{z}_i^3\right]$$

$$I_{Z_i} = \frac{(H_i - h_i)B_i^3 + h_i(B_i - b_i)^3}{12}$$

$$A_i = B_i(H_i - h_i) + h_i(B_i - b_i)$$

$$y_{P_i} = B_i/2$$

<u>FOR CONFIGURATION 7 ONLY:</u>

$$z_{P_i} = \bar{z}_i$$

<u>FOR CONFIGURATION 8 ONLY:</u>

$$z_{P_i} = \bar{z}_{T_i}$$

<u>CONFIGURATIONS 9 AND 10:</u>

T-BEAMS WITH FLANGE TO THE LEFT (SHOWN) AND FLANGE TO THE RIGHT RESPECTIVELY:

FIG XII

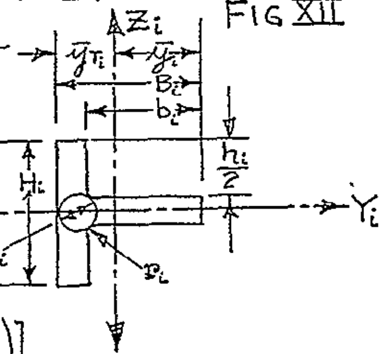

<u>FOR BOTH CONFIGURATIONS 9 & 10:</u>

LET

$$b' = B_i - b_i$$
$$d' = H_i - h_i$$
$$K_i = K_1 + K_2 + \alpha D_i^4$$

WHERE:

$$K_1 = H_i(B_i - b_i)^3\left[\frac{1}{3} - 0.21\frac{B_i - b_i}{H_i}\left(1 - \frac{[B_i - b_i]^4}{12H_i^4}\right)\right]$$

$$K_2 = b_i(H_i - h_i)^3\left[\frac{1}{3} - 0.105\frac{H_i - h_i}{b_i}\left(1 - \frac{[H_i - h_i]^4}{192 b_i^4}\right)\right]$$

TEST:
IF $b' < d'$ THEN $t = b'$ AND $t_1 = d'$
IF $b' > d'$ THEN $t = d'$ AND $t_1 = b'$

THEN

$$\alpha = \frac{t}{t_1}\left(0.15 - 0.10\frac{r}{b'}\right)$$

$$\bar{y}_i = B_i - \frac{1}{2}\frac{(H_i - h_i)B_i^2 + h_i(B_i - b_i)^2}{(H_i - h_i)B_i + \frac{h_i}{2}(B_i - b_i)}$$

$$\bar{y}_{T_i} = B_i - \bar{y}_i$$

$$I_{Z_i} = \frac{1}{3}\left[H_i \bar{y}_{T_i}^3 - h_i (b_i - \bar{y}_i)^3 + (H_i - h_i)\, \bar{y}_i^3\right.$$

$$I_{Y_i} = \frac{1}{12}\left[(B_i - b_i) H_i^3 + b_i (H_i - h_i)^3\right.$$

$$A_i = H_i(B_i - b_i) + b_i(H_i - h_i)$$

$$z_{P_i} = H_i/2$$

<u>FOR CONFIGURATION 9 ONLY:</u>

$$y_{P_i} = \bar{y}_{T_i}$$

<u>FOR CONFIGURATION 10 ONLY:</u>

$$y_{P_i} = \bar{y}_i$$

WIND TUNNEL STING BALANCES

TASK CORPORATION
1009 E. Vermont Avenue
Anaheim, California

Appendix C

WIND TUNNEL STING BALANCES

Richard R. Tracy
Task Corporation

INTRODUCTION The fundamental tool of the experimental gas dynamicist or aerodynamicist is the wind tunnel. Of the many measurements made in wind tunnels, the most important, at least from an engineering standpoint, is the determination of aerodynamic forces and moments acting on a body. In early tunnels, the model support struts attached to beam balances and the forces were measured by direct comparison with dead weights. The balances were necessarily situated outside the tunnel working section. Such "external balances" are still in use in some present facilities. However, although servo-driven self-balancing devices (and more recently, the replacement of balance beams by force transducers) have reduced the tedium and time involved in making force measurements, the external balance exhibits several undesirable features:

1. Large tares due to the weight of the model support system (and pitching system when measurements are in "wind axes").
2. Large force transfer due to balance location away from model.
3. Support struts must be windshielded, hence pressure sealing may present a formidable problem.

These difficulties were largely overcome by locating the "balance" (as it is still called) within the model or between the model and a supporting strut. Where such an arrangement is employed, the support strut extends downstream from the model base and is called a "sting"; hence, the name "sting balance".

The construction of the internal (or sting) balance was made possible as a consequence of the invention of the resistance strain gage. Early examples were little more than instrumented stings; strain gages were located in such positions as to give signals "proportional" to the applied aerodynamic forces and moments. Despite the subsequent refinement of both strain gages and balance geometry, single piece balances were generally characterized by significant coupling effects (interactions), large deflections, and limited load carrying capacity.

A reduction of strain gage physical size later permitted the consideration of an entirely different type of internal balance. It was conceptually very similar to the external balance in that the aerodynamic forces and moments were mechanically resolved by a statically determinant array of members, each of which was instrumented with strain gages. Thus, each member (or element) was a single force transducer isolated from the remaining forces by pivots located at each of its ends. Supported on the six elements was a model attachment frame or sleeve, giving this type its name - "floating frame balance". Despite the similarity of function, size, and location of the two types of internal balances, it is edifying to examine the important aspects in which they differ.

THE SINGLE PIECE BALANCE The single piece balance is essentially a cantilever beam supporting a model at its end and instrumented with strain sensitive devices. If such a member is loaded at its end by some combination of forces and moments, the state of stress (and hence strain, for an elastic material) is completely determined throughout the member. Since it is impossible to completely determine the state of strain throughout a body, the loads on the member must be determined from a knowledge of the surface strains at a few discrete locations. That is, if several combinations of one, two, or four gages are each wired to give an electrical output (for example, a Wheatstone Bridge) proportional to local surface strain, is it possible to equate each output to, say, a linear combination of the six applied forces and their products?

$$(\text{OUTPUT})_n = \sum_{p=1}^{6} (k_n)_p F_p + \sum_{p=1}^{6} \sum_{q=1}^{6} (k_n)_{pq} F_p F_q$$
$$+ \sum_{p=1}^{6} \sum_{q=1}^{6} \sum_{r=1}^{6} (k_n)_{pqr} F_p F_q F_r + \dots$$
$$+ \sum_{p=1}^{6} \dots \sum_{u=1}^{6} (k_n)_{pqrstu} F_p F_q F_r F_s F_t F_u \tag{1}$$

Such a representation is sufficiently general; however, if the above equations for the outputs of a six component balance were written out in full, they would involve 335,916 coefficients! Even though only 5,562 of these are independent (under the assumption that outputs depend only upon load combinations rather than loading sequence), the calibration required for their determination and the problem of inversion (solution for the forces from a set of output signals) would be formidable. The practical limit for calibration and data reduction requires a system whose outputs may be represented by:

$$(\text{OUTPUT})_n = \sum_{p=1}^{6} (k_n)_p F_p + \sum_{p=1}^{6} \sum_{q=1}^{6} (k_n)_{pq} F_p F_q \tag{2}$$

and further that the calibration slope constant of each component, $(K_n)_n$, be much greater than the remaining coefficients. That is, each output depends predominantly on only one applied load component. It is rather surprising that a cantilever member can be constructed and instrumented with strain gages whose component outputs meet these requirements.

In the general case, a bridge of strain gages is applied to an especially machined section: one such for each force or moment component to be measured. Each section is configured and the gages mounted on it so as to be sensitive to strains resulting from the application of only one force component and, insofar as possible, insensitive to the strains produced by application of the forces. The achievement of this end is approached by:

1. Thoughtful design and careful machining
2. Careful matching of gage sensitivities within each bridge
3. Precise gage placement

It is further apparent that the ratios between applied forces to be measured must be in the neighborhood of unity. That is, a section greatly weakened to measure a very light force is incapable of supporting the remaining large forces, not to mention the inability to remain insensitive to the large strains imposed. (Note that moments may be approximately compared with forces by dividing each moment by the largest balance dimension lying in the plane of the moment's action.)

The above limitation renders this type of balance unsatisfactory for measurement of chord (model axis) forces in most aerodynamic problems. Balances which must measure relatively light chord forces are equipped with a pivoted axial element, isolated from the remaining forces by a flexured cage. In this sense the balance is partially of the floating frame type. The most successful recent examples of the single piece balance, group more than one measuring component at each station. In fact, it is not now uncommon to sense five forces or moment components at one elaborately machined section and chord force as described above. The section offers multiple parallel load paths to the applied forces and in philosophy approaches the floating frame balance.

THE FLOATING FRAME BALANCE The floating frame balance consists of a cantilever member which supports a model mounting frame or sleeve by means of a statically determinant array of one-component force transducer links. Each link or element is provided with pivots at each end in order to permit only one component of load to be transmitted through the element under any combination of applied loads.

In general, there are any number of possible orientations of the elements which provide mechanical resolution of applied forces and moments into single force components through each element. For a specified combination of capacity loads, a particular configuration usually provides optimum resolution and over-all accuracy; however, the wind tunnel internal balance is confined within a very specialized package shape. The most usual external shape is that of an elongated circular cylinder whose axis is aligned with the model axis. Somewhat fortuitously, these spatial confinements are compatible with the element arrangement most suitable for resolution of the usual force and moment combinations.

Broadly, this arrangement may be described as a pair of vertically situated elements spaced apart longitudinally; another pair of elements similarly spaced but lying in a horizontal plane; an axial element; and a concentrically placed torque tube. The result is a rectilinear arrangement of normal force, side force, and axial force members and a pure moment measuring element. It should be emphasized that each element is capable of transmitting only one component of force (or moment) by virtue of its placement and the pivots provided at each end, and that, additionally, the transducer associated with each element is designed to be sensitive only to the applied force. Consequently, the output of each transducer is proportional only to the value of its associated applied force and not upon any other applied force or combination of applied forces.

The preceeding discussion applies strictly to an idealized internal balance (rigid support structure, perfect pivots, perfect initial alignment, negligible transducer deflections, and transducer output proportional to load). These effects are an approximation to the behavior of a real balance, albeit, a very close approximation in several important cases - notably the lower force range balances. The reasons for departures from the ideal behavior may generally be attributed to the following real effects:

1. Distortion of the model support frame ("outer sleeve")
2. Deflections of the cantilever supporting member ("inner rod").
3. Imperfect pivots preventing complete force separation and resolution.
4. Deflection of elements (including transducer) under loading.
5. Transducer sensitivity to incidental non-primary loads.
6. Transducer failure to produce output proportional to load.

A final important source of abberative behavior not heretofore considered is:

7. Sensitivity to thermal environment.

Before investigating in detail the results of these deviations from ideal, it is well to state some general consequences which may be inferred.

Initial misalignment will be a source of first order interactions, as will be the finite stiffness of the pivots in transmitting small spurious loads to a slightly "cross-sensitive" transducer. These are minimized by careful pivot and transducer design.

About one-third of the mathematically possible second order interactions will necessarily exist. Their magnitudes are in proportion to the degree of misalignment produced by applied loads, and may be approximately calculated from estimated element and structure deflections. Several of these are usually negligible and the rest are reduced by minimizing angular deflections under loading.

Third order interactions are, at most, on the order of second order terms squared. Hence, they may generally be considered negligible since second order terms rarely exceed about 1 percent even under the most adverse circumstances.

Transducer inaccuracies impose a fundamental restriction on ultimate balance performance. Non-linearity, non-repeatability, hysteresis, electrical signal zero drift with time, drift under load, thermal change of sensitivity, thermal zero drift, and sensitivity to other environmental conditions are all potential errors which must be minimized.

A very important aberration to which the floating frame balance is susceptible is the introduction of thermal forces arising from temperature gradients (or dissimilar materials) through the balance. These are actual forces and not the thermal strains to which the transducer may also be sensitive (in these as well as in the single piece balances). Thermal forces always exist in a multiply connected body (i.e., one with holes) in the presence of temperature gradients.

Generally, these forces tend toward zero as the pivot stiffness decreases. Furthermore, since the thermal gradients encountered are rather consistently similar in most applications, it is particularly important to employ the particular configuration which renders the thermal forces a minimum under the anticipated conditions. The most successful approach to this problem will be described in a later section of this paper.

FLOATING FRAME BALANCE COMPONENTS: The design of a floating frame balance involves the application of several branches of engineering technology. Although, in balance design practice, these several fields are intimately interconnected, an attempt will be made here to deal with them as separately as is meaningful in order to emphasize the primary function of each of the components and to bring out the principal considerations influencing their design. The balance problem may be subdivided as follows:

1. Mechanical force resolution
2. Strength of structural support members
3. Pivots
4. Transducers and strain gage techniques
5. Attachments
6. Calibration and operation
7. Balance selection

1. Mechanical Force Resolution The arrangement of the forces resolving linkage system has been briefly mentioned previously. The general nature of the applied forces and the restriction on shape dictate a particular arrangement of the pivoted links as shown schematically in Figure 1. A pair of elements placed on vertical diameters (of the circular cylindrical package) sense normal force and pitching moment. Another pair on horizontal diameters sense side force and yawing moment. Axial (chord) force is carried by a central longitudinal element and rolling moment is taken by a concentric tube around the chord force element.

The above arrangement effectively solves the force resolution problem in a manner compatible with structural, pivot, and transducer requirements. However, a radial temperature gradient introduces an axial thermal force which may be significant compared to the axial force capacity. Thermal error proved to be a severe limitation on the usefulness of this arrangement and for several years a variety of devices were employed in an attempt to cancel or compensate the spurious thermal output. The first balance to successfully overcome this difficulty employed a deceptively apparent and minor mutation of element arrangement which eliminated the troublesome thermal force even in the presence of the radial temperature gradient.

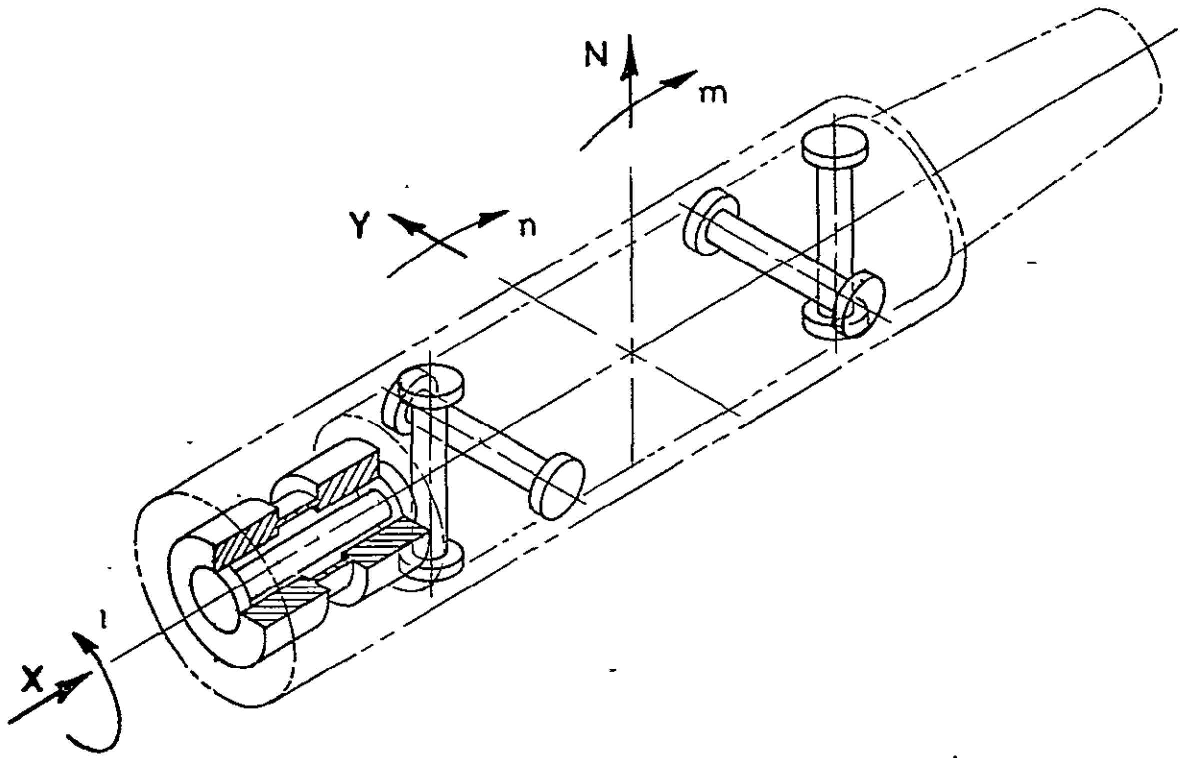

Figure 1. Schematic of early arrangement for force resolving links.

In order to understand the method of averting thermal forces in the balance, it is necessary to examine the basic problem. If the roll and axial members are imagined to be removed, the resulting differential expansion between the inner rod and outer sleeve is "centered" at a point midway between the forward and aft sets of normal and side force elements. At any other station there is a relative axial displacement between the inner rod and outer sleeve. With the axial force element installed at the balance forward end, the relative displacement there cannot exist and an axial force is developed of magnitude such as to overcome the normal and side force elements' pivot stiffness in removing the displacement. In other words, the differential expansion is forcibly "centered" at the axial element station and if this does not coincide with the "natural" center (with axial element removed) of expansion, then a thermal axial force will result. It is, therefore, clear that the natural solution of the problem is to place the axial force element at the "thermal center". The "Series - D" balances (after Robert Davie who first realized this configuration) employ dual (tandem) axial elements acting in parallel and positioned symmetrically with respect to the thermal center or "center of forces". The dual chord force permits the otherwise impossible achievement of a completely symmetrical central position and, in addition, provides electrical cancellation of thermal forces arising from a temperature difference between the inner rod and axial elements. The tandem axial elements are attached at their common center to the outer sleeve and at their ends to the inner rod. An applied axial force produces forces of opposite sense in each element while forces due to temperature differences between inner rod and axial element are of the same sense in each, thus producing no net signal from the combined outputs. An example of this arrangement is depicted in Figure 2.

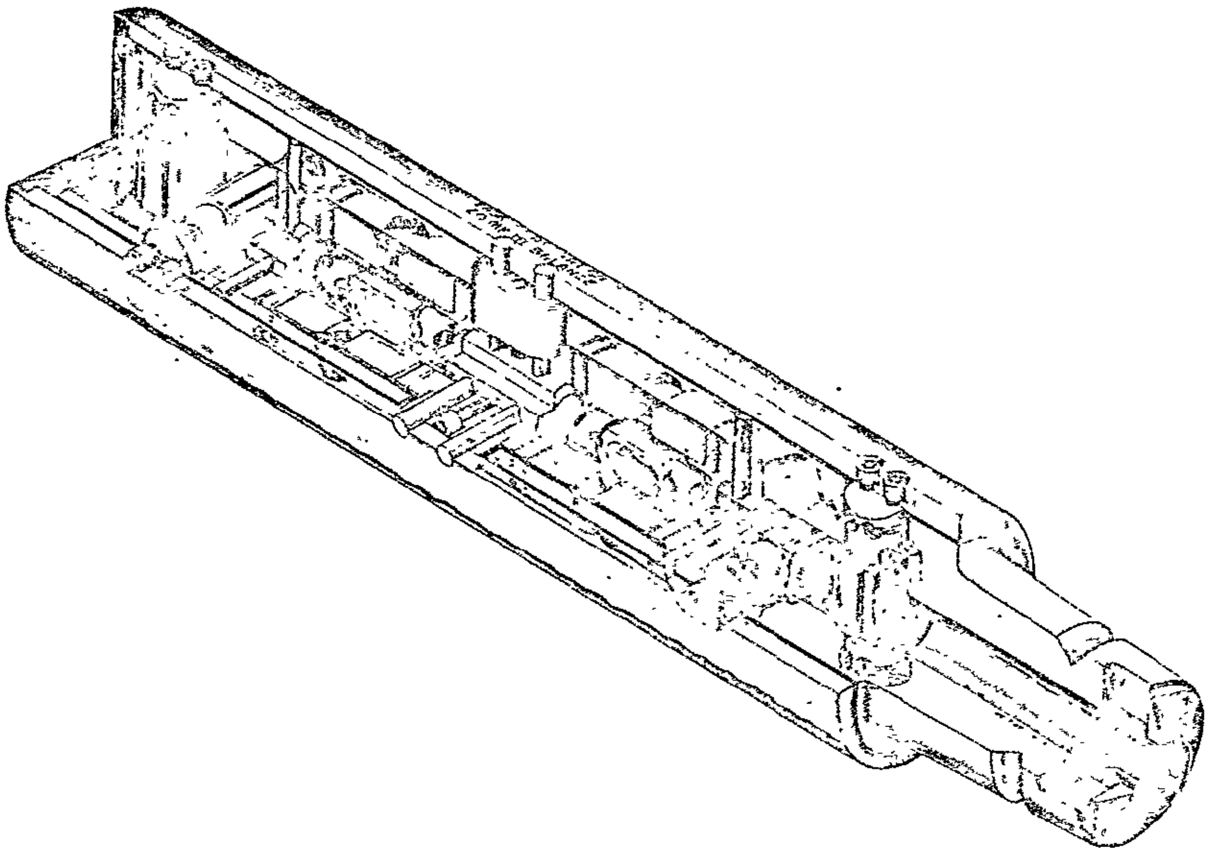

Figure 2. Cutaway view of a modern force balance.

As a natural consequence of the arrangement the roll element becomes a dual member attached as is the chord force, and placed concentrically around it. Additional benefits are the virtual elimination of second order interactions involving normal forces times chord force or rolling moment, and side force times chord force or rolling moment. Also, the second order interactions arising from pitching or yawing moment times chord force or rolling moment are substantially reduced.

Because of its many advantages, this arrangement of force resolving members is now practically in universal use for floating frame balances. Minor changes in relative spacing of elements, etc., are dictated by each particular combination of loads to be measured and the permissible physical size of the balance.

<u>2. Strength of Structural Support Members</u> The strength of the inner rod and outer sleeve is a relatively straightforward stress analysis problem. The outer sleeve should occupy as little space as possible yet provide adequate attachment for each of the elements and sufficient strength and rigidity to carry the loads from the model attachment device.

Generally, the inner rod occupies all of the space not taken by the outer sleeve or the elements. This is done, not only to maximize rigidity, but because the inner rod, rather than the elements, is a limiting component in the maximum load carrying capacity of a balance! Since, as shown in Figure 2, the inner rod is machined to provide clearance holes (as well as mounting seats) for the elements, the size and shape of each element is to some extent governed by the structural requirements of the inner rod. The inner rod is provided with a means of attachment to the supporting sting. Most usually this is accomplished by a tapered joint which is locked and keyed. While the design of this joint is not of fundamental importance in balance performance, it is a very critical area and will be discussed presently.

3. Pivots The pivots used at each end of the elements have a definitive effect upon balance performance. While they need not deflect through large angles, they must be compact, rotationally free, axially rigid, and absolutely without axial backlash or rotational hysteresis. The only pivot which approaches these qualities is the elastic pivot employing integral flexible portions or "flexures".

The simplest elastic pivot providing the two degrees of rotational freedom required (universal joint) consists of a pair of flat strap flexures in tandem at right angles to each other. The only defect of the elastic pivot is its elastic restoring moment resisting angular deflection. This pivot stiffness introduces redundancy into the ideally statically determinant system. However, if the actual forces in each element are "closely approximated" by a statically determinant analysis, then it may be expected that, except for slight change in the apparent sensitivity of each transducer, the balance will behave substantially as if it had perfect pivots. A crude calculation serves to establish the degree to which the real balance approaches the statically determinant ideal. Consider six identical elements, each comprised of a pair of flat strap flexures at each end and an intermediate strain gage transducer as shown schematically in Figure 3. The lateral force, S, required to deflect each element a distance, δ, is related to the restoring moment of the flexures, M:

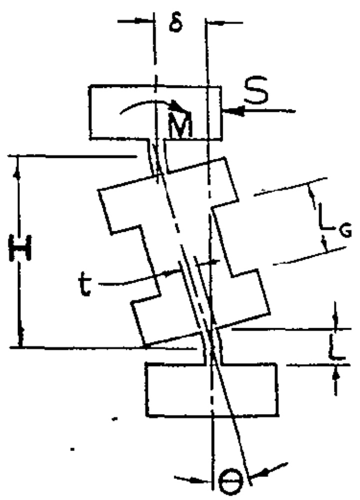

Figure 3. Schematic arrangement of typical flexural element.

$$S = \frac{2M}{H} \tag{3}$$

where H is the flexure spacing.

The moment is dependent on the deflection angle, θ, and the flexure geometry

$$M = K_\theta = \frac{EI}{L}\theta = \frac{Ebt^3\theta}{12L} = \frac{EAt^2\theta}{12L} \tag{4}$$

where E is Young's Modulus and A is the flexure cross-sectional area. L is the flexure length and b and t are its width and thickness, respectively. The angular deflection is the result of the axial deflection of one element carrying the primary load, P:

$$\delta = 4\,\delta_{\text{flexure}} + \delta_{\text{transducer}}$$

$$= 4\frac{PL}{AE} + \frac{PL_g}{A_g E}$$

$$\therefore \theta = \frac{\delta}{H} = 4\frac{PL}{AEH} + \frac{PL_g}{A_g EH}\,, \tag{5}$$

where θ is the angular deflection, L_g and A_g are transducer length and cross-sectional area respectively.

Inserting these in the expression for the lateral force, summing the lateral forces, S, produced by each of the remaining five elements and dividing by P, the primary force acting on the component under consideration gives the fraction of applied load diverted by the flexures of the remaining element:

$$\sum_{n=1}^{5} \delta = 5\left[\frac{2}{H}\ \frac{EAt^2}{12L}\ \left(4\frac{PL}{AEH} + \frac{PL_g}{A_g EH}\right)\right] = \Delta P \tag{6}$$

$$\therefore \frac{\Delta P}{P} = \left[\frac{10}{3} + \frac{5}{6}\left(\frac{L_g}{L}\right)\left(\frac{A}{A_g}\right)\right]\left(\frac{t}{H}\right)^2 \tag{7}$$

Typically, L_g/L is of order 10 and A/A_g of order 1/3 (for "tension-type" elements), hence:

$$\frac{\Delta P}{P} \cong 6\left(\frac{t}{H}\right)^2 \tag{8}$$

Thus, the fraction of an applied load that is "lost" due to the redundancy of the system is very small if the flexures' thicknesses are small compared with the dimension separating each pair. The above formula is a result of great oversimplification and serves only to verify that the use of properly designed elastic pivots will permit the balance to function substantially as anticipated.

Each flexure is a thin strap comprising the material remaining between parallel holes drilled through the element shank. Not only is this type of flexure straightforward to manufacture with great precision but it possesses very desirable behavior under load. Another advantageous feature is that all of the machine work on an element may be completed before the flexures are "sawed-free" to permit the flexures to deflect.

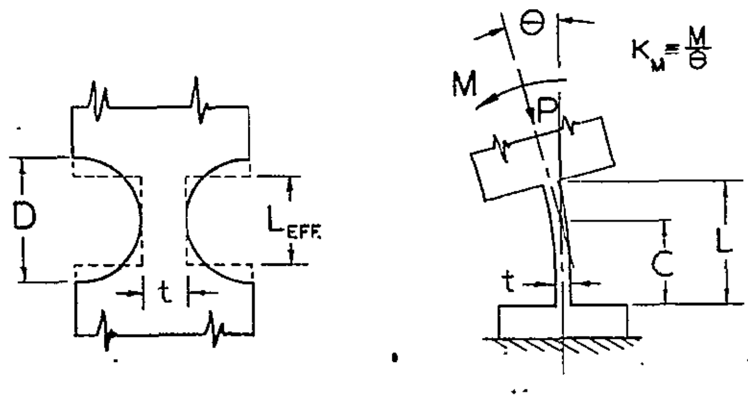

Figure 4. Typical flexure used in force balance.

Occasionally, compatibility or stress requirements indicate a longer flexure than can be obtained with "circular arc" types. In these cases the strap is elongated by milling slots on each side of the flexure rather than by drilling larger holes.

The term, "compatibility" is used herein to describe the ease with which the elastic pivots permit each element to comply with the lateral deflections imposed on them by the axial deflections of a loaded element. A synonymous term is "compliance": it is the reciprocal of the spring constant.

The behavior of a flexure in bending while subjected to axial force is in itself a problem of some complexity. The beam-column analysis required has been presented by Eastman and others for the case of a flat strap, constant thickness, flexure for several possible modes of loading. The results of importance for balance application are that as axial force increases:

1. The position of the center of the center of rotation shifts
2. The allowable angle of rotation decreases rapidly
3. The apparent restoring moment or angular spring constant changes.

The proper axial force parameter is the ratio of applied force to critical buckling load. These effects are shown quantitatively in Figure 5, with terms explained in the sketch of Figure 4. The surprising consequence is that the effective spring constant in bending increases with compressive load and decreases with tension!

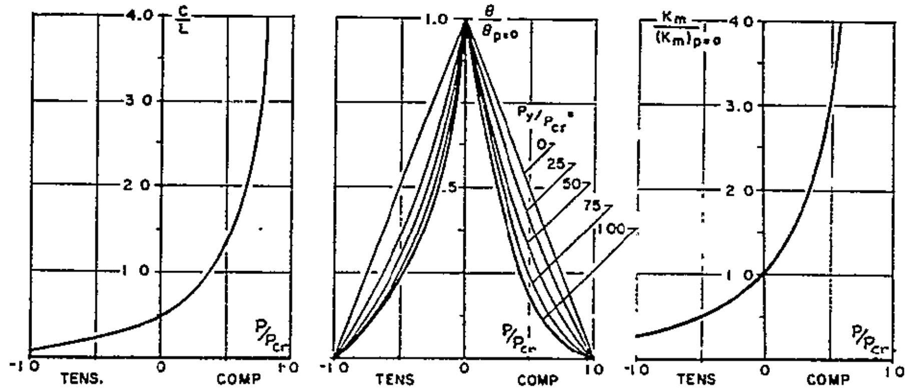

Figure 5. Flexure behavior under axial loading.

The flexures used in the internal balance under discussion are usually of the "circular arc" type with sides formed by parallel drilled holes such that the thickness varies continuously along their length. It is possible to define an effective flat strap length of this type of flexure in bending and also for axial deflection. These are plotted as effective length over thickness (Le/t) versus flexure hole diameter (arc diameter) over minimum thickness (D/t) in Figure 6.

Immediately apparent are the two shortcomings of circular arc flexures:

1. The axial deflection is somewhat greater than that of an equivalent flat-strap flexure
2. The longitudinal space required is much larger than that occupied by the equivalent flat strap

These are usually unimportant concessions compared with the benefits accrued.

The usual range of D/t is from about 3 - 8 resulting in Leff./b of about 1.5 - 2.5 in bending. (Greater D/t is usually ineffectual while very small D/t results in poor compliance and excessive bending stress.)

Even for the extreme case of L/t = 2.5, the flexure working load is only about 20 percent of the conservatively calculated buckling load. Since this case corresponds to a very compliant flexure, and since stiffer flexures are typically working at P/P_{cr} less than 10 percent, it may be reasonably expected that the effects portrayed in Figure 5 will be very recessive in affecting balance performance. In a few instances where load capacity has necessitated thick flexures and bending stress limitations dictated large flexure diameters (or flexure elongation), excessive second order interactions were traced in part to the variation of restoring moment of such flexures with applied axial force. This points up the fallacy of excessively increasing flexure length to gain compliance. There is a point of diminishing returns beyond which increasing flexure length does little but increase

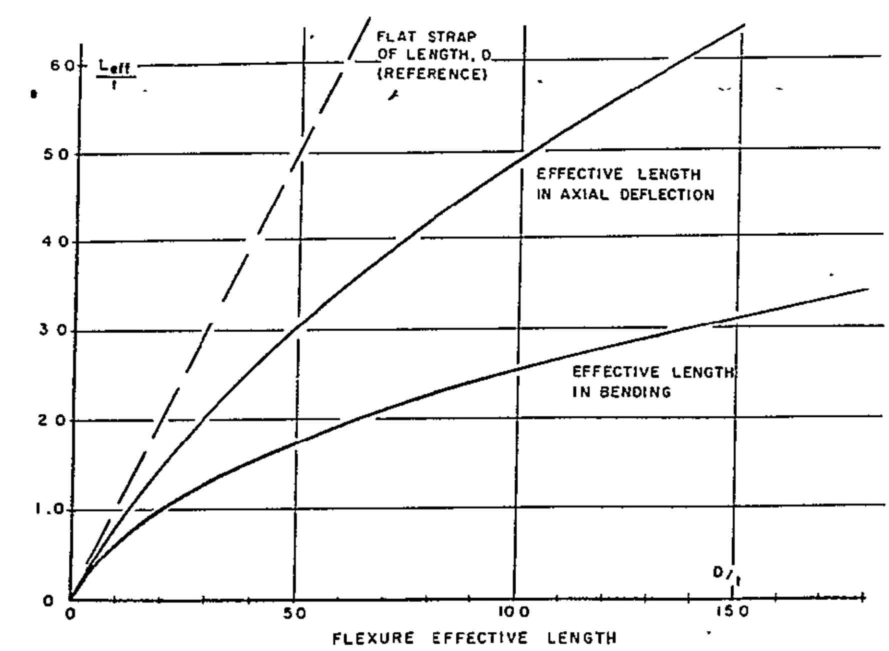

Figure 6. Effect of flexure geometry when exposed to axial and transverse loading.

over-all balance deflection. Flexure lengths of greater than about 3 times their thickness are rarely useful except to reduce otherwise intolerable bending stress levels. In fact, it is apparent that very long flexures in a moderately non-compliant balance will lead to significant non-linearity in the second order interactions (tantamount to a third order interaction) due to the non-linearity of restoring moment depending upon load. Long flexures are justified only when the transducers involved are much more deflective than "tension-type" or when the reduction of flexure bending stress permits the flexure to be substantially thinner.

A general practice appropos the above discussion is to design the balance with maximum flexure spacing and very thin flexures (so that the direct flexure stress is near the permissible working stress). Excessive bending stresses should be reduced first by increasing flexure diameter and only then, if necessary, increasing flexure thickness. Only in severe cases will elongation of flexures be necessary.

It is of value at this point to note (with a little hindsight) that an estimate of the limiting loads for which the balance may be expected to operate as a nearly statically determinant system can be made from flexure considerations alone. If each normal force element has the dimensions shown in Figure 7, where "D" is the diameter of the model cavity (and balance outside diameter), then the average fraction of applied load "lost" through flexure stiffnesses is found from the previously obtained expression:

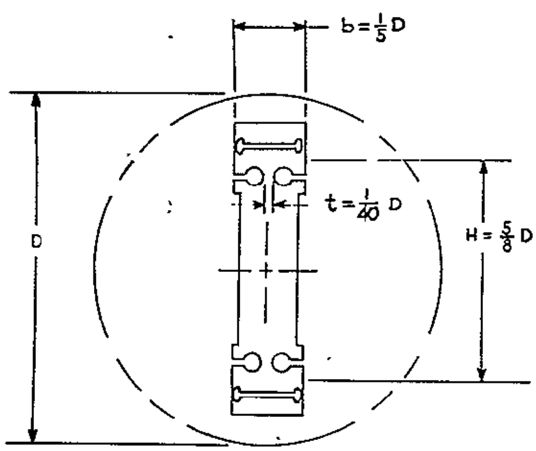

Figure 7. Typical dimensions for force element flexures.

$$\frac{\Delta P}{P} \approx 6\left(\frac{t}{H}\right)^2 \approx 6\left(\frac{D/40}{5D/8}\right)^2 \approx 1 \text{ percent.} \qquad (9)$$

If the greatest ratio between capacity loads is of order ten, then about 10 percent of the lightest load may be diverted by the flexures of the other elements. The normal force capacity of this balance, assuming a direct flexure stress of 50,000 psi, is

$$N_{TOTAL} \approx (2)\sigma A_{Flex.} = (2)\sigma bt$$
$$\doteq (2)(50 \times 10^3)\left(\frac{D}{5}\right)\left(\frac{D}{40}\right) = 500\ D^2 \qquad (10)$$

Hence, for ideal behavior it would appear necessary to limit the normal force load parameter, R_n:

$$R_n \equiv \frac{N_{TOTAL}}{D^2} < 500 \qquad (11)$$

Experience has shown that, other factors given due consideration, balances meeting this requirement have very good performance and are considered "standard-range" balances.

If the flexure thickness is doubled, then

$$\frac{\Delta P}{P} \approx 4 \text{ percent} \qquad (12)$$

and nearly half of a light load component (one tenth normal force capacity) may be diverted through other elements. This may be considered to be the absolute limit for balances having behavior approximating the mechanical resolution concept. Thus, balances for which the load parameter lies in the range,

$$500 \leq R_n \leq 1{,}000 \qquad (13)$$

are considered "high-range" balances. Balances for which $R_n > 1000$ are "extended range" balances and are generally subject to aberrative behavior.

A similar "analysis" may be applied to rolling moment capacity taking as typical dimensions those of Figure 8 from which the average fraction of applied load diverted through roll element type flexures is

$$\frac{\Delta P}{P} \approx 6 \left(\frac{t}{H}\right)^2 \approx 6 \left(\frac{3/250\ D}{3/10\ D}\right) \approx 1 \text{ percent} \tag{14}$$

And again, light load elements may be of the order of 90 percent effective. Then recalling that the rolling moment, l, is carried in parallel by two such roll elements and that each pivot has four flexure straps sharing the load:

$$l \approx 8\sigma A_{flex.} R \approx 8\sigma btR$$

$$\approx (8)\ (50 \times 10^3)\ \left(\frac{3}{20} D\right) \left(\frac{3}{250} D\right) \left(\frac{9}{40} D\right)$$

$$\approx 160\ D^3 \tag{15}$$

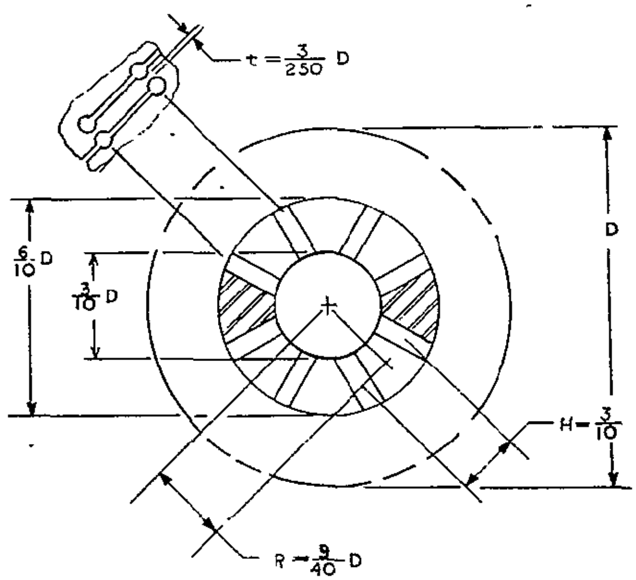

Figure 8. Typical dimensions for roll element flexures.

Hence, the maximum value of the roll load parameter for standard-range balances (here again supported by empirical results), is taken to be:

$$R_l \equiv \frac{l}{D^3} < 160 \tag{16}$$

And for high-range balances the parameter will have a value,

$$160 \leq R_l \leq 320 \tag{17}$$

R_l in excess of 320 generally determines a balance to be in the extended-range category.

Other factors, of course, influence the relationship between balance load capacity and the expected approach to ideal behavior. Generally favorable to good performance are large balance physical size and component capacities such that their load parameters are of the same order of magnitude.

Define for this purpose

$$R_N = \frac{N_{TOTAL}}{D^2} \qquad R_l = \frac{l}{D^3}$$

$$R_Y = \frac{Y_{TOTAL}}{D^2} \qquad R_m = \frac{m}{S_n D^2}$$

$$R_X = \frac{X}{D^2} \qquad R_n = \frac{n}{S_y D^2}$$

where S_n and S_y are the distances from the balance center to the normal and side force elements, respectively.

It should be emphasized that the above load limits do not represent the maximum loads for which a balance can be designed. As was mentioned earlier, the force measuring elements generally do not impose an absolute limit on load carrying capacity. In fact, the high dynamic pressures now available in some tunnels have necessitated construction of balances whose operating capacity resulted in load parameters nearly twice those corresponding to extended range balances! It is, frankly, startling, not that such a balance exhibits anomalies, but rather that it yields data of nearly the same order of reducible accuracy as a standard-range balance.

4. Transducers and Strain Gage Techniques   The transducers integral with each element may be considered the heart (or better, nervous system) of the balance. The fundamental requirement of each transducer is that it be of a size commensurate with the available space and that it produce the required output from the load component it is to sense. The additional objectives of

1. low deflection
2. linear output
3. low hysteresis or non-repeatability
4. insensitivity to extraneous forces and moments
5. insensitivity to thermal environment
6. insensitivity to pressure change and humidity
7. ease of fabrication
8. ruggedness

are each separately achievable but difficult to attain simultaneously at an acceptable level. The transducer configurations possible are literally unlimited; however, a number of specific types have found repeated application by virtue of their general satisfaction of at least most of the requirements. The most common species are:

1. tension-type
2. eccentric columns
3. ring-types

Before describing and comparing these specifically, consider a few generalities.

The deflection of a body under external loading is generally determined by applying the principal of conservation of energy:

$$W - U = \text{Const.} = 0 \tag{18}$$

Where W is the external work done by the applied loading and U is the strain energy of the body; hence, for the case of uni-axial loading of a linearly elastic body the equation becomes,

$$\frac{P\delta}{2} = \frac{1}{2} \iiint\limits_{\text{volume}} \sigma\varepsilon \; d(\text{vol.}) = \frac{E}{2} \iiint\limits_{\text{volume}} \varepsilon^2 \; d(\text{vol.}) \tag{19}$$

The formula is already specialized to the case where only one significant component of strain (stress) is developed in the body due to the applied loading, P.

For the case of a prismatic member of length, L, width b, and thickness t, loaded axially such that the axial strain is uniform throughout the member:

$$\delta = 8\frac{E}{P} \int_0^{\frac{L}{2}} \int_0^{\frac{b}{2}} \int_0^{\frac{t}{2}} \varepsilon^2 \, dx \; dy \; dz$$

$$= \frac{E}{P} \varepsilon^2 \; tbL \equiv \frac{E}{P} \varepsilon^2 \, \forall \tag{20}$$

from which it would appear that for a given strain gage output (or strain level) and for the minimum volume, v, on which a strain gage may be mounted with adequate power dissipation (which also places a lower limit on the body thickness), the deflection decreases without limit as the load capacity of the transducer increases. Unfortunately, there is a constraint between strain load and cross-sectional area such that the proper expression is

$$\delta = \varepsilon L \ . \tag{21}$$

Hence, for a fixed minimum length for gage mounting and fixed output, the deflection is independent of load.

For the case of a prismatic member in pure bending such that the bending stress (and strain) vary linearly through the thickness and upon which is superimposed a uniform stress due to the axial load P,

$$\delta = 8 \frac{E}{P} \int_0^{\frac{L}{2}} \int_0^{\frac{b}{2}} \int_0^{\frac{t}{2}} (\varepsilon \frac{2x}{t})^2 \ dx \ dy \ dz$$

$$= \frac{1}{3} \frac{E}{P} \varepsilon^2 \ tbL = \frac{1}{3} \frac{E}{P} \varepsilon^2 v \tag{22}$$

There is an apparent reduction of deflection by a factor of three compared with the direct tension transducer element for the same minimum strain gage mounting volume. Furthermore, it is possible here to use a four-active gage Wheatstone Bridge circuit while the tension-type element has only two active, or at best, two fully active and two 0.3 active gages when Poisson's Ratio effect is utilized. The net result is that this idealized bending member has only about 22 percent the deflection of the optimum tension-type element for a given sensitivity. There is, furthermore, no longer the restrictive condition relating load, strain, and cross-sectional area since the bending moment may be arbitrarily adjusted to achieve the desired strain at the minimum practical cross-sectional area independent of load. It must be noted that the vanishing deflections indicated as load P, increases are not attainable. The shear strains in a cantilever member or the axial strain for an eccentric column are not negligible as the load increases and the section is kept small. The result for the eccentric column including strain due to axial loading as well as bending is

$$\delta = \frac{1}{3} \frac{E}{P} \varepsilon^2 \ tbL \left[\!\left[1 + \frac{1}{12} (\frac{t}{e})^2 \right]\!\right] \tag{23}$$

where e is the eccentricity of the active portion of the column. There is now an additional relationship between load, eccentricity, strain and section dimensions:

$$E \varepsilon = \frac{6Pe}{bt^2} \ ; \tag{24}$$

so that the proper expression for deflection is

$$\delta = 2 \varepsilon L \left[\!\left[(\frac{e}{t}) + \frac{1}{12(e/t)} \right]\!\right] \tag{25}$$

The deflection is minimized at $e/t = 0.288$ for which

$$\delta_{min.} = 1.154 \ \varepsilon L \tag{26}$$

At the same strain, then, the best eccentric column is about 15 percent more deflective than the best tension-type element; however, in terms of electrical sensitivity, the eccentric column is about 25 percent <u>less</u> deflective!

This difference is not very significant in the light of the many practical considerations such as load magnitude, linearity, sensitivity to temperature and extraneous loads, and physical size which usually govern the final choice. It is apparent that the transducer deflection may usually be estimated for preliminary design purposes by considering a simply tension-type element.

The same principles apply to a shear sensitive section with the important result that where such a section can be employed it may be much less deflective. This is because the shear web on which the gages are mounted may be made an order of magnitude thinner than the tensile or bending sections discussed previously since the unstressed flanges which are usually associated with a shear section serve as heat sinks to dissipate the electrical strain gage power generated. However, only a particular combination of circumstances permit the advantageous utilization of shear transducers in a floating frame balance, since practical shear transducers are ungainly in size and shape.

A tension-type element is most simply a prismatic post whose cross-sectional area is determined by the strain level requirements and whose lateral dimensions permit attachment of strain gages. Even where only two gages are active in a bridge circuit, thermal compensation dictates that the two dummy gages be located proximate the active ones. In practice, low sensitivity to extraneous loads is obtained by maintaining large lateral dimensions. Typically, an "I" or "H" section is used. Commonly, the active gages are mounted to the outer surface of the flanges and the lateral gages are mounted on the web. In this case, it is often possible to realize a slight increase in sensitivity by taking advantage of a secondary ring bending effect. An even more successful arrangement is to mount the primary gages on the web which is aligned with the adjacent flexures for a local augmentation of stress, and to mount the lateral gages on the outer surface of the flanges. The flanges are (with proper design) subject to a secondary lateral bending similar to anticlastic bending such that the net output may approach that of a four active gage bridge operating at the average axial strain level. Furthermore, sensitivity to extraneous loads are even more reduced. Many other arrangements are, of course, possible and most have been tried at one time or another.

Strain gage elements of this type always exhibit "negative" non-linearity (less output in compression than in tension) due to

1. Poisson's Ratio change of area under loading
2. the logarithmic dependency of "natural" strain (to which the strain gage is sensitive) upon total strain.

These two effects result in a quadratic non-linearity of from 0.1 percent to 0.3 percent at a nominal sensitivity of one millivolt output per volt input.

The eccentric column is simply a member displaced from the axis of loading, dimensioned to develop the proper bending strain under the influence of the resultant bending moment, and instrumented to sense only the bending strain with four active gages. The bending takes place in the same plane as that permitted by the inboard flexures of the element so that the column bending moments are nearly statically determinant. Depending upon the relative bending stiffness of the inboard flexures, the transducer is to a greater or lesser extent dependent on extraneously applied moments in the plane of the eccentricity. This undesirable effect is eliminated by splitting the column longitudinally into two halves, each of which is eccentric, but on opposite sides of the axis of loading. Hence, the sense of bending is always opposite in these two members such that a net extraneous bending moment of the same sense in both members is electrically cancelled. These elements may be made to be sensitive to much smaller applied forces than the tension-type element. They are always non-linear in a positive sense (increased output in compression) due to the change in eccentricity caused by loading. The magnitude of non-linearity is calculable to be proportional to:

$$\frac{(L/t)^2 - 2\mu}{(e/t)} \qquad (27)$$

where L/t is column length-thickness ratio, μ is Poisson's Ratio, and e/t is as defined previously. Rarely is it possible to reduce L/t to the order of twice Poisson's Ratio; hence, linearity is "positive" and may be further decreased by increasing eccentricity. This is contrary to the deflection criterion which indicates e/t ratios of about 0.3. The necessary compromise is a difficult one to make; the usual course being to minimize length as much as possible and to favor the deflection in selecting low eccentricities at the price of non-linearities ranging between 1/4 and 3/4 percent at one millivolt per volt. Again, many other factors enter in the final choice.

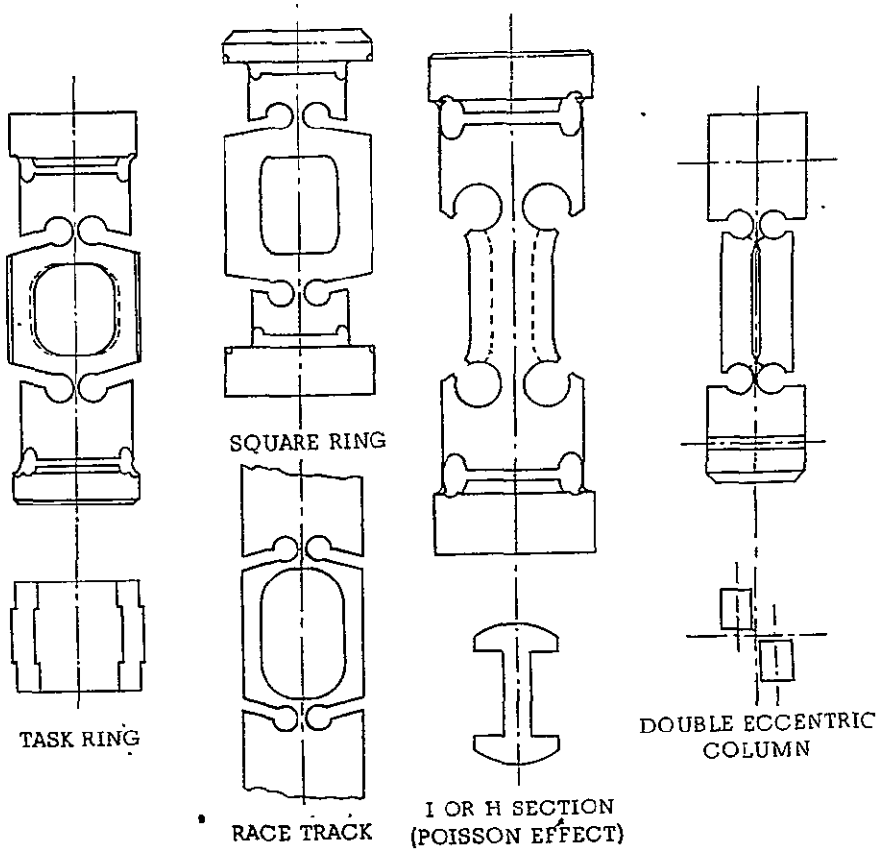

Figure 9. Flexure configurations used in force balances.

The "ring-types" are variations of the eccentric column, or rather the double-eccentric column described last. Initially, they were made to approximate circular rings of constant cross-section for ease of stress analysis and design synthesis. These were difficult to machine, overly deflective, space consuming, and presented only curved surfaces for gage mounting. Even so, such rings were not exactly predictable by simple ring formulae. The modified ring or "race-track" element has found wise use in internal balances. Its advantages are

1. the width of the gaged portion is great enough to permit "stress-balancing" such that the gage bonds in each case "see" only the useful bending strain and need not electrically cancel the net axial strain
2. the distance between the inboard flexures is greater than that for an equivalent eccentric column
3. it is very rugged and virtually unaffected by extraneous loads.

The second feature is an advantage only in moderately large balances where maximum flexure spacing is desirable with minimum active gage length. Despite these features, the "race-track", like all ring types, exhibits positive non-linearities and its deflections are greater than the eccentric column which would replace it. Its large deflection argues against its use except in some light load components of moderately large balances and for light load applications in very small balances where size restrictions prevent "doubling" of the eccentric column and loads are too light for a tension-type member. This application has led to the "square-ring": short because of length restriction; broad to enable gages to be applied to the inner faces. The result is a practically linear output but very large deflections (relative to a comparable tension-type element).

The single eccentric column is often used in the dual chord force arrangement where space is limited and loads are very light. The moment sensitivity and non-linearity of the two (long) single columns cancel in the net output of such a push-pull axial force element.

It may be mentioned that in high load parameter balances the chord force output is limited when the axial force requirement is very small. The compliance of the remainder of the balance to axial deflections may be less than that of the axial force element itself! In this case, increasing the sensitivity of the element may reduce its stiffness (increase compliance) enough to offset the sensitivity increase, while stiffening may likewise be offset by the resulting reduced sensitivity. This problem mutually involves flexure and transducer design.

The most effective rolling moment transducer is simply a thin-walled circular tube on which strain gages are placed at 45° to the axis of the tube in order to sense only the shearing strain produced by torsion. The deflection follows the same law found for tension-type members and non-linearity is negligible.

These by no means exhaust the transducer possibilities, since a complete morphology would be voluminous. Suffice it to say that others have been tried and still others are under development, some of which offer great promise for standard and special applications.

Likewise, a discussion of strain gages, their selection, application, connection, temperature and output compensation, protection, and operating environment would be a treatise beyond the scope of the present paper. With regard to balance design and practice, several (often conflicting) requirements should be approached as closely as possible:

1. Locate the gages of a bridge near one another with good thermal connection;
2. Locate gages away from fibers strained by extraneous loads;
3. Locate gages on surfaces as flat as possible;
4. Use four fully active gage bridges where possible;
5. Avoid mounting on thin surfaces (generally take .02" - .03" as a minimum);
6. Use large-high resistance gages with maximum gage length;
7. Design for surface strains of 500 to 1000 microinches per inch macimum;
8. Use super-clinical cleanliness and care in preparing and mounting strain gages.

5. Attachments The balance fittings and attachments are quite ordinary and yet require the utmost care to avoid their compromising the balance's strength and accuracy potential.

The model must fit very closely on the balance diameter. The balance outer sleeve is a structural member and as such is subject to deformation necessitating the tightest possible fit in the model cavity. Axial and roll loads are carried by one or more very closely fitting pins between model and outer sleeve. It is strongly felt that a significant contribution to hysteresis and non-repeatability (especially those of first and second order interactions) can be traced to poor calibration body and model fits on the balance. This should not be too surprising since the only joint on the balance system that is not either screwed or heavily pressed together is the model-balance attachment.

The normal and side force elements are customarily attached to the inner rod and outer sleeve with specially machined cap screws. Clearance is provided at the outer sleeve joint to permit adjustments of element alignment to be made. This is one of the most important features of the floating frame balance in that eight important first order interactions of the thirty possible may be often reduced virtually to zero. (Only a half dozen or less of the remaining twenty-two are generally significant.)

The axial and roll members are attached at each extreme end to the inner rod with hardened steel pins pressed in burnished holes. At their center two rows of similarly pressed pins carry axial and roll loads from the outer sleeve.

The balance connection to the sting is the most difficult area of the balance to properly analyze. The "sting-socket" tapered joint must carry bending and shear in two planes and axial and rolling moment (with the aid of two pins or keys). The most common modes of failure, aside from bearing failure of the roll restraint pin slots, are:

1. Fracture at the base of sting,
2. Bearing failure at base of sting,
3. "Bell-mouthing" or cracking of socket lip.

The first two above are ameliorated at the expense of the third and vice versa. When the sting "gage diameter" is adjusted accordingly, the remaining course is to lengthen the joint. When this has been done, excessive galling of the mating surfaces resulted from the inevitable motion between sting and socket in bending. In short, the limitation of balance lateral force and moment capacity currently lies at this joint rather than with the complex system of pivots and transducers within the balance itself.

Stimulated by the need for thermal stability in the presence of continuous hypersonic tunnels with high stagnation temperatures (and model temperatures), an external water jacket for balance cooling has been introduced. This accessory has far exceeded its expectations. Most important, it permits maintenance of constant balance temperatures under virtually any conditions, thus practically eliminating thermal errors. In addition, the slight pressure expansion of the jacket securely locks the balance in the model. Even where temperatures can be withstood by a balance without cooling, such a jacket can greatly improve over-all accuracy.

6. Calibration and Operation The calibration sequence begins with a load check to determine what, if any, alignment is necessary. Following alignment, a minimum calibration consists of step loading each individual component to rated load (both tension and compression) and return, and recording outputs to determine sensitivities and first order interactions. For a performance calibration, this may be sufficient (although some second order interactions may be checked). Thermal zero drift should be monitored along with the thermocouple outputs for several thermal cycles. It may be necessary to determine change of sensitivity of each component with temperature. For a full calibration, it will usually be necessary to check virtually all of the second order interactions to ascertain their values or non-existence. Third and higher order load combinations are normally unnecessary and, in any event, are often difficult to apply with sufficient accuracy.

The use of a balance requires, block diagram-wise,

1. power supply,
2. balance,

3. amplification,
4. analog to digital converter,
5. visual readout or card, tape or typewriting system,
6. manual or digital data reduction and presentation.

This equipment may be very simple and yet very accurate, or it may be very elaborate. The primary advantage of an automatic readout and data reduction system is the increased rate at which data may be taken and presented in final form. A facility which is expensive to operate is usually economically justified in installing a high speed automatic data acquisition system. Closer study of each case is needed to make the decision as to the use of automatic storage and a low speed computer, or direct data reduction requiring greater computer capacity. Such a sophisticated system is no assurance a priori of high accuracy. In fact, greater care is indicated in ascertaining that a highly automated data handling system does not impose errors whose magnitudes are of the same order or greater than balance inaccuracies. On the other hand, it is not prudent to employ a balance whose accuracy is less than desired when the remainder of the system is capable of much greater accuracy and a relatively small additional expenditure could secure an instrument (balance) of greater precision. All this is to say that the data acquisition and handling system should not compromise the best balance to be employed, while on the other hand the balance quality should be such that truly necessary accuracies may be obtained if at all possible. Finally, the choice of A-C or D-C; direct reading, fractional resistance change, or null readout; magnetic tape, card punch, type-out, or automatic plotting, etc., do not materially affect the design or instrumentation of the balance itself and will not be belabored herein, with the exception that the readout system should be sensitive to a maximum balance output level of four millivolts for a very small balance increasing to not more than about twice this for a large balance. The errors induced by self-heating of the strain gages due to excessive input voltage (power) can be in excess of all other balance errors!

7. Balance Selection   Proper determination of size and load requirements for a floating frame balance can materially affect the accuracy of the data. Generally speaking, the load parameters should be as small as possible and the ratios of applied loads should approach unity. (The exception to the above is that lateral forces of much below one hundred pounds and axial forces much below fifty pounds introduce difficulties in transducer design, although they can be generally overcome.)

If the desired normal force and balance diameter result in a value of $R_n (= N/D^2)$ much greater than 500 or if roll capacity indicates $R_1 (= 1/D^3)$ much above 160, every effort should be made to employ a larger balance. When it is realized that a 50 percent increase in balance diameter reduces R_n by more than one-half and R_1 by more than two-thirds and that associated errors may be reduced by even greater amounts, the difficulty of employing the very largest possible balance is seen to be well justified.

A second possibility is that the high loads desired are needed for starting or emergency stop conditions. If such is the case, overload stops can be provided in the balance without the detrimental effects otherwise associated with high load balances. Normal to side force ratios greater than 3 or 4 and normal to chord force ratios greater than 10 or 12 are rarely needed and should be avoided. The absolute error of a very light load element will generally be minimized if the above ratios are not exceeded even if only a portion of rated capacity of the light element is used!

In the attempt to fully utilize the range of existing instrumentation, high input voltage and output sensitivity is often specified. Carried to excess, both of these requirements can introduce balance errors which overwhelm the gains anticipated from full use of instrument range. A rule of thumb for excitation voltage is

$$V_{max.} \approx 4\sqrt{D} \quad , \qquad (28)$$

while transducer sensitivities of 1.0 to 1.5 millivolts per volt are usually optimum.

Rationally, the accuracy of a six-component balance should not be expected to equal that of a precision single-component transducer, especially when the balance loads approach those which would destroy a solid piece of steel of the same external configuration! The wind tunnel balance is often treated as the stepchild of the instrumentation field, yet it finds more "experts" ready to delve into its mysteries than many a simpler device. These balances are, unquestionably, the most complex and compact transducers yet achieved; capable of separating and measuring six different but interrelated variables simultaneously. It is truly a tribute to those persons who have contributed to wind tunnel balance technology that such a device can be made; and that it will perform with an accuracy that does, in fact, place it in the precision transducer class.

1 - CONTROL NUMBER: U261426
4 - ACCESSION NUMBER: N77-83285
B3 - COLLECTION CODE: 4
B6 - MANAGEMENT CODE: XF
B7 - PROCESS ACTNG CD: 01 B7A-REGISTRATION FEE: 00000
B8 - PRODUCT MANAGER: H
B9 - RECEIPT TYPE: 1 B9A-LOAN DUE OUT:
B10- TRANSACTION: TN B10A-DUPE/PRIOR/SUPER:
B12- RETURNS: 0 B12A-RETURN DATE:
B13- PROCESSING: 1
B14- PAT. POTENTIAL: 0
B17- FORM/PRICE: 12001
B18- ANNOUNCE: 0000
B19- PUBLICATION-1: u8201 B20- PUBLICATION-2:
B21- LIMITATION: 0
B23- PC BIN: 000
B24- STOCK: 0000 B24A-STOCK TYPE CODES: N
B25- PAGES/SHEETS: 00120
B26- PC PRICE CODE: A06
B27- DOMESTIC PRICE: 0000000 B28- FOREIGN PRICE: 0000000
B29- ACTION CODES: BX
B33- MN PRICE CODE: X00
B34- DOMESTIC PRICE: 0000000 B35- FOREIGN PRICE: 0000000
B36- ACTION CODES: XM
B37- RELEASABILITY CD: A
B38- MF PRINT: D
B39- ADDITIONAL INFO: n
B40- PRINT PC: n
B41- PC DUE: n
B42- SOURCE ORDER: n
B42A-GENERATE RDP: 0
B42B-SUPPLIER SRC CD:
06)Proceeding o Western regional St
ran Gage Committe.¢
11)1977,¢
14 I-C) NASA-TM-74879¢

1. CONTROL NUMBER
U 261426

INVENTORY ONLY

BATCH NUMBER 96852F

3. COL. CD. 4

2. SOURCE CODE NASA

4. ACCESSION NUMBER

2A. RECOGNITION NUMBER NASA-TM-74879

10. TRANSACTION N NEW D DUPLICATE P PRIOR S SUPERSEDES
N
10A.

6 MGT. CD. C D A R K V
V X K

7. PROCESS ACCTG. CD. Q1

7A. REGISTRATION FEE

8. PROD MGR. H

9 RECEIPT TYPE 1
0 N/A 1 RETAIN 2 LAST 3 ERRATA 4 LOAN

9A. LOAN DUE OUT Y Y D D D

11. PRICE 1. STD. 2. EXC.

12. RETURNS 0 N/A 1 PAGES 3 REPRO 4 BDS 5 REST. 8 MISC.

12A. RETURN DATE Y Y M M D D

13 PROCESS 0 STANDARD 1 INVENTORY 2 HIGHLIGHT 3 UNEDIT 4 REANNOUNCE 5 SPECIAL BIB

14. PAT. POTENTIAL 0 NO 1 POOR 2 FAIR 3 GOOD 4 EXCEL.

16. BILL

17 FORM/PRICE

18. ANNOUNCE GRA WGA 0 D/8

19 PUBLICATION-1 U

20. PUBLICATION-2

20A. PUBLICATION-3

21. LIMITATION 0 N/A 1 DISCLAIMER 2 COLOR 3 COMBO

23. PC BIN STOCK 24A. PAGES/SHEETS PRICE CODE DOMESTIC PRICE FOREIGN PRICE ACTION CD.
QQD 0 N 120

MICROFICHE
37. REL. CD. 38. MF PRINT

39. ADD. INFO.

40 PRINT PC

43. 43A) ORDER ADD'L STOCK & CODE/ADDR 43B) BIN MSG 43C) STK UNIT COST 43D) SET ID 43E) CAMERA CONTROL 43F) REFER TO ADDR

41. PC DUE

42 SOURCE ORDER

42A RDP. 0 N/A 1 RDP 2 42B. SUPPLIER SOURCE

COPYRIGHT
YES NO INITL

RD

44 BATCH NO.

02C) COM CAT.

03S) ADDITIONAL SOURCE CLIENTS

03L) LANGUAGE

03C) COMP. ENTRY CODE

34) SERIAL

35) CORP. AUTHOR CD.

MGT CD. CAT REV KEY VER

45 REMARKS (DO NOT KEY)